

Traditional to Transformers: A Survey on Current Trends and Future Prospects for Hyperspectral Image Classification

Muhammad Ahmad, Salvatore Distifano, Manuel Mazzara, and Adil Mehmood Khan

Abstract—Hyperspectral image classification is a challenging task due to the high dimensionality and complex nature of Hyperspectral data. In recent years, deep learning techniques have emerged as powerful tools for addressing these challenges. This survey provides a comprehensive overview of the current trends and future prospects in Hyperspectral image classification, focusing on the advancements from deep learning models to the emerging use of transformers. We review the key concepts, methodologies, and state-of-the-art approaches in deep learning for Hyperspectral image classification. Additionally, we discuss the potential of transformer-based models in this field and highlight the advantages and challenges associated with these approaches. Comprehensive experimental results have been undertaken using three Hyperspectral datasets to verify the efficacy of various conventional deep-learning models and Transformers. Finally, we outline future research directions and potential applications that can further enhance the accuracy and efficiency of Hyperspectral image classification.

The Source code is available at <https://github.com/mahmad00/Conventional-to-Transformer-for-Hyperspectral-Image-Classification-Survey-2024>.

Index Terms—Spatial-Spectral Feature; Hyperspectral Image Classification (HSC); Convolutional Neural Networks (CNNs); Spatial-Spectral Transformers (SSTs).

I. INTRODUCTION

HYPERSPECTRAL Sensors capture detailed spectral information across a broad range of electromagnetic wavelengths [1]. Unlike traditional methods, Hyperspectral Images (HSIs) provide a continuous spectrum through numerous narrow bands, enabling precise material characterization and valuable Earth surface information extraction [2], [3]. Its significance in remote sensing lies in overcoming the limitations of multispectral imaging, allowing discrimination of subtle differences in material properties, and facilitating accurate land cover classification [4].

HSI's key advantage lies in its ability to distinguish materials with similar visual appearances but distinct spectral properties [5]. This specificity is crucial in various applications, such

M. Ahmad is with the Department of Computer Science, National University of Computer and Emerging Sciences, (NUCES), Pakistan, and the Dipartimento di Matematica e Informatica-MIFT, University of Messina, 98121 Messina, Italy. e-mail: mahmad00@gmail.com.

S. Distifano is with the Dipartimento di Matematica e Informatica-MIFT, University of Messina, 98121 Messina, Italy. e-mail: sdistefano@unime.it

M. Mazzara is with the Institute of Software Development and Engineering, Innopolis University, 420500 Innopolis, Russia. e-mail: m.mazzara@innopolis.ru

A. M. Khan is with the School of Computer Science, University of Hull, Hull HU6 7RX, UK. e-mail: a.m.khan@hull.ac.uk

as agriculture, forestry, urban planning, environmental monitoring, mineral exploration, disaster management, bloodstain identification, meat processing, contamination detection in red chili, and bakery products [6]–[19]. Figure 1 illustrates some HSI applications, while Figure 2 outlines HSI research trends from 2010 to 2024.

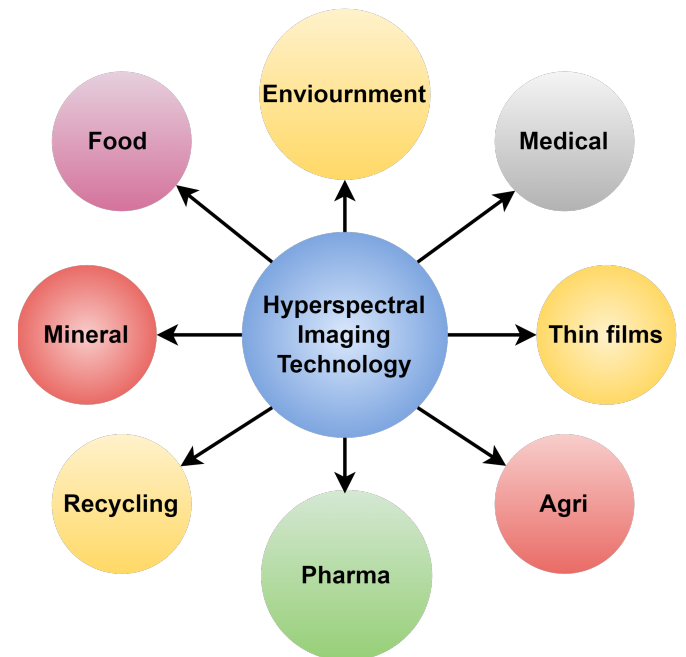


Fig. 1: Various real-world applications of HSI.

In agriculture [6], HSI monitors crop health, detects diseases, and estimates vegetation properties like chlorophyll content, optimizing irrigation and pest control for enhanced crop management. In forestry, HSI assesses forest health, and species composition, and detects pests and diseases early, aiding conservation efforts. It is crucial for monitoring deforestation and ecosystem changes caused by human activities. In geological studies [8], [9], [12] and mineral exploration [10], [11], HSI identifies mineral deposits through unique spectral signatures, supporting resource exploration, mining, and environmental impact assessments. Additionally, HSI assists urban planning by identifying land cover types, analyzing urban heat islands, monitoring urban expansion, and assessing environmental quality for sustainable development and infrastructure planning.

In short, HSI provides detailed spectral information, enhanc-

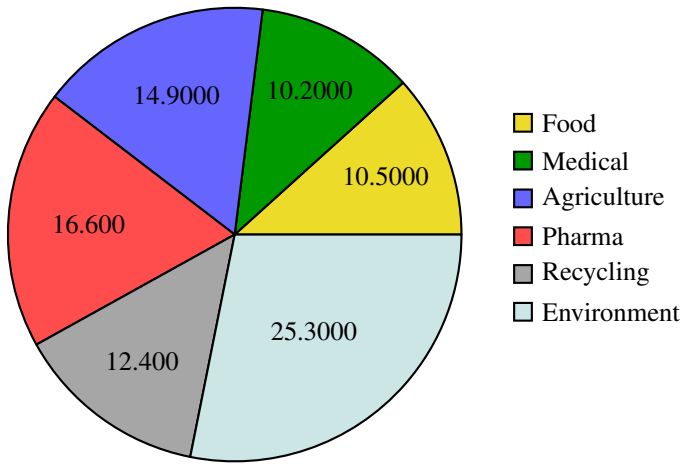


Fig. 2: Distribution of published papers across domains in the recent years. Data sourced from Google Scholar accessed on 18-02-2024.

ing understanding of the Earth’s surface and supporting land cover classification, environmental assessment, change monitoring, and decision-making [20]. As technology advances and HS sensors become more accessible, HSI will play a vital role in addressing environmental challenges and facilitating sustainable resource management. This survey focuses on the field of Hyperspectral Image Classification (HSC), which has seen significant advancements, especially with the rise of deep learning (DL) models [21], [22]. The survey aims to comprehensively overview commonly used DL techniques for HSC. It will address primary challenges in HSC, not effectively tackled by conventional machine learning (TML) methods, and emphasize how DL improves HSC performance.

A. Significance of Accurate Classification

Accurate classification in HSI analysis is crucial due to the wealth of complex information within the data’s numerous spectral bands. HSIs provide unique details about observed objects, making precise classification essential for diverse applications. The significance of accurate classification lies in extracting meaningful information about land cover types and land-use patterns [23]. HSC techniques identify and map different land cover classes, aiding land management, resource planning, and environmental assessments [24], [25]. This precision is vital for monitoring changes in land cover, facilitating insights into deforestation, urban expansion, and ecosystem degradation for conservation and sustainable land-use practices [26].

Accurate classification is crucial for environmental monitoring and assessment [9]. HS imagery detects factors like water quality, pollution sources, and ecosystem health, allowing identification of areas of concern, tracking changes, and evaluating environmental management strategies. This information is vital for ecosystem health, biodiversity conservation, and mitigating environmental risks. In agriculture, precise HSC supports crop monitoring, disease detection, and yield estimation [6]. It identifies stressed vegetation, enabling targeted

interventions like irrigation or pesticide application. HSC also aids precision agriculture by providing information on soil composition, nutrient levels, and plant health, optimizing resource allocation for improved productivity.

In mineral exploration, precise classification of HS data identifies and maps mineral deposits and geological formations [10], [11]. Distinct spectral signatures of minerals aid prospecting and resource estimation, crucial for sustainable resource management, reducing exploration costs, and minimizing environmental impacts. Urban planning and infrastructure development benefit from accurate HSC [8]. Accurate classification of land cover types and urban features enables assessing urban growth patterns, monitoring changes, and planning for future development. It supports urban heat island analysis, transportation planning, and identifying green spaces, contributing to sustainable and livable cities.

Therefore, accurate HSC is highly significant, improving our understanding of the Earth’s surface, supporting informed decision-making, and enabling sustainable management practices. With advancing HSI technology, accurate classification techniques will play a crucial role in addressing complex challenges and fostering sustainable development.

B. Brief Introduction to Deep Learning

Deep models, like CNNs, have revolutionized HSC, outperforming conventional methods by leveraging neural networks and attention mechanisms [27], [28]. CNNs excel in learning hierarchical representations and capturing spatial and spectral dependencies within HS data [29]. Their ability to automatically extract discriminative features makes them well-suited for accurate classification in HSI [30], [31]. RNNs, designed for sequential data, show promise in HSC for temporal analysis [32]. Exploiting the temporal dimension, RNNs capture contextual information for tasks like tracking land cover changes or monitoring dynamic environmental processes. Autoencoders (AEs), a neural network type, find application in HSC [33]. Comprising an encoder and decoder network, AEs compress input data into a low-dimensional representation (latent space) and attempt to reconstruct the original input [34]. In HSI, AEs are used for unsupervised feature learning and dimensionality reduction [35]. Training AEs on unlabeled HS data enables effective feature extraction and classification by capturing the underlying data structure [36].

More recently, Transformers have gained significant attention in various domains, including natural language processing and computer vision [2], [4], [11], [30]. Transformers are based on a self-attention mechanism that allows the model to capture dependencies between different positions within a sequence. In the context of HSC, transformers have shown promise in learning long-range dependencies and capturing non-local spectral relationships. By modeling the interactions between different spectral bands, transformers can effectively exploit the rich spectral information in HS data. This has led to improved classification performance and the ability to capture complex spectral patterns. Transformers can handle variable-length input sequences, making them suitable for

HSIs of different spatial dimensions. Additionally, transformers offer interpretability, as the attention mechanism allows for visualizing the importance of different spectral bands in the classification process. This interpretability can be valuable for understanding the reasoning behind the model's predictions and enhancing domain knowledge. In short, DL models, including CNNs, RNNs, AEs, and Transformers, demonstrate substantial potential in HSC. Leveraging their capacity to learn intricate representations, capture spatial and spectral dependencies, and exploit temporal information, these models contribute to significant advancements in accurate HSC, enhancing our understanding of the Earth's surface across diverse applications.

The following sections are organized as follows: Section II provides an in-depth description of the HS dataset, covering spectral, spatial, and spectral-spatial representation. In Section III, various learning mechanisms for HSI processing are outlined. Section IV examines conventional methods for HSC along with their limitations. Section V explores the advantages of employing DL for HSC. Section VI elaborates on CNN models for spectral, spatial, and spectral-spatial models. Section VII outlines Deep Belief Networks (DBN) for HSC and potential research directions. Section VIII discusses Recurrent Neural Networks (RNNs) for HSC and potential research directions. Section IX details Autoencoders (AEs) for HSC and potential research directions. Section X concludes trivial deep learning approaches and suggests future research directions. In Section XI, an extensive discussion on state-of-the-art deep models, specifically Transformers, includes a comparison with traditional deep models, benefits, and challenges for HSI analysis. Subsequently, Section XI explores emerging trends and advancements in state-of-the-art models for HSI analysis. Section XII discusses Explainable AI and Interoperability in HSC, while Section XIII outlines challenges and research questions. In Section XIV, detailed experimental results for traditional deep learning models and Transformer-based deep models are presented. Finally, Section XV concludes the survey and suggests immediate research directions.

II. HYPERSPECTRAL DATA REPRESENTATION

HS data is typically a 3D hypercube, denoted as $\mathbf{X} \in \mathcal{R}^{B \times (N \times M)}$, containing spectral and spatial information of a sample [37]. Here, B is the number of spectral bands, and N and M represent the spatial components (width and height) [38]. Figure 3 illustrates an HSI cube from the University of Houston dataset.

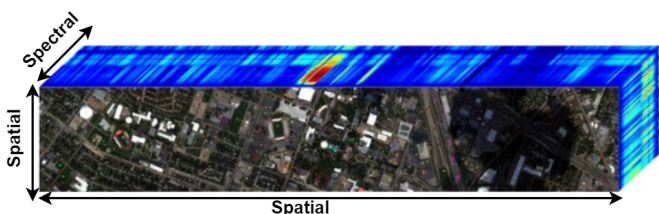


Fig. 3: University of Houston: Hyperspectral Image Cube representation.

In spectral representation, each pixel vector, denoted as $x_i \in \mathcal{R}^B$, is processed independently based on its spectral signature. The value of B represents the spectral channels, which can be the actual number or a reduced set obtained through dimensionality reduction (DR) techniques. A lower-dimensional representation is preferred to reduce redundancy and enhance class separability without significant information loss [39]. Unsupervised DR techniques, like Principal Component Analysis (PCA), [40] and Locally Linear Embedding [41], transform HSI data without using class labels. Supervised DR methods, such as linear discriminant analysis (LDA) [42], [43], local Fisher discriminant analysis (LFDA) [44], local discriminant embedding (LDE) [45]–[47], and nonparametric weighted feature extraction (NWFE) [48], utilize labeled samples to improve class separability. LDA and LFDA, for instance, enhance class separability by maximizing the distance between classes while minimizing within-class distance. However, spectral mixing challenges differentiation between classes solely based on spectral reflectance. This underscores the need for advanced techniques beyond spectral information for accurate HSI class differentiation.

To overcome spectral representation limitations, spatial information of pixels can be utilized. In this approach, pixels in each spectral band are represented as a matrix, denoted as $x_i \in \mathcal{R}^{N \times M}$. Spatial representation considers neighboring pixels due to high spatial correlation, enhancing class coherence. Neighbors are identified using kernels or pixel-centric windows [49]. Various methods extract spatial information from the HSI cube, including morphological profiles (MPs) [39], Gabor filters for texture features [50], gray-level co-occurrence matrix (GLCM) [51], local binary patterns (LBP) [52], and Deep Neural Network (DNN)-based methods. MPs capture geometrical characteristics, with extensions like extended morphological profiles (EMPs) [39] and multiple-structure-element morphological profiles [53]. Texture extraction methods like Gabor filters capture textural details, while LBP [52], [54] provides rotation-invariant representations. GLCM [51], [55] determines spatial variability based on relative pixel positions. DNNs can extract spatial information by treating each pixel as an image patch, learning spatial features. Combining multiple methods, as seen in studies like Zhang et al. [56], enhances spatial information extraction. In this study, Gabor filters and differential MPs were combined for an RNN-based HSC framework, showcasing the potential of integrating techniques for leveraging spatial information.

Spatial-spectral approaches in HSI process pixel vectors by incorporating both spectral features and spatial-contextual information. Two common strategies exist for the simultaneous use of spectral and spatial representations. The first strategy concatenates spatial details with the spectral vector, demonstrated in studies by Chen et al. [57], [58], merging both into a single feature representation. The second strategy processes the three-dimensional HSI cube, preserving its structure and contextual information. Paoletti et al. [59] showcase this approach, maintaining the HSI's three-dimensional nature and utilizing DL techniques to extract features capturing both spectral and spatial characteristics. Both strategies aim to enhance HSI analysis and classification tasks by leveraging

the complementary nature of spectral and spatial information. While many DNN models focus on spectral representation [60], recognizing its limitations, recent efforts aim to integrate spatial information into the classification process [60]. Joint exploitation of spectral and spatial features has gained interest, leading to improved accuracy [61].

III. LEARNING CATEGORIES

Machine learning models for HSC can employ different learning strategies, four of which are presented in Figure 4.

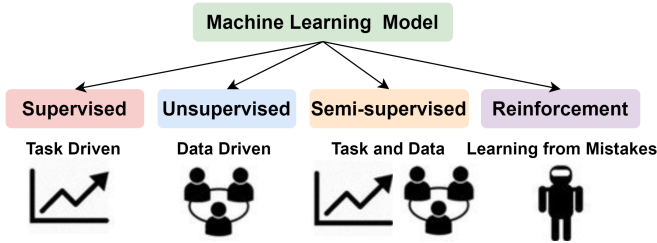


Fig. 4: Major Learning Categories.

Supervised Learning In supervised learning, models are trained on labeled data, associating each example with a target output. The model adjusts its parameters iteratively during training to improve accuracy in predicting outputs. Effective training requires a substantial amount of labeled data, making these models suitable for scenarios with abundant labeled data. DNNs excel in learning complex patterns and making accurate predictions in such scenarios. **Unsupervised Learning** Unsupervised learning involves training models on unlabeled data to uncover patterns without predefined target labels. Measuring accuracy can be challenging, but it is useful when learning intrinsic structures of datasets with limited labeled training data. Techniques like PCA learn low-dimensional representations by identifying directions of maximum variance. K-means clustering groups data into clusters, revealing patterns or similarities among instances [62].

Semi-Supervised Learning strategy combines elements of both supervised and unsupervised learning. It utilizes a limited amount of labeled data along with a larger set of unlabeled data for training. The model learns from the labeled data to make predictions on both labeled and unlabeled instances, leveraging the additional unlabeled data for improved performance [63], [64]. **Reinforcement Learning**, an agent interacts with an environment and learns to take actions to maximize cumulative rewards. The agent receives feedback in the form of rewards or penalties based on its actions, allowing it to learn optimal decision-making policies through trial and error [65]. **Transfer Learning** involves leveraging knowledge or representations learned from one task or domain and applying them to a different but related task or domain. This approach can be beneficial when labeled data is scarce or when pre-trained models can provide useful feature representations [66], [67]. **Online Learning** also known as incremental learning, involves updating the model continuously as new data becomes available. The model learns from each instance of data sequentially, adapting to changing patterns or concepts over time [68], [69].

IV. BRIEF OVERVIEW OF CONVENTIONAL METHODS

The main goal of HSC is to assign distinct labels to pixel vectors in the HSI cube based on their spectral or spatial characteristics [70]. Mathematically represented as $\mathbf{X} = [x_1, x_2, x_3, \dots, x_B]^T \in \mathcal{R}^{B \times (N \times M)}$, where B is the total number of spectral bands with $N \times M$ samples per band [71]. These samples belong to Y classes, each $x_i = [x_{1,i}, x_{2,i}, x_{3,i}, \dots, x_{B,i}]^T$ represents the i^{th} sample with a class label $y_i \in \mathcal{R}^Y$. The classification task is treated as an optimization problem, where a mapping function $f_c(\cdot)$ operates on the input data \mathbf{X} [29], aiming to minimize the disparity between the obtained output and actual labels [72] as shown in equation 1.

$$\mathbf{Y} = f_c(\mathbf{X}, \theta) \quad (1)$$

where the parameter θ adjusts transformations applied to the input data \mathbf{X} for the mapping function $f_c : \mathbf{X} \rightarrow \mathbf{Y}$. HSC research has seen a trend influenced by computer vision methodologies [1]. Conventional machine learning-based HSC relies on handcrafted features like shape, texture, color, spectral, and spatial details. Common methods include texture descriptors (LBPs [73], HOG [74], PHOG [75]), SIFT [76], GIST [76], Random Forests [77], kernel-based SVM [78], KNN [79], and ELM [36].

Color histograms are simple and effective but lack spatial context, making them sensitive to illumination changes. HOG captures edge orientations effectively, finding applications in remote sensing studies [80], [81]. SIFT is robust and invariant but computationally intensive. GIST provides a global image description based on statistical properties like roughness and openness [76]. Texture descriptors like LBPs are common in remote sensing image analysis for capturing texture around each pixel [73], [82]. Color histograms, GIST, and texture descriptors are global features, capturing statistical characteristics, while HOG and SIFT are local features describing geometric information. They are used in BoVW models [83], [84] and HOG-based models. For enhanced BoVW models, Fisher vector coding, SPM, and PTM are popular pooling strategies [85]–[87]. Combining these features is a common practice in HSC [88]. LBPs are computationally efficient, involving simple binary operations on local pixel neighborhoods. In contrast, SIFT is more complex, requiring convolutions, gradient computations, and orientation assignments, making it computationally intensive. GIST, as a global descriptor, computes statistical properties over image sub-regions, with complexity generally lower than SIFT. LBPs are the least computationally complex, followed by GIST, while SIFT is the most intensive [89].

Hand-crafted features, while effective, face challenges in real-world data due to varying optimal feature sets, subjectivity in human-driven design, biases, and limitations. Traditional HSC approaches encounter the curse of dimensionality, struggle with feature selection and extraction, lack spatial information consideration, exhibit limited robustness to noise, face scalability issues, and may not adapt well to complex data distributions. These challenges, including the curse of

dimensionality, reliance on domain expertise, and limited spatial information, have prompted the exploration of DL-based methods, such as CNNs and RNNs, for HSC. DL techniques offer automated feature learning, potentially overcoming the limitations of traditional methods and improving classification accuracy by capturing intricate spatial-spectral relationships in HSIs [90], [91].

V. ADVANTAGES OF DEEP LEARNING

Deep Learning (DL) architectures, exemplified in Figure 5, can discern patterns and features from data without prior knowledge of its statistical distribution [92]. Unlike conventional methods, DL models extract both linear and non-linear features without pre-specified information, making them suitable for handling HS data in spectral and spatial domains, individually or combined [1], [93]. With flexible architectures and varying depths, DL models accommodate different layers, allowing adaptation to diverse machine learning strategies—supervised, semi-supervised, and unsupervised. This adaptability makes DL architectures optimized and tailored for specific classification tasks across various domains and applications [94].

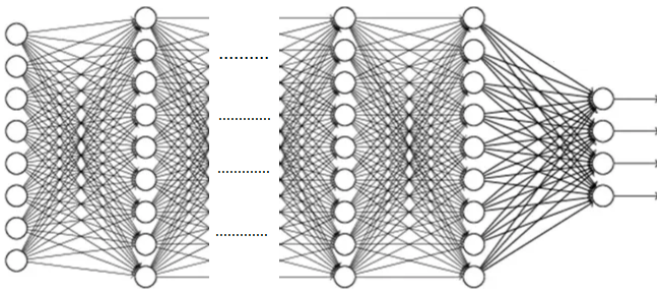


Fig. 5: Example of Deep Artificial Neural Network.

Leveraging DL enhances HSI data processing, leading to heightened classification accuracy and the ability to capture intricate relationships. DL models automatically learn and extract informative features from high-dimensional HSI data, addressing inherent complexity and variability [95]. Overall, DL architectures present a promising approach for HSC, learning from data without prior distribution knowledge, extracting both linear and non-linear features, and offering architectural and learning strategy flexibility [96]. These capabilities make DL models well-suited for overcoming challenges and complexities in HSI data analysis.

Automatic feature learning: DL models autonomously learn relevant features from data, creating hierarchical representations at various abstraction levels [97]. Unlike traditional methods relying on hand-crafted features, DL adapts and extracts discriminative features from HSIs, reducing the need for manual engineering and potentially capturing complex spectral-spatial patterns. **Spatial-spectral fusion:** DL models effectively capture spatial and spectral characteristics by integrating both types of information [98]. CNNs exploit spatial structure through convolutional layers, discerning local patterns [99]. Combining spectral and spatial details enhances accuracy, especially for classes with similar spectra but distinct spatial distributions.

End-to-end learning: DL models are trained end-to-end, optimizing the entire model, including feature extraction and classification, jointly [100], [101]. This simultaneous learning of features and classifiers can lead to superior performance compared to separate stages in traditional approaches. **Adaptability to complex data distributions:** DL models, particularly CNNs, with their non-linear transformations, effectively capture complex data distributions and intricate relationships between features and classes [102]. This adaptability enables better handling of variability and nonlinearity in HSIs.

Transfer learning and pre-training: DL models benefit from transfer learning, leveraging knowledge from one task or dataset for another [103]. Pre-training on large-scale datasets, followed by fine-tuning on smaller HS datasets, enhances classification performance, especially with limited labeled data [31]. **Scalability:** DL models efficiently handle large-scale datasets, enabling quick classification for real-time applications. Advances in hardware and DL frameworks, like GPUs, accelerate training and inference processes, making DL applicable to larger and more complex HS datasets [104], [105]. Despite these advantages, DL models for HSC face challenges, including the need for large labeled datasets, computational requirements, and potential overfitting. However, ongoing developments in DL techniques and increased HS dataset availability mitigate these challenges, establishing DL as a promising approach for accurate and automated HSC.

VI. CONVOLUTIONAL NEURAL NETWORKS FOR HSC

The CNN architecture, inspired by Hubel and Wiesel’s biological visual system [106] and Fukushima’s Neocognitron model [107], comprises two main stages: Feature Extraction (FE) and classification. The FE network, with convolutional and pooling layers, extracts hierarchical representations of input data. The subsequent classification stage utilizes these features, demonstrating CNN success in tasks like image classification and object detection. The FE network includes stacked layers—CONV, activation, and pooling—each contributing to meaningful FE. The CONV layer, sharing kernels across the input, captures local patterns efficiently, reducing model complexity and enhancing training ease.

In a CNN, convolved results undergo non-linear transformations through an activation layer, extracting crucial non-linear features for capturing complex data patterns. Following activation, pooling reduces feature map resolution, achieving shift-invariance and retaining essential information. Typically, a pooling layer follows each CONV layer, coupled with activation. This hierarchical process extracts increasingly complex features from input data for subsequent analysis and classification. The classification stage incorporates Fully Connected (FC) layers and a Softmax operator to determine class probabilities. Global average pooling, an FC layer alternative, summarizes spatial information and reduces parameters, mitigating overfitting. Softmax normalizes outputs into a class probability distribution, aiding predictions. While Softmax is common, studies explore SVM as an alternative for classification in CNNs, offering different optimization objectives and decision boundaries. Overall, the classification stage utilizes FC layers

or global average pooling, followed by a Softmax operator or alternatives like SVM, for predicting class memberships in input patterns. Subsequent sections detail three CNN architectures tailored for HSC: i) Spectral CNN, ii) Spatial CNN, and iii) Spectral-spatial CNN.

A. Spectral CNN

Spectral CNNs exclusively process 1D spectral data ($x_i \in \mathcal{R}^B$), where B denotes the original or reduced spectral bands [108]. Tailored for HS data, they treat each pixel’s spectral information as a 1D vector, capturing spectral intensity at different wavelengths. Unlike conventional 2D CNNs for image classification, these models consider HSIs as 1D sequences, where each element represents spectral intensity. The input is the pixel’s spectral profile, either the original full-dimensional vector or a dimensionality-reduced representation, presenting a focused approach to handle spectral dimensionality.

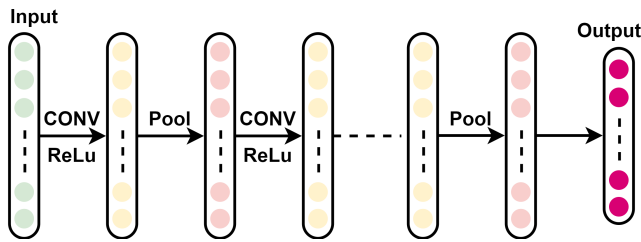


Fig. 6: Basic example of Spectral Convolutional Neural Network.

A crucial element in spectral CNNs is the CONV layer, applying filters to capture local spectral patterns and generate feature maps by element-wise operations. Commonly, pooling layers, such as max or average pooling, downsample and reduce dimensionality. Additional layers like fully connected or recurrent layers can be added for enhanced discriminative power. In [109], a CNN addressed overfitting by using 1×1 CONV kernels, increased dropout rates, and a global average pooling layer instead of fully connected layers. For handling high correlation among HSI bands, [110] introduced a CNN architecture transforming the 1D spectral vector into a 2D feature matrix with cascading 1×1 and 3×3 CONV layers. This design allowed feature reuse across different spectral bands. Similar to [109], [110] employed a global average pooling layer to reduce trainable parameters and extract high-dimensional features.

In HSC, [111] proposed a hybrid model combining CONV and recurrent layers for extracting both position-invariant middle-level features and spectral-contextual details. Similarly, in [112], a hybrid architecture effectively classified healthy and diseased wheat heads by transforming spectral information into a 2D structure for improved analysis. In spectral-based identification of rice seed varieties, [113] demonstrated CNN’s superiority over SVM and KNN, showcasing its effectiveness in accurately identifying rice seed varieties based on spectral characteristics. A similar application in [114] identified various Chrysanthemum varieties using CNN on spectral data represented by the first five Principal Components (PCs) obtained

through PCA, a widely-used dimensionality reduction method. In medical HSI, [115] used PCA as a preprocessing step, fusing CNN kernels with Gabor kernels for classification, highlighting the efficacy of hybrid architectures and the superiority of CNN over traditional algorithms in spectral-based classification tasks in HSC.

Advantages: Firstly, they capture local spectral patterns effectively through CONV operations, facilitating discriminative feature extraction [108]. Secondly, by integrating pooling operations, spectral CNNs manage high-dimensional HS data, reducing computational complexity. Thirdly, the inclusion of fully connected or recurrent layers enables learning high-level representations and capturing spectral-contextual dependencies, enhancing classification accuracy. **Limitations:** Challenges include limited labeled HS datasets, restricting model training and evaluation. Additionally, computational complexity and memory requirements due to numerous spectral bands in HS data may lead to intensive training and deployment processes. In summary, despite challenges like limited data and computational complexity, spectral CNNs offer a potent approach for HSIC, showcasing potential for advancements and demonstrating promising results in diverse applications.

B. Spatial CNN

Spatial CNNs, focusing on spatial information in HSIs, address the spatial dimensionality of HS data. Unlike spectral CNNs concentrating on spectral details, spatial CNNs treat the HSI as a 3D volume—width and height as spatial dimensions and the third representing spectral data at each pixel. The input is a 3D HSI, with CONV filters capturing local spatial patterns by considering both spectral and neighboring spatial information as shown in Figure 7.

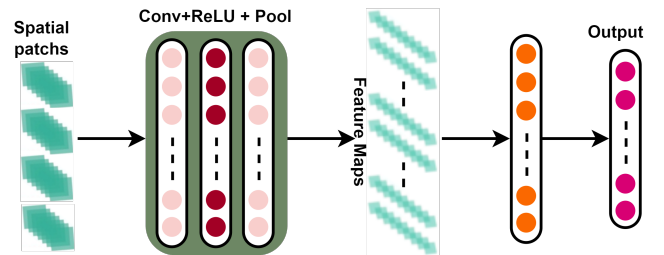


Fig. 7: Basic example of Spatial Convolutional Neural Network.

Pooling layers, like max or average pooling, commonly feature in spatial CNNs to condense feature maps and capture key spatial information. Additional layers, including FC layers, are often integrated to grasp high-level spatial features and enhance classification. In studies by Li et al. [116], Haut et al. [117], and Xu et al. [118], PCA-derived PCs were employed to infuse refined spatial information into CNN frameworks, demonstrating approaches to bolster DL models for HSC. Wang et al. [119] proposed a novel probabilistic neighborhood pooling-based attention network (PNPAN) aiming to enhance model robustness and combat overfitting in HSC. These strategies, including PCA-driven spatial information, random patch networks, and innovative techniques like PNPAN, seek

to address challenges linked to limited training samples and overfitting in DL models for HSC.

Ding et al. [120] extracted patches from 2D input images (representing different spectral bands) to train a 2D-CNN architecture. Data-adaptive kernels were learned to capture pertinent features from hyperspectral (HS) data. Chen et al. [121] proposed a 2D-CNN augmented with Gabor filtering to address overfitting concerns, effectively preserving spatial details. Zhu et al. [122] introduced a deformable HSC network using adaptive deformable sampling locations based on spatial features, enhancing the extraction of complex structures. These methods leverage data-adaptive kernels, handcrafted features like Gabor filters, and deformable sampling locations to improve HSC by capturing relevant spatial information and overcoming challenges such as overfitting with limited training samples.

Advantages: in capturing vital spatial-contextual information for hyperspectral classification, facilitating the understanding of spatial patterns and relationships. This capability is crucial for handling spatially varying features in HSIs, including structures, textures, and localized objects. Another strength lies in their ability to fuse spatial and spectral features, enhancing classification accuracy by leveraging the complementary aspects of these dimensions. **Limitations:** They demand substantial labeled training data, posing a hurdle in acquiring datasets with diverse spatial characteristics. Moreover, their computational intensity, attributed to the 3D input data and numerous parameters, can result in time-consuming training and inference processes. In summary, spatial CNNs provide a potent solution for hyperspectral classification, capitalizing on spatial information, though challenges like data requirements and computational complexity persist.

C. Spectral-Spatial CNN

Spectral-spatial CNNs exploit both spectral and spatial dimensions of HSIs simultaneously, unlike traditional CNNs focusing solely on spatial aspects (depicted in Figure 8). Treating the HSI as a 3D volume, with two dimensions for width and height and a third for spectral information at each pixel, Spectral-Spatial CNNs receive 3D HSI input, where each pixel contains a spectral profile. Comprising three key components: **Spectral Convolution** utilizes 1D CONV filters to capture spectral patterns. **Spatial Convolution** employs 2D CONV filters for spatial patterns and local dependencies. Finally, **Fusion and Classification** combines features from both dimensions, enhancing accuracy by leveraging complementary spectral and spatial information.

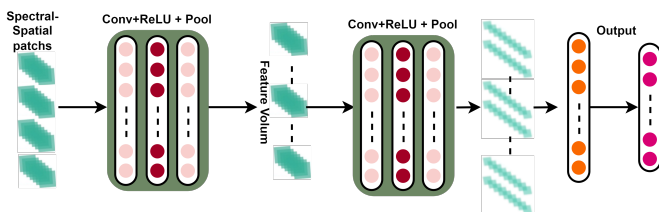


Fig. 8: Basic example of Spatial-Spectral Convolutional Neural Network.

Integrating spatial features with spectral information enhances spectral-spatial pixel-wise HSC. For instance, Ran et al. [123] introduced spatial pixel pair features (PPF), emphasizing immediate neighborhood pairs with identical labels for enhanced discriminative power. Zhong et al. [124] proposed a Spectral-Spatial Residual Network (SSRN) utilizing 3D-CONVs in spectral and spatial residual blocks to extract joint representations. Paoletti et al. [125] presented a 3D CNN framework effectively capturing spectral-spatial relationships for improved classification accuracy. Li et al. [126] employed adaptive weight learning for dynamic adjustment of spatial information importance, capturing variations in spatial context. Roy et al. [127] proposed adaptively determined adjustable receptive fields, enhancing joint feature extraction in a spectral-spatial residual network. Additionally, Roy et al. [128] fused maximum and minimum CONVal features, reported to enhance classification performance in HSC tasks.

Paoletti et al. [129] addressed 3D CNN limitations in exploiting rotation equivariance by introducing translation-equivariant representations, enhancing spatial feature robustness in HSC tasks. Zhang et al. [130] proposed an end-to-end 3D lightweight CNN to counter overfitting and gradient vanishing challenges with limited labeled samples. Jia et al. [131] introduced spatial-spectral Schroedinger eigenmaps (SSSE) to balance numerous trainable parameters and scarce labeled samples. Roy et al. [132] incorporated a lightweight bag-of-feature paradigm into a spectral-spatial squeeze-and-excitation residual network. Roy et al. [133] introduced Morphological CNN (MorphCNN), combining spectral and spatial features for effective information utilization.

Li et al. [126] proposed a two-stage framework with adaptive learning of input patch weights in the first stage, extracting joint shallow features and obtaining deep hierarchical features through a Stacked Autoencoder (SAE) network. Classification is performed using a Multinomial Logistic Regression (MLR) layer. Li et al. [134] introduced a 3D-CNN model, comparing its performance with spectral-based Deep Belief Networks (DBN), SAE, and 2D-spatial CNNs. Roy et al. [135] presented a bilinear fusion mechanism combining global pooling and max-pooling branches. Jiao et al. [136] introduced a deep multiscale spectral-spatial feature extraction approach, learning discriminative features from spatially diverse images using a Fully CONVal Network (FCN). These spatial features are fused with spectral information using a weighted fusion strategy for accurate pixel-wise classification.

He et al. [137] use PCA-transformed images to generate multi-scale cubes, extracting handcrafted features with multi-scale covariance maps to capture spectral-spatial details. Zhang et al. [138] implement a dual-channel CNN framework, employing a 1D-CNN for spectral and a 2D-CNN for spatial hierarchical feature extraction, combining both for classification. He et al. [139] introduce a multiscale 3D deep CNN for end-to-end HSC, jointly learning 1D spectral and 2D multiscale spatial features without pre-processing like PCA. Dong et al. [140] embed a band attention module within a CNN to selectively focus on informative bands, reducing redundancy and noise in HSC. Cheng et al. [141] combine CNN with a metric learning-based framework, using CNN

for deep spatial information extraction and metric learning for spectral and spatial feature fusion. Gong et al. [142] merge a multi-scale CONV-based CNN with diversified deep metrics based on determinantal point process (DPP) priors [143], employing multi-scale filters and DPP-based diversified metrics for enhanced HSI representational ability.

Liu et al. [144] introduce an HSC framework for multi-scale spatial feature extraction, constructing a three-channel RGB image from HSIs to leverage existing networks. Selami et al. [145] present an adaptive band selection-based semi-supervised 3D CNN, jointly exploiting spectral-spatial features. Ma et al. [146] propose a two-branch Deep CNN, with one branch extracting spatial information and the other utilizing a contextual DNN for spectral features. Mei et al. [147] use a 3D CONV AE for unsupervised simultaneous exploitation of spectral-spatial features. Roy et al. [148] explore a dual-attention-based AE-decoder network for unsupervised HS band selection and joint feature extraction. Roy et al. [149] introduce a lightweight HetConv3D for HSC with noisy labels, combining spectral and spatial kernel features. Roy et al. [150] propose a hybrid 3D-2D CNN architecture for HSC, first extracting joint spectral-spatial features with a 3D-CNN and then capturing spatial contextual information with a 2D-CNN. Zhang et al. [151] use an adaptive MRF with a CNN to extract joint spectral-spatial features and refine classification results. Paoletti et al. [152] present a separable attention network dividing input feature maps for global contextual information encoding. Roy et al. [153] introduce G2C-Conv3D to combine intensity-level semantic information and gradient-level detailed information during CONV operations.

Advantages: Spectral-Spatial CNNs offer enhanced discriminative power by capturing detailed relationships between spectral bands and spatial patterns, enabling effective differentiation of land cover classes. These models incorporate spatial convolutional filters to grasp spatial contextual information, crucial for handling spatial structures and textures in hyperspectral classification. The fusion of spectral and spatial features in Spectral-Spatial CNNs takes advantage of the complementary nature of these dimensions, resulting in improved classification performance through the exploitation of unique information from both spectral and spatial components. **Limitations:** The computational complexity of Spectral-Spatial CNNs is elevated due to the 3D nature of hyperspectral data and the fusion of spectral and spatial information, demanding extensive computational resources for training and inference, particularly in the context of large-scale hyperspectral images. Additionally, the effectiveness of Spectral-Spatial CNNs relies on the availability of substantial labeled hyperspectral datasets that encompass diverse spectral and spatial characteristics. Acquiring such datasets is challenging and resource-intensive, involving expert annotation and data collection efforts. Despite these challenges, Spectral-Spatial CNNs present a potent approach for hyperspectral classification, offering enhanced discriminative capabilities, capturing spatial contextual information, and facilitating complementary feature fusion. Their potential for advancing hyperspectral classification is evident through promising results in diverse applications.

D. Graph Convolutional Networks for HSC

Graph Convolutional Networks (GCNs) have garnered attention for their adeptness in processing non-grid high-dimensional data and their adaptable network architecture [154]. These characteristics open up possibilities for efficient handling of hyperspectral (HS) data [155]–[164]. GCNs are particularly proficient in capturing relationships between data or samples, making them well-suited for modeling spatial relationships among spectral signatures in hyperspectral images (HSIs), as depicted in Figure 9. However, the construction of large graphs poses challenges due to computational demands, limiting the popularity of GCNs in hyperspectral classification (HSC) compared to Convolutional Neural Networks (CNNs). Despite this, exploratory studies have begun to leverage GCNs in certain HSC tasks [165].

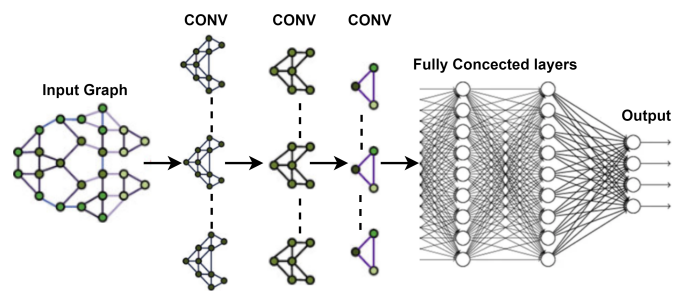


Fig. 9: Basic example of Graph Convolutional Neural Network.

Here are some details on how GCNs can be used for HSC: In HSIs, the graph representation assigns each pixel as a node, utilizing the spectral signatures as node features. The construction of the graph involves connecting neighboring pixels based on spatial proximity, with the edges denoting spatial relationships between pixels. The fundamental component of GCNs is the graph CONV layer, facilitating information propagation and aggregation across the graph. In each layer, node features are updated by aggregating information from neighboring nodes, employing a CONV operation that considers both node features and edge connections. Graph pooling operations can be applied to handle the high-dimensional nature of HS data, reducing spatial resolution while retaining essential information. These pooling operations aggregate nodes based on importance or connectivity, resulting in a coarser graph representation. To further enhance GCNs, graph attention mechanisms can be integrated to weigh the importance of neighboring nodes during information aggregation, enabling adaptive attention to nodes based on their significance in the classification task.

By incorporating graph structures and spatial relationships, Graph Convolutional Networks (GCNs) provide a robust framework for hyperspectral image classification (HSC), capturing intricate interactions between spectral signatures and leveraging spatial context for improved accuracy. Despite their potential, it is crucial to address computational complexities and scalability issues with large hyperspectral datasets. Researchers have proposed strategies to mitigate these challenges. For instance, a second-order GCN in [166] models spatial-

spectral relations on manifolds to reduce computational costs, while [167] utilizes superpixel segmentation to enhance GCN efficiency in handling larger pixel sets for land cover classification. However, fundamental issues persist. Hong et al. proposed miniGCN in [165], training GCNs in a mini-batch fashion akin to CNNs, effectively reducing computational costs and enabling quantitative comparisons and fusion with CNNs, leading to the development of FuNet for HSC.

Transfer learning is a valuable technique for GCNs in HSC. By pre-training a GCN on a large or related dataset, it captures generic spatial patterns, and fine-tuning on the target HSC task with a smaller labeled dataset enhances performance, especially when labeled HS data is limited. Moreover, integrating GCNs with other deep learning models, such as CNNs, proves effective. A two-stream architecture can be employed, where one stream utilizes GCNs for spectral information, and the other employs CNNs for spatial information. The fusion of outputs from both streams contributes to the final classification decision, leveraging the complementary strengths of the two models.

E. Future Research Directions

While CNNs have demonstrated impressive performance in HSC, integrating spatial and spectral information poses a challenge. Existing frameworks often sacrifice spectral details in pursuit of enhanced spectral-spatial representation through DR techniques. Future research should prioritize the development of robust HSC models that effectively integrate spatial and spectral information without compromising spectral details. However, such approaches increase computational complexity, demanding efficient solutions for real-time deployment on resource-constrained platforms. Utilizing parallel processing techniques with Field-Programmable Gate Arrays (FPGAs) and Graphics Processing Units (GPUs) can address these challenges, ensuring both computational efficiency and performance accuracy.

In addition to computational concerns, the depth of CNNs requires abundant labeled training data, which is limited in HSI. To overcome this, integrating CNNs with unsupervised or semi-supervised learning approaches is crucial. Leveraging unlabeled or partially labeled data enhances the training process, improving classification performance. Furthermore, the generalization ability of CNNs needs exploration beyond traditional grid structures. Investigating their applicability to diverse data formats can be addressed by combining CNNs with GCNs, creating a versatile and generalized framework. This integration allows the capture of spatial relationships in non-grid data, contributing to a more adaptable HSC approach. Overcoming challenges related to data availability, generalization, and incorporating GCNs will advance CNNs for HSC, unlocking their full potential for efficient and accurate classification tasks. Ongoing research in these areas is essential for further advancements in the field.

VII. DEEP BELIEF NETWORK FOR HSC

Introduced by Hinton et al. in 2006 [168], the Deep Belief Network (DBN) is a hierarchical Deep Neural Network

(DNN) that utilizes unsupervised learning to sequentially learn features from input data as shown in Figure 10. Constructed with multiple layers using Restricted Boltzmann Machines (RBMs), RBMs are two-layer neural networks where visible units connect to hidden units [169]. RBMs play a crucial role in extracting informative features from input data, forming a layer-by-layer architecture in DBNs. This hierarchical structure enables greedy training, with each RBM capturing progressively abstract features from HS data.

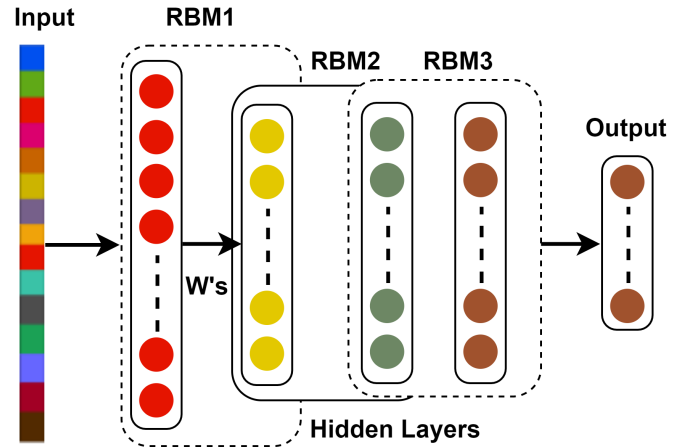


Fig. 10: Basic example of three layered Deep Belief Network for HSC.

Widely applied in HSC, DBNs, such as in Ayhan et al.'s work [170], have been utilized for land cover classification, emphasizing the integration of spectral and spatial information. The typical training process involves unsupervised pre-training with unlabeled samples, followed by supervised fine-tuning using labeled samples. However, this approach may lead to co-adaptation issues among hidden units and activation neuron sparsity, limiting the diversity of learned features. Addressing these challenges [171], [172], Zhong et al. proposed a diversified DBN model [173]. This model introduces a regularization technique during both pre-training and fine-tuning stages, promoting diversity among hidden units and activation neurons. By mitigating co-adaptation and enhancing activation selectivity, the diversified DBN model provides a potential solution to improve DBN classification performance in HSC, enhancing representation power and discriminative capabilities.

In HSC, researchers have introduced diverse strategies for efficient texture feature extraction. Li et al. proposed a DBN-based texture feature enhancement framework [174], incorporating band grouping, sample band selection, and guided filter techniques to improve texture features. Another approach by Tan et al. implemented a parallel layers framework [175], using a Gaussian-Bernoulli RBM for high-level, local invariant, and nonlinear feature extraction, followed by a logistic regression layer for classification. Both methods utilize DBN-based frameworks and parallel layers architectures to enhance texture features, emphasizing the importance of effective feature extraction for accurate HSC.

To improve classification accuracy, studies have focused on

integrating spectral and spatial information [174]. Li et al. presented a DBN framework with a logistic regression layer, showcasing that joint exploitation of spectral-spatial features enhances accuracy [176]. Similarly, Sellami et al. proposed a spectral-spatial graph-based RBM method [177], constructing a spectral-spatial graph to measure similarity based on both spectral and spatial details. The RBM extracted joint spectral-spatial features, contributing to improved classification performance when integrated into a DBN and logistic regression layer. These approaches highlight the significance of considering both spectral and spatial information for effective HSC.

The above discussion highlighted the limited use of DBNs in HSC compared to other DNNs, emphasizing the need for robust techniques integrating spatial and spectral features. A promising avenue for research involves refining the pre-training and fine-tuning processes in DBNs to address issues like inactive or over-tolerant neurons. Improving the training process can enhance performance and generalization in HSC applications. Further advancements in HSC should explore DBN-based approaches that efficiently combine spatial and spectral features while focusing on regularization techniques to overcome challenges related to neuron activity. These efforts can contribute to more effective and resilient DBN-based methods for accurate HSC.

VIII. RECURRENT NEURAL NETWORKS FOR HSC

RNNs, featuring loop connections that link current and previous steps, excel in learning from temporal sequences [178]. In the context of HS data, RNNs treat spectral bands as sequential time steps, providing a temporal processing advantage [179]. Three fundamental RNN models include Vanilla, LSTM, and GRU (Figure 11), each offering distinct strategies to address challenges related to learning and capturing long-term dependencies in sequential data. While Vanilla RNNs are straightforward, they may struggle with extended sequences, prompting the use of LSTM and GRU models designed to mitigate the vanishing gradient problem and handle long-term dependencies more effectively. Leveraging the temporal aspects of RNNs for sequential processing in HSI data allows researchers to harness their power in capturing and modeling temporal dynamics.

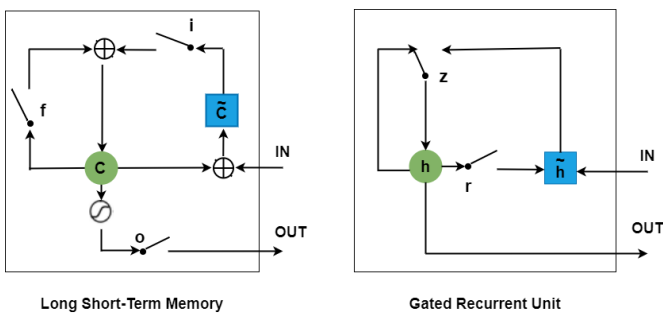


Fig. 11: Internal architecture of LSTM and GRU [1]

Vanilla RNN, the simplest RNN form, can face information degradation issues, impacting its performance with high-dimensional data like HSI due to the vanishing/exploding

gradient problem. LSTM models, developed to tackle this, introduce cell and hidden states along with input, forget, and output gates, enabling selective information control. LSTM excels at capturing and retaining relevant information over long sequences, addressing the temporal dependencies in data. GRU, a variant simplifying LSTM by combining gates, offers comparable performance while being computationally efficient. Vanilla RNNs suffer from information degradation, LSTM mitigates it with gates, and GRU provides a simpler alternative while maintaining high performance.

Hang et al. [180] proposed an RNN framework using the novel parametric rectified tanh activation function and GRU for sequential HS data analysis. Zhang et al. [56] introduced an RNN-based local spatial sequential (LSS) method, fusing Gabor filters and differential morphological profiles for low-level feature extraction, followed by RNN modeling for high-level feature extraction. Zhou et al. [181] employed separate LSTM networks for spectral and spatial features, combining their outputs using a decision fusion strategy. Sharma et al. [182] utilized LSTM cells for multi-temporal and multi-spectral information, capturing complex patterns and dependencies in HSI for effective land cover classification.

Wu et al. [111] introduced a CONV RNN model for HSC, using initial CONV layers to extract position-invariant middle-level features and recurrent layers to capture spectral-contextual details. In a semi-supervised setting, Wu et al. [183] applied a similar CRNN model, incorporating pseudo-labels for leveraging unlabeled data. Zhou et al. [184] proposed an integrated CNN and GRU-based fusion network, where CNN extracts spatial features and GRU performs both feature-level and decision-level fusion. Luo et al. [185] introduced a CNN-parallel GRU-based RNN architecture, simplifying GRU training and enhancing performance by combining it with the CNN component. Liu et al. [186] presented the Bidirectional CLSTM model, jointly exploiting spectral-spatial features of HSI. Shi et al. [187] combined multiscale local spectral-spatial features from a 3D CNN with a hierarchical RNN. Yang et al. [188] proposed recurrent 2D CNN and 3D CNN models for HSC. Seydgar et al. [189] integrated CNN with CLSTM in a cascaded architecture, using a 3D CNN for low-level features and CLSTM for higher-level features. Hang et al. [180] introduced a cascade RNN architecture with two layers of GRU-based RNNs, reducing redundant spectral bands in the first layer and learning features in the second layer.

The aforementioned discussion explored recent advances in RNN-based techniques for HSC, acknowledging their notable success in classification performance. However, challenges exist, particularly in handling lengthy input sequences that may lead to overfitting. Addressing this, future research should explore strategies to reduce input sequence length, preserving spectral and spatial information. Additionally, investigating parallel processing tools can enhance computational efficiency, and alternative approaches like spectral band grouping merit exploration for improved discrimination. Another promising direction involves extending RNN-based HSC frameworks to multi-temporal HS imagery, enabling models to capture dynamic changes over time for more accurate and robust results. These efforts will not only overcome challenges but

also enhance the practical utility of RNN-based models in real-world scenarios and contribute to advancements in RS applications.

IX. AUTOENCODERS FOR HSC

The Autoencoder (AE) is a widely adopted symmetric neural network in HSC for unsupervised feature learning. It prioritizes generating a compressed feature representation of high-dimensional HS data instead of direct classification. The AE architecture typically includes an input layer, a hidden or encoding layer, a reconstruction or decoding layer, and an output layer as shown in Figure 12. During training, the AE learns to encode input data into a latent representation that accurately reconstructs the original input. This is achieved by minimizing the reconstruction error, measuring the difference between the input and output, enabling effective learning of a compressed feature representation.

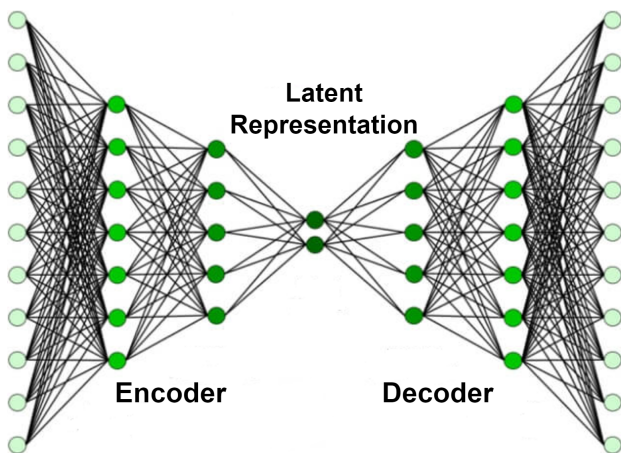


Fig. 12: Autoencoder architecture.

The AE is designed to extract essential features from input data, discarding irrelevant information through unsupervised learning. This process yields compact representations, beneficial for tasks like classification in HSC. The Stacked AE (SAE) extends this architecture, stacking multiple AE layers to learn increasingly abstract features. The Denoising AE (DAE), another variant, intentionally corrupts input data with noise, forcing the model to reconstruct the original signal. This enhances the DAE's ability to handle noisy input, making it useful in scenarios with data corruption. Overall, the AE, SAE, and DAE are powerful tools in HSC for learning compressed, abstract features and handling noisy input.

In Zhu et al.'s [190] approach, multi-layer AEs with maximum noise fraction were combined to learn high-level representations from HS data. Hassanzadeh et al. [191] employed a multi-manifold learning framework combined with the Counteractive AE for unsupervised HS classification. Zhang et al. [192] proposed a framework utilizing a Recursive AE (RAE) network to jointly exploit spectral-spatial features, focusing on recursive feature extraction from neighboring pixels based on spectral similarity. Hao et al. [193] introduced a two-stream DNN with a class-specific fusion scheme, incorporating a SAE for spectral features and a CNN for spatial information.

Sun et al.'s architecture [194] integrated PCA, guided filters, and sparse AEs with batch-based training to fuse spectral and spatial information. In Zhao et al.'s framework [195], an HSC approach involved selecting spatial resolution from HSIs and utilizing stacked sparse AEs for high-level feature extraction, with classification performed using Random Forest. The hybrid architectures in Sun et al. [194] and Zhao et al. [195] effectively combined PCA, guided filters, and sparse AEs for feature extraction in both spectral and spatial domains.

Wan et al. [196] employed SAEs to extract diverse representations, including spectral-spatial features and multi-fractal features, alongside higher-order statistical representations. Lv et al. [197] proposed a combination of SAEs and Extreme Learning Machines (ELMs), where features were segmented, transformed using SAEs, and rearranged for input to an ELM-based classifier. Ahmad et al. [36] introduced a computationally efficient multi-layer ELM-based AE for HSC, aiming to enhance feature learning efficiency and effectiveness. Zhou et al. [198] addressed intra-class variability and inter-class similarity challenges in HSC by incorporating a local Fisher discriminant regularization technique for learning compact and discriminative features. Lan et al. [199] combined a k-sparse denoising AE with spectral-restricted spatial features to handle high intra-class variability in spatial features. Paul et al. [200] segmented spectral components in HSI based on mutual information measure, reducing computation time during feature extraction using SAE and incorporating spatial information with Empirical Mode Decomposition (EMD). Liu et al. [201] utilized an SAE-based approach for classifying oil slicks on the sea surface, jointly exploiting spectral-spatial features to improve accuracy.

The above discussion explored recent advancements in AE-based techniques for HSC. While these approaches demonstrate strong predictive performance and generalization, there remains a need for more sophisticated methods. Many discussed techniques underutilize spatial information in HSIs, prompting further research to effectively harness joint spatial and spectral information for improved HSC. Moreover, challenges such as high intra-class variability and inter-class similarity persist in HSC, impacting classification accuracy. While some reviewed methods address these issues, additional research is crucial. Exploring strategies like pre-training, co-training, and adaptive neural networks within AE-based frameworks could offer promising solutions to enhance accuracy and robustness. In summary, the development of innovative approaches, including pre-training, co-training, and adaptive neural networks, holds potential to advance AE-based HSC frameworks.

X. LIMITATIONS OF TRADITIONAL DEEP LEARNING

Applying DL to HSC faces challenges arising from the unique characteristics of Hyperspectral Imaging (HSI). These challenges include a large number of narrow spectral bands, high spectral resolution, low spatial resolution, and limited labeled training data. The curse of dimensionality, exacerbated in high-dimensional data scenarios, impacts classification performance, particularly when labeled data is insufficient. The

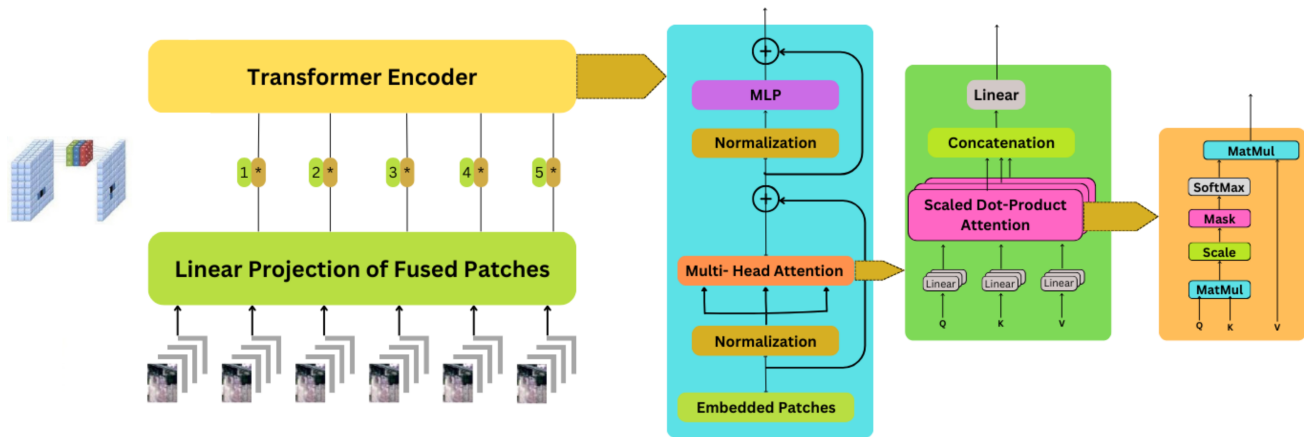


Fig. 13: Spatial-Spectral Transformer architecture.

Hughes phenomena, associated with small labeled datasets, can lead to overfitting and poor generalization. Scarcity of labeled HS data, a time-consuming and expensive task, hampers model training. Addressing these challenges requires strategies like feature selection, dimensionality reduction, and augmenting training data through unsupervised or semi-supervised learning. Efficient labeling methods can enhance dataset availability. High intra-class variability, instrumental noise, redundant spectral bands, and spectral mixing further complicate HSC. Researchers are exploring techniques involving domain knowledge, denoising algorithms, feature extraction, and spatial-spectral fusion to tackle these challenges, improving the robustness and accuracy of HSC models. Following are some main challenges that come across when DL is applied to HSC:

Complex Training: Training deep models for hyperspectral analysis, belonging to the NP-complete problem class, poses challenges in convergence, especially with a large number of parameters [29], [202]. Optimization techniques like SGD, SGDM, RMSProp, Adam, AdamW, diffGrad, RAdam, gradient centralization, and AngularGrad have addressed this, enhancing training efficiency and convergence for hyperspectral analysis [203]–[211]. **Model Interpretability:** The interpretability of DNNs remains challenging due to their black-box nature. Despite efforts to enhance interpretability, DNNs are inherently complex, impacting understanding and decision-making during optimization. **Limited Training Data:** Supervised deep models in hyperspectral imaging (HSI) face challenges due to limited labeled data, risking overfitting, known as the Hughes phenomena [212]. The high dimensionality of HSI exacerbates this challenge, requiring careful adjustments during training [72]. **High Computational Burden:** DNNs handling large datasets encounter challenges in memory, computation, and storage. Advances in parallel and distributed architectures, along with high-performance computing, enable efficient processing of large datasets in hyperspectral imaging [213]–[216]. **Training Accuracy Degradation:** The assumption that deeper networks yield higher accuracy is not always valid. Deeper networks may face challenges like the exploding or vanishing gradient problem, adversely affecting convergence [217], [218]. By mitigating these artifacts and

advancing robust techniques, researchers can enhance the reliability and accuracy of HSC, facilitating applications in remote sensing, agriculture, and environmental monitoring.

XI. TRANSFORMERS FOR HSC

The Transformer architecture, introduced by Vaswani et al. [219] in 2017, has emerged as a powerful DL model for various tasks, such as machine translation, language understanding, text generation, etc. Unlike traditional RNNs or CNNs, the Transformer architecture relies on a self-attention mechanism to capture dependencies between different elements in a sequence, enabling it to effectively model long-range dependencies. This self-attention mechanism allows the model to attend to different parts of the input sequence to build contextualized representations. The Transformer architecture has also found applications in the field of HSC as shown in Figure 13. HSC involves the classification of each pixel in an HSI into different land cover or material classes [11]. The Transformer architecture offers several advantages in this context:

- 1) **Capturing Spectral-Spatial Dependencies:** The Transformer architecture can effectively capture dependencies between spectral bands and spatial locations in HSIs. By attending to both the spectral and spatial dimensions, the model can learn to extract discriminative features that leverage the rich information present in HS data [220].
- 2) **Handling Long-Range Dependencies:** HSIs typically exhibit long-range dependencies, where the spectral characteristics of a pixel may depend on distant pixels in both spectral and spatial dimensions [221]. The self-attention mechanism in the Transformer architecture allows the model to capture these long-range dependencies, enabling it to model complex relationships between pixels and make more accurate predictions [163].
- 3) **Contextualized Representation Learning:** The Transformer architecture can generate contextualized representations for each pixel in an HSI. By considering the entire image context, the model can learn to encode information about neighboring pixels and their classes, leading to improved classification accuracy.

4) **Interpretability:** The attention mechanism in the Transformer architecture provides interpretability by highlighting the relevant spectral and spatial features that contribute to the classification decision [222]. This can help in understanding the reasoning process of the model and identifying important features for classification.

In recent studies, researchers have explored different variations of the Transformer architecture for HSC [2], [223]–[245], including adaptations like the HS Transformer Network and the Spectral Transformer Network [234]. These models have shown promising results in HSC tasks, achieving competitive performance compared to traditional approaches like CNNs and RNNs. Overall, the Transformer architecture offers a powerful and flexible framework for HSC. Its ability to capture spectral-spatial dependencies, handle long-range dependencies, and generate contextualized representations makes it a promising approach for extracting discriminative features from HS data and improving classification accuracy.

The Swin Transformer (ST) showcases significant strengths, primarily deriving from its hierarchical attention mechanism, which enables the model to efficiently capture information across different scales, analyzing both local and global features [246]–[248]. Furthermore, the utilization of windowing-based processing enhances the scalability of STs in contrast to traditional transformers, facilitating the effective handling of large images with reduced computational complexity [249]. The adaptability of the architecture to diverse tasks makes STs suitable for various applications [250]. In the domain of HSC, STs have demonstrated SOTA performance, outperforming traditional transformers and CNNs in specific scenarios, underscoring their efficacy for HSC tasks [251], [252]. However, despite these achievements, STs have limitations. While excelling in capturing spatial relationships, they may encounter challenges in dealing with sequential data, rendering tasks reliant on spectral dependencies less optimal for them [253]. Additionally, the hierarchical attention mechanism introduces added complexity. Training large ST models necessitates substantial computational resources, posing challenges for researchers with limited access to high-performance computing. Moreover, akin to other deep models, the interpretability of STs raises concerns, particularly in complex tasks like HSIC, necessitating ongoing research to understand their decision-making processes [248].

Likewise, the vision and spatial-spectral transformers (SSTs) stand out in their ability to capture global contextual information [254]–[261]. The self-attention mechanism enables the model to consider relationships between all HSI regions simultaneously, providing a comprehensive understanding of the visual context [262]. Unlike CNNs, SSTs demonstrate robust scalability to high-resolution HISs, effectively processing large HSI datasets without the need for complex pooling operations. This versatility has led to successful applications of SSTs in HSC, and their adaptable architecture contributes to their broad applicability. Moreover, SSTs reduce reliance on handcrafted features by directly learning hierarchical representations from raw pixel values [234], simplifying the model-building process and often yielding improved performance. Additionally, the attention maps generated by SSTs offer insights into the

model’s decision-making process, enhancing interpretability by highlighting the image regions most influential in specific predictions [263].

Despite the accomplishments of SSTs, they do come with certain limitations. Notably, training large SSTs can pose significant computational challenges, particularly as the model size increases [221], [264]. The self-attention mechanism introduces quadratic complexity with respect to sequence length, potentially impeding scalability [265]. Unlike CNNs, which inherently possess translation invariance through shared weight convolutional filters, SSTs may struggle to capture spatial relationships that remain invariant to small translations in the input [266]. Moreover, SSTs rely on dividing input images into fixed-size patches during the tokenization process, which may not efficiently capture fine-grained details [267], [268]. The quadratic scaling of self-attention poses challenges, particularly when dealing with long sequences. Additionally, achieving optimal performance with SSTs often requires substantial amounts of training data. Attempting to train these models on smaller datasets may lead to overfitting, thus limiting their effectiveness in scenarios with limited labeled data [11].

Considering these limitations, various potential solutions have been proposed in the literature, including the integration of SSTs with other architectures. For instance, a hybrid model could leverage the strengths of both approaches by combining the global context understanding of SSTs with the local feature extraction capabilities of CNNs [4], [269]. However, a potential drawback of hybrid transformers is the increased complexity in model architecture. Integrating different transformer variants or combining transformers with other architectures might introduce additional intricacy, rendering the model more challenging to interpret and potentially demanding more computational resources for training and inference.

Moreover, there exists a realm for exploration in fine-tuning the attention mechanism, where endeavors concentrate on sparse attention patterns or alternative attention mechanisms aimed at tackling the computational complexity challenges [257], [270], [271]. Capturing long-range dependencies and integrating global and local features in transformers entails the challenge of finding a delicate equilibrium between model complexity and computational efficiency. Although optimizing attention patterns can elevate performance, it may concurrently heighten computational requirements, rendering the model more demanding on resources and possibly constraining its utility in scenarios with limited resources.

Expanding the capabilities of SSTs to accommodate multi-modal inputs emerges as a promising avenue for further research [272]. This extension has the potential to widen their applicability and augment their ability to comprehend intricate relationships within diverse data types [273]–[275]. However, integrating information from various modalities necessitates thoughtful consideration of feature representations and alignment. The model might encounter difficulties in effectively learning meaningful cross-modal relationships, and crafting architectures capable of efficiently fusing and processing diverse data sources remains an ongoing research challenge. Additionally, gathering and annotating large-scale multi-modal datasets for training can be resource-intensive. Lastly, developing effi-

cient tokenization strategies is crucial, aiming to capture fine-grained details while alleviating the quadratic scaling issue. Such strategies could significantly boost the performance of SSTs in tasks requiring high spatial resolution. In summary, while both ST and SST are transformer-based architectures tailored for image classification tasks, they diverge in their approach to handling image data. Here are some of the major differences between ST and SST:

Image Patch Processing: ST adopts a hierarchical structure by initially dividing the image into non-overlapping patches. It then processes these patches hierarchically using a window-based self-attention mechanism, efficiently capturing both local and global context. In contrast, SST divides the input image into fixed-size non-overlapping patches, linearly embeds each patch, and subsequently flattens the 2D spatial information into a 1D sequence for input into the transformer.

Hierarchical Self-Attention: ST introduces a shifted window-based self-attention mechanism, where instead of attending to all positions equally, it employs local self-attention windows that slide across the sequence hierarchically. This approach enables the model to effectively capture both local and long-range dependencies. On the other hand, SST utilizes a single self-attention mechanism across the entire sequence of patches.

Positional Encoding: In ST, shifted windows in self-attention are utilized, eliminating the need for explicit positional embeddings. The local windows implicitly encode positional relationships. Conversely, SST relies on positional embeddings to furnish the model with information regarding the spatial arrangement of patches.

The transformer-based models as compared to the traditional DL models for HSC are a nuanced exploration that delves into the strengths and weaknesses of each approach. HSC is a critical task in remote sensing, where the goal is to assign each pixel in an image to a specific land cover class based on the spectral information acquired across numerous bands. Traditional DL models, especially CNNs, have been the workhorse for HSC. CNNs are adept at learning hierarchical spatial features from the data, enabling them to capture intricate patterns and relationships. However, HS data introduces unique challenges due to the high dimensionality of the spectral information. Traditional models may struggle to effectively handle the complex interactions between different spectral bands and to capture long-range dependencies. Whereas, transformer-based models were originally designed for natural language processing tasks. Transformers, with their attention mechanism, can capture global dependencies and model interactions between distant spectral bands effectively. This mechanism allows the model to assign varying levels of importance to different parts of the HS spectrum, enabling more nuanced feature learning.

One of the primary advantages of transformer-based models in HSC lies in their capacity to handle long-range dependencies. The self-attention mechanism allows the model to weigh the importance of different spectral bands dynamically, facilitating the learning of complex spectral-spatial relationships. This can be particularly beneficial in scenarios where understanding the interactions between distant bands is crucial for

accurate classification. However, the success of transformer-based models in HSC is contingent on several factors. One significant consideration is the amount of available training data. Transformers often require large datasets to generalize well, and HS data can be inherently limited due to acquisition costs and data availability. Conventional DL models may still perform admirably when faced with smaller datasets.

Computational resources also play a role in this comparison. Transformer-based models, with their self-attention mechanisms, are computationally more demanding compared to traditional CNNs. The feasibility of deploying transformer-based models may be restricted by the available hardware and processing capabilities. Moreover, the complexity of the classification task influences the performance of these models. In cases where the spectral patterns are relatively simple, traditional models may achieve satisfactory results without the need for the more complex architecture of transformers. In short, the comparison of transformer-based models with traditional DL models for HSC is a multifaceted analysis. While transformer-based models hold promise in capturing global dependencies and intricate spectral-spatial relationships, their effectiveness depends on factors such as data size, computational resources, and the complexity of the classification task. Conventional DL models continue to be valuable and efficient, especially in scenarios with limited data and less intricate spectral patterns. The choice between these approaches should be made judiciously, considering the specific characteristics of the HS data and the goals of the classification task.

A. Benefits and Challenges of Transformers in HS Analysis

The application of transformers in HSI analysis introduces a range of benefits and challenges, reflecting the unique characteristics of HS data and the capabilities of transformer-based architectures. Here we first discuss the Benefits of transformers for HSI analysis, later the drawbacks will be portrayed.

Global Contextual Understanding: Transformers excel at capturing global dependencies and long-range interactions within data. In HSI analysis, this ability is crucial for understanding the complex relationships between different spectral bands. Transformers can consider the entire spectrum simultaneously, allowing for a more comprehensive contextual understanding of the HS scene. **Adaptive Feature Learning:** The attention mechanism in transformers enables adaptive feature learning, allowing the model to assign varying levels of importance to different spectral bands. This adaptability is particularly valuable in HS data, where certain bands may contain more discriminative information for specific classes or features. Transformers can dynamically focus on relevant bands, enhancing their ability to extract meaningful features. **Efficient Handling of Spectral-Spatial Information:** Transformers are well-suited for capturing spectral-spatial interactions in HSIs. The self-attention mechanism facilitates the modeling of relationships between distant pixels, enabling the identification of intricate patterns and structures. This is especially beneficial in scenarios where spatial context is essential for accurate classification. **Transferability Across**

Tasks: Pre-trained transformer models on large datasets for general computer vision tasks can be fine-tuned for HSI analysis. The transferability of pre-trained models reduces the need for extensive HS-specific training data and can lead to improved performance in scenarios with limited labeled examples.

While transformers offer several benefits for HS analysis, there are also some challenges associated with their use. For instance: **Computational Demands:** Transformers are computationally more demanding than conventional DL models, such as CNNs, RNN, AEs, etc. The self-attention mechanism involves processing interactions between all pairs of pixels, leading to a quadratic increase in computational complexity with the size of the input. This can pose challenges in terms of training time and hardware requirements, particularly for large HSIs. **Limited Data Availability:** HS datasets are often limited in size due to the high cost and complexity of data acquisition. Transformers, known for their data-hungry nature, may struggle to generalize effectively when faced with insufficient training samples. This limitation could lead to overfitting or suboptimal performance, especially in the absence of extensive HS-specific pre-training data. **Model Interpretability:** Transformers, being complex models with numerous parameters, might lack interpretability compared to simpler models. Understanding how the model arrives at specific classification decisions in HSI analysis is essential, especially in applications where interpretability is critical, such as in scientific research or decision-making processes. **Hyperparameter Sensitivity:** Transformers often involve a large number of hyperparameters, and their performance can be sensitive to these choices. Fine-tuning the hyperparameters for optimal performance on HS data may require extensive experimentation, and the optimal configuration might vary depending on the specific characteristics of the dataset.

In short, the use of transformers in HSI analysis brings notable advantages in terms of global contextual understanding, adaptive feature learning, and efficient handling of spectral-spatial information. However, challenges related to computational demands, limited data availability, model interpretability, and hyperparameter sensitivity must be carefully addressed to harness the full potential of transformer-based architectures in HS applications. Researchers and practitioners need to strike a balance between the benefits and challenges, considering the specific requirements and constraints of their HSI analysis tasks.

B. Emerging Trends and Advancements

As HS technology continues to evolve, several emerging trends and advancements in HSC have garnered attention within the RS and image-processing communities. These trends reflect ongoing efforts to enhance the accuracy, efficiency, and applicability of HS data analysis. The integration of DL and transformer-based models has revolutionized HSC. DL architectures excel at automatically learning hierarchical and complex features from HS data, improving classification accuracy. Transformers, with their ability to capture global dependencies, are being explored to address challenges related

to long-range spectral interactions. In the recent past, several trends have emerged, aiming to enhance the overall generalization performance of DL models, and a few of them are enlisted in the following.

1) **Domain Adaptation and Transfer Learning:** With the limited availability of labeled HS datasets, domain adaptation, and transfer learning have emerged as key strategies to leverage pre-trained models from other domains or modalities. This approach aids in addressing the data scarcity issue by transferring knowledge learned from one dataset to another, enhancing classification performance even with limited labeled HS samples. Depending on the presence of labeled training instances, transfer learning frameworks can be classified into supervised or unsupervised transfer learning. Typically, it is assumed that both the source and target domains are related but not identical. In scenarios like HSC, where the categories of interest are consistent but data in the two domains may differ due to distinct acquisition circumstances, the distributions may not be the same.

In DNN-based HSC, the model undergoes hierarchical feature learning, with lower layers typically extracting generic features when trained on diverse images. Consequently, the features acquired by these lower layers can be transferred to train a new classifier for the target dataset. For example, Yang et al. [276] employed a two-branch spectral-spatial CNN model, initially trained on a substantial amount of data from other HSIs. The lower layers of this pre-trained model were then applied to the target network, ensuring robust classification of the target HSI. To capture target-specific features, the higher layers of the target network were randomly initialized, and the entire network underwent fine-tuning using limited labeled instances from the target HSI. Similarly, Windrim et al. [277] introduced an effective method for pre-training and fine-tuning a CNN network, making it adaptable for the classification of new HSIs. The study conducted by Liu et al. [278] incorporated both data augmentation and transfer learning approaches to address the shortage of training data, aiming to enhance the performance of HSC.

As discussed above, data in the source and target domains may differ in various aspects. For instance, in the context of HSIs, the dimensions of two HSIs may vary due to acquisition from different sensors. Addressing such cross-domain variations and facilitating knowledge transfer between them is referred to as heterogeneous transfer learning, and a comprehensive survey of such methods can be found in [279]. Within the literature on HSC, numerous studies have been put forth to bridge the gap and transfer knowledge between two HSIs with varying dimensions and/or distributions. For instance, an effective framework for HSC based on heterogeneous transfer learning was introduced by Lin et al. [280]. This framework demonstrates efficacy with both homogeneous and heterogeneous HSIs. Another approach, proposed by Li et al. [281], utilizes an iterative re-weighting mechanism within a heterogeneous transfer learning framework for HSC. Similarly, a work by Liu et al. [282] advocates a band selection-based transfer learning approach to pre-train a CNN, maintaining a consistent number of dimensions across various HSIs. Additionally, Lin et al. put forward an unsupervised transfer

learning technique designed to classify entirely unknown target HSIs. Furthermore, Pires et al. [283] demonstrate that networks trained on natural images can enhance the performance of transfer learning for RS data classification compared to networks trained from scratch using smaller HS datasets.

2) **Data Augmentation:** is a proven and effective technique in HSC to address the challenge of limited training samples. It involves generating new samples from the original training data without the need for additional labeling costs. Data augmentation approaches can be broadly categorized into two main strategies: **Data Wrapping:** This strategy focuses on encoding invariances such as translational, size, viewpoint, and illumination variations by applying geometric and color-based transformations while preserving the original labels. These transformations help create new samples that exhibit similar characteristics to the original data but with variations that can improve the model's robustness and generalization. Examples of data wrapping techniques include geometric transformations like rotation, scaling, and flipping, as well as color-based transformations like brightness and contrast adjustments. **Oversampling:** Oversampling-based augmentation methods aim to inflate the training data by generating synthetic samples based on the original data distribution [284]. These techniques help address class imbalance issues and provide the model with a more balanced representation of different classes. Oversampling techniques include mixture-based instance generation, where new samples are created by blending existing samples from the same class, and feature space augmentations, where new samples are generated by perturbing the feature vectors of existing samples.

In the realm of HSC literature, various frameworks utilizing data augmentation techniques have been implemented to enhance classification performance and mitigate potential overfitting issues, often stemming from limited training data availability. For example, Yu et al. [285] improved training data by applying three augmentation operations (flip, rotate, and translation), leveraging this augmented dataset to train CNN for HSC. Li et al. [286] conducted a thorough comparison of commonly used HS data augmentation techniques, proposing a pixel-block pair-based approach that integrates both spectral and spatial information to synthesize new instances for training CNN models in HSC. The study by Cao et al. [287] assessed the classification performance of a combination of CNN and Active Learning, both with and without data augmentation techniques, demonstrating higher accuracy when employing data augmentation. Similarly, in another comparative study [288], a data augmentation-based CNN exhibited a 10% increase in HSC accuracy compared to a PCA-based CNN model.

The aforementioned approaches employ offline data augmentation methods, which involve increasing the training data by generating new instances during or before the model training process. A recent innovative data augmentation framework for HSI is introduced in [289]. In contrast to expanding the training data, this framework generates samples at test time. A DNN trained on the original training data, coupled with a voting scheme, is utilized to determine the final class label. To enhance the generalization capability of DNN models, [289]

also puts forth two rapid data augmentation techniques for high-quality data synthesis. Additionally, a similar online data augmentation strategy based on PCA is proposed in [290]. This strategy synthesizes new instances during the inference phase rather than during the training phase.

3) **Generative Adversarial Networks:** The Generative Adversarial Network (GAN), introduced by Goodfellow et al. [291], consists of two neural networks: a generator and a discriminator. GANs can learn and replicate samples by leveraging intricate details within the data distribution. In the context of Semi-Supervised Learning-based HSC, Zhan et al. [292] presented a GAN approach that relies on spectral features. In a similar vein, He et al. [293] introduced a GAN-based framework for spectral-spatial HSC. Likewise, Zhu et al. [294] devised 1D-GAN and 3D-GAN architectures, based on CNN, aimed at enhancing classification performance. Zhan et al. [295] employed a customized 1D-GAN to generate spectral features, utilized by a CNN for subsequent feature extraction, and concluded the process with majority voting in HSC. Recently, Feng et al. [296] presented a Spatial-Spectral Multi-Class GAN (MSGAN) employing two generators to produce spatial and spectral information through multiple adversarial objectives. In addressing data imbalance issues for HSC, Zhong et al. [297] proposed a semi-supervised model combining GAN with Conditional Random Fields (CRFs).

Similarly, Wang et al. [298] explored the Caps-TripleGAN model, which efficiently generates new samples through a 1D structure Triple GAN (TripleGAN) and classifies the generated HSI samples using the capsule network (CapsNet). Additionally, Xue et al. [299] suggested the adoption of a 3D CNN-based generator network and a 3D deep residual network-based discriminator network for HSC. To learn high-level contextual features, the combination of a capsule network and a Convolutional LSTM (ConvLSTM) based discriminator model was introduced by Wang et al. [300] in the context of HSC. The study conducted by Alipour et al. [301] aimed to overcome the limitation of scarce training examples by employing a GAN model. In this approach, the discriminator's performance is enhanced through an auxiliary classifier, generating more structurally coherent virtual training samples. Additionally, Roy et al. [302] introduced a generative adversarial minority oversampling-based technique to augment model performance. This approach specifically addresses the persistent challenge of class-wise data imbalance in HSC.

4) **Active Learning:** Given the cost and effort associated with acquiring labeled HS data, active learning strategies are becoming more prevalent. These techniques involve selecting the most informative samples for annotation, iteratively improving the model's performance with minimal labeled data. Active learning helps in optimizing the learning process, making HSC more efficient and cost-effective. The process of selecting the most informative samples is performed to ensure that the chosen samples are both informative and representative of the overall input distribution, ultimately enhancing accuracy. Depending on the criteria for adding new instances to the training set, Active Learning frameworks can be categorized as either stream-based or pool-based. In the stream-based selection, one instance is drawn at a time from

an existing set of unlabeled samples, and the model determines whether to label it or not based on its perceived usefulness. Conversely, in the pool-based strategy, samples are queried from a pool or subset of unlabeled data. This selection is based on ranking scores computed from various measures to assess the sample's usefulness. The study by Ganti et al. [303] observed that stream-based selection yields lower learning rates compared to pool-based selection, primarily due to the former's tendency to query additional instances. In pool-based selection, emphasizing diversity within the pool of samples is crucial to prevent redundancy. Typically, the selection or querying of the most valuable samples centers around three main aspects: heterogeneity behavior, model performance, and representativeness of samples.

Heterogeneity-based selection: These strategies focus on selecting samples that exhibit greater heterogeneity compared to the instances already encountered. This heterogeneity is assessed in terms of model diversity, classification uncertainty, and discord among a committee of diverse classifiers. Models based on heterogeneity include uncertainty sampling, expected model change, and query-by-committee. **Performance-based Selection:** These methods take into account the impact of adding queried samples on the model's performance. They aim to optimize the model's performance by minimizing variance and error. Performance-based sampling can be broadly categorized into two types i.e., Expected Error Reduction [304] and Expected Variance Reduction [305]. **Representativeness-based selection:** Representative sampling tends to query instances that are representative of the overall input distribution, thus steering clear of outliers and unrepresentative samples. These methods assign a higher importance to the denser input region during the querying process. Representativeness sampling approaches, such as density-weighted techniques like information density, consider both the representativeness of samples and heterogeneity behavior. These models are often referred to as hybrid models [304].

Active Learning has gained substantial prominence in recent times within HSC. Liu et al. [306] introduced a feature-driven active learning framework, aiming to establish a well-constructed feature space for HSC. Zhang et al. [307] proposed a semi-supervised active learning method based on Random Forest, leveraging spectral-spatial features to formulate a query function. This function is employed to select the most informative samples as target candidates for the training set. Guo et al. [308] introduced a framework that integrates the spectral and spatial features of superpixels. Likewise, Xue et al. [309] incorporated neighborhood and superpixel information to augment the uncertainty of queried samples. In a recent study, Bhardwaj et al. [310] leveraged attribute profiles to integrate spatial information within an active learning-based HSC framework.

The diversity of samples becomes crucial in batch-mode techniques to prevent redundancy. A multi-criteria batch-mode method introduced by Patra et al. [311] defines a novel query function based on diversity, uncertainty, and cluster assumption measures. These criteria leverage the properties of KNN, SVM, and K-means clustering, respectively. Genetic algorithms are subsequently employed to choose the most

effective batch of samples. Similarly, Zhang et al. [312] proposed a regularized multi-metric batch-mode framework for HSC, exploiting various features of HSI. A Multiview active learning (MVAL) framework was introduced by Xu et al. [313]. This framework analyzes objects from various perspectives and gauges sample informativeness through multiview Intensity-based query criteria. Similarly, Pradhan et al. [314] embraced the concept of multiview learning, employing the Fisher Discriminant Ratio to generate multiple views. In another study, Zhang et al. [315] put forth an innovative adaptive MVAL framework for HSC, simultaneously leveraging spatial and spectral features in each view. More recently, Li et al. [316] proposed an MVAL technique utilizing pixel-level, subpixel-level, and superpixel-level details to generate multiple views for HSC. Furthermore, the proposed method exploits joint posterior probability estimation and dissimilarities among multiple views to query representative samples.

Sun et al. [317] combined an AE with an active learning technique, while Liu et al. [318] introduced a DBN-based active learning framework for HSC. Similarly, Haut et al. [319] married a Bayesian CNN with the active learning paradigm for spectral-spatial HSC. More recently, Cao et al. [287] proposed a CNN-based active learning framework to effectively leverage unlabeled samples for HSC. Several studies have incorporated active learning with transfer learning for HSC [31]. For instance, Lin et al. [320] introduced a framework that identifies salient samples and utilizes high-level features to establish correlations between source and target domain data. Another approach, suggested by Deng et al. [321], presented an Active Transfer Learning technique based on Stacked Sparse AE. This technique jointly utilizes both spectral and spatial features for HSC. Additionally, Deng et al. [322] combined domain adaptation and AL methods, incorporating multiple kernels for HSC.

Active learning in HSC introduces sophisticated frameworks aimed at improving the generalization capabilities of models. For example, Ahmad et al. [323] presented a fuzziness-based to enhance the generalization performance of both discriminative and generative classifiers. This method calculates the fuzziness-based distance for each instance and the estimated class boundary. Instances with higher fuzziness values and smaller distances from class boundaries are selected as candidates for the training set. Recently, a non-randomized spectral-spatial framework for multiclass HSC was introduced in [324]. This framework combines the spatial prior fuzziness approach with Multinomial Logistic Regression via a Splitting and Augmented Lagrangian classifier. The authors conducted a comprehensive comparison of the proposed framework with state-of-the-art sample selection methods and diverse classifiers.

5) **Graph-based Approaches:** Graph-based methods are gaining popularity for HSC, especially in scenarios where spatial-spectral relationships are crucial. GCNs and graph attention networks (GATs) enable the modeling of intricate interactions between neighboring pixels, capturing both spectral and spatial information. These methods have shown promise in improving classification accuracy, particularly in urban and complex landscapes.

6) **Explainable AI for HS Analysis:** As HS data finds applications in critical decision-making processes, the demand for explainable AI has grown. Researchers are working on developing models that provide interpretable results, enabling end-users to understand the reasoning behind classification decisions. This is especially crucial in fields such as environmental monitoring, agriculture, and defense.

7) **Integration of Multimodal Data:** Combining HS data with other imaging modalities, such as Light Detection and Ranging (LiDAR) or Synthetic Aperture Radar (SAR), is an emerging trend. The fusion of multimodal data sources enhances the overall understanding of the scene, providing complementary information for improved classification accuracy and discrimination of complex land cover classes.

8) **Edge Computing for Real-time Processing:** The need for real-time HSC in applications like precision agriculture and disaster response has led to the exploration of edge computing solutions. Deploying lightweight models on edge devices allows for on-site processing, reducing latency and enabling timely decision-making.

9) **Development of Benchmark Datasets:** Efforts are being made to create standardized benchmark datasets for HSC, facilitating fair comparisons among different algorithms and approaches. These datasets help in evaluating the generalization capabilities of models and advancing the reproducibility of research findings.

In short, the field of HSC is witnessing rapid advancements driven by innovations in DL, domain adaptation, graph-based methods, active learning, explainable AI, multimodal data integration, edge computing, and the establishment of benchmark datasets. These trends collectively contribute to the refinement of HS data analysis techniques and expand the applicability of HSI in various domains. As technology continues to progress, further breakthroughs will likely shape the future landscape of HSC.

XII. EXPLAINABLE AI AND INTEROPERABILITY

Explainable AI (XAI) and interpretability play crucial roles in HSC, enabling users to understand and trust the decision-making process of the models. Here is a detailed discussion on XAI and interpretability in this context:

- 1) **Importance of Explainable AI:** In HSC, where accurate and reliable decisions are vital, it is essential to understand why and how a model arrives at a particular classification result. EAI techniques aim to provide transparency and interpretability to the decision-making process of complex models. By gaining insights into the model's reasoning, users can assess the model's reliability, detect biases, identify important features, and diagnose potential errors or limitations.
- 2) **Interpretability Techniques:** Various techniques are employed to achieve interpretability in HSC:
 - **Feature Importance:** Feature importance methods, such as permutation importance or feature saliency maps, help identify the most influential spectral bands or spatial locations contributing to the classification decision. These methods provide insights

into which features are critical for classification and can guide further analysis or data collection.

- **Attention Mechanisms:** Attention mechanisms, commonly used in transformer-based models, allow users to visualize the attention weights assigned to different spectral bands or spatial locations. By highlighting the relevant regions, attention maps provide interpretability by revealing which parts of the HSI are crucial for classification.
 - **Rule Extraction:** Rule extraction techniques aim to extract human-understandable rules or decision trees from complex models. These rules provide explicit conditions that determine the classification outcome for a given input, making the decision process more transparent and interpretable.
 - **Model Visualization:** Visualizing the internal representations of the model, such as intermediate feature maps or activation patterns, can aid in understanding how the model processes and represents the HS input data. Visualization techniques help identify patterns, correlations, or anomalies that contribute to the classification outcome.
- 3) **Domain Expert Collaboration:** In HSC, the collaboration between AI experts and domain experts is crucial to achieving interpretability. Domain experts possess in-depth knowledge of the spectral signatures and spatial characteristics of the objects or materials of interest. By involving domain experts in the interpretability process, their expertise can be leveraged to validate and refine the explanations provided by the AI models, ensuring that the interpretations align with domain-specific knowledge.
 - 4) **Transparency and Trust:** EAI and interpretability techniques help build transparency and trust in HSC models. By providing understandable and justifiable explanations, users can assess the model's reliability, understand its limitations, and make informed decisions based on the model's outputs. This transparency is particularly important in critical applications, such as environmental monitoring, precision agriculture, or target detection, where the consequences of misclassifications can be significant.
 - 5) **Regulatory and Ethical Considerations:** In some domains, regulatory frameworks or ethical considerations may require explanations for AI-based decisions. For example, in healthcare or RS applications, it may be necessary to explain the reasons behind a diagnosis or land cover classification. Incorporating interpretability techniques in HSC models can help meet these requirements and ensure compliance with regulations and ethical standards.

There are certain challenges as well, for instance:

- 1) **Trade-off with Performance:** Achieving high interpretability may come with a trade-off in terms of model performance. Simpler models or interpretable methods might not capture the complexity of HS data as effectively as more complex models.

- 2) **Interpretable DL:** DL models, particularly CNNs and transformers, can be challenging to interpret due to their hierarchical and non-linear nature. Balancing interpretability with the power of DL is an ongoing research challenge.
- 3) **Human Understanding:** The interpretability provided by a model should align with the human understanding of the data. It is essential to present information in a way that is meaningful and relevant to domain experts and end-users.

In short, EAI and interpretability play a pivotal role in HSC, addressing issues of trust, ethics, and regulatory compliance. Choosing appropriate interpretability methods and balancing them with model performance and ethical considerations, identifying important features, detecting biases, collaborating with domain experts, and complying with regulations are essential for building trustworthy and effective HSC systems. Ongoing research in this area aims to develop more advanced techniques that strike an optimal balance between interpretability and predictive accuracy.

XIII. OPEN CHALLENGES AND RESEARCH QUESTIONS

HSC poses several challenges and prompts various research questions, reflecting the complexity and unique characteristics of HS data. Addressing these challenges and answering pertinent research questions is essential for advancing the field and improving the accuracy and applicability of HSC. Below is a detailed discussion of some key challenges and associated research questions:

- 1) **Limited Labeled Training Data: Challenge:** Acquiring labeled training data for HSIs can be expensive and time-consuming. Limited labeled data may hinder the development of accurate and robust classification models. **Research Questions:** How can transfer learning be effectively applied to leverage knowledge from related domains or existing labeled datasets to improve classification performance with limited labeled HS data? What active learning strategies can be employed to strategically select and query the most informative samples, optimizing the use of limited labeled data?
- 2) **Curse of Dimensionality: Challenge:** HS data typically exhibits high dimensionality due to the large number of spectral bands. This high-dimensional space can lead to the curse of dimensionality, affecting the performance of traditional classification algorithms. **Research Questions:** How can dimensionality reduction techniques be tailored to HS data to preserve relevant information while mitigating the challenges associated with the curse of dimensionality? What DL architectures or AE can effectively capture and represent the intrinsic structure of HS data in a lower-dimensional space?
- 3) **Spectral-Spatial Complexity: Challenge:** HSIs often contain intricate spectral-spatial patterns that are challenging to capture using traditional classifiers. **Research Questions:** How can advanced machine learning models, such as DNNs, be designed to effectively integrate spectral and spatial information for improved classification accuracy? What role do graph-based models or

attention mechanisms play in capturing spectral-spatial dependencies, and how can they be optimized for HSC?

- 4) **Class Imbalance and Rare Events: Challenge:** Class imbalance is prevalent in HS datasets, where certain classes may have fewer instances. Additionally, rare events or anomalies may be crucial but challenging to detect. **Research Questions:** How can HSI classifiers handle class imbalance, and what techniques can be employed to address the challenge of rare events or anomalies in the data? What role can generative models, such as GANs, play in augmenting rare class samples and enhancing classification performance?
- 5) **Robustness to Environmental Variability: Challenge:** HS data may be sensitive to variations in environmental conditions, such as lighting, atmospheric effects, and seasonal changes, leading to reduced model generalization. **Research Questions:** How can HS classifiers be made robust to environmental variability, and what preprocessing or normalization techniques are effective in reducing the impact of these variations? What transfer learning strategies can be employed to adapt models trained in one environment to perform well in different environmental conditions?
- 6) **Explainability and Interpretability: Challenge:** DL models and complex classifiers may lack interpretability, hindering user understanding and trust in the classification results. **Research Questions:** What methods and tools can be developed to provide explainability and interpretability in HSC, especially for DL models? How can the interpretability of models be aligned with the specific needs and expectations of domain experts and end-users in different application domains?
- 7) **Real-Time Processing and Resource Constraints: Challenge:** In certain applications, HSC needs to operate in real-time or under resource constraints, necessitating efficient algorithms. **Research Questions:** How can lightweight and efficient models be designed for real-time HSC, considering the constraints of processing power, memory, and energy consumption? What trade-offs can be made between model complexity and accuracy to achieve optimal performance in resource-constrained environments?

In short, addressing these challenges and answering the associated research questions is crucial for advancing the field of HSC. Innovative solutions to these issues will contribute to the development of more accurate, robust, and interpretable HSC models, enabling their successful application in various domains such as agriculture, environmental monitoring, and RS.

XIV. EXPERIMENTAL RESULTS AND DISCUSSION

Research-oriented publications in the literature commonly provide a thorough experimental evaluation to elucidate the strengths and weaknesses of the proposed methodologies. Nonetheless, these works might adopt varying experimental configurations, such as the assignment of training, validation, and test samples. While the number or percentage of samples

in these sets might be the same, the actual samples could differ as they are often selected randomly. Therefore, ensuring a fair comparison among different works from the literature necessitates the adoption of consistent and identical experimental settings. The standardized experimental settings should entail identical samples, ensuring that geographical locations remain consistent for all selected models rather than varying between them. Furthermore, the number of samples chosen for each round of training within the cross-validation process must be uniform. Typically, these samples are selected randomly, creating a potential discrepancy if models are executed at different times, as they might use different sets of samples.

TABLE I: Summary of the HSI datasets used for experimental evaluation.

—	IP	PU	UH
Year	1992	2001	2013
Source	AVIRIS	ROSIS-03	CASI
Spatial	145×145	610×610	340×1905
Spectral	220	115	144
Wavelength	400 – 2500	430 – 860	0.35 – 1.05
Samples	21025	207400	1329690
Classes	16	9	15
Sensor	Aerial	Aerial	Aerial
Resolution	20 <i>m</i>	1.3 <i>m</i>	2.5 <i>mpp</i>

Another concern prevalent in recent literature is the overlap between training and test samples. In many cases, training and validation samples are randomly chosen (considering or disregarding the aforementioned point) for the training and validation phases. However, during the testing phase, the entire dataset is often passed through, leading to a highly biased model, as the model has already encountered the training samples, thereby inflating accuracy results. In this study, while the training and test samples are selected randomly (as all models are executed simultaneously), special attention has been given to the above issue. Specifically, measures have been taken to ensure that there is no overlap among these samples, preserving the integrity of the evaluation process. Table I furnishes a concise overview of each dataset utilized in the subsequent experiments and further details regarding the experimental datasets are provided in the following.

The **University of Houston (UH)** dataset, released by the IEEE Geoscience and Remote Sensing Society as part of the Data Fusion Contest in 2013 [325], was collected by the Compact Airborne Spectrographic Imager (CASI). With dimensions of 340×1905 pixels and 144 spectral bands, the dataset features a spatial resolution of 2.5 meters per pixel (MPP) and a wavelength range from 0.38 to 1.05 μm . The ground truth for this dataset encompasses 15 distinct land-cover classes. Detailed class descriptions and ground truth maps are depicted in Figure 14. Moreover, Table II illustrates the selection of class-wise disjoint training, validation, and test samples used to train, validate, and test the models.

The **Indian Pines (IP)** dataset was acquired by the Airborne Visible/Infrared Imaging Spectrometer (AVIRIS) [326] over the Indian Pines test site in North-western Indiana. Comprising 224 spectral bands within a wavelength range of 400 to 2500 *nm*, the dataset excludes 24 null and corrupted bands. The image has a spatial size of 145×145 pixels, with a spatial

resolution of 20 meters per pixel (MPP). It encompasses 16 mutually exclusive vegetation classes. Disjoint Training/Test sample maps are illustrated in Figure 15. Moreover, Table II illustrates the selection of class-wise disjoint training, validation, and test samples used to train, validate, and test the models.

The **University of Pavia (UP)** dataset, captured by the Reflective Optics System Imaging Spectrometer (ROSIS) sensor during a flight campaign over the university campus in Pavia, Northern Italy [327], features dimensions of 610×340 pixels. With 103 spectral bands spanning the wavelength range from 430 to 860 *nm* and a spatial resolution of 2.5 meters per pixel (MPP), the dataset includes 9 urban land-cover classes. Detailed class descriptions and ground truth maps can be found in Figure 16. Moreover, Table II illustrates the selection of class-wise disjoint training, validation, and test samples used to train, validate, and test the models.

To substantiate the outlined concepts in this survey and validate the claims, recent contributions encompass a variety of models, including 2D CNN, 3D CNN, Hybrid CNN, 2D Inception Network, 3D Inception Net, Hybrid Inception Net, 2D Xception Net, (2+1)D Extreme Exception Net (EX Net), Attention Graph CNN, SCSNet: Sharpend Cosine Similarity-based Neural Network, and Spatial-Spectral Transformer. A comparative analysis of experimental results has been conducted by considering representative works for each model as shown in Table III, Table IV, TableV and Figure 17, Figure 18, and Figure 19. To a certain degree, all the aforementioned studies rely on Convolutional Networks and undergo evaluation using three benchmark HSI datasets, namely IP, PU, and Houston University Scene. This survey specifically focuses on assessing the robustness of these models, taking into account the challenge of classifying HSI with a limited sample size in the training data for joint spatial-spectral classification. Comparative methods tend to misclassify samples with similar spatial structures, exemplified by the confusion between Meadows and Bare Soil classes in the Pavia University dataset, as illustrated in the Table III, Table IV, and TableV and Figure 17, Figure 18, and Figure 19. Furthermore, the overall accuracy for the Grapes Untrained class is lower compared to other classes, attributed to the reasons mentioned earlier. In summary, it can be concluded that higher accuracy can be attained by augmenting the number of labeled training samples. Therefore, a larger set of labeled training samples has the potential to yield improved accuracies across all competing methods.

In general, the Hybrid CNN and 3D Inception nets consistently outperform other comparative methods, particularly when dealing with a smaller number of labeled training samples. This suggests that these works exhibit stability and are less sensitive to variations in the number of training samples. While the accuracies of these methods improve with an increase in the number of training samples, it is noteworthy that other methods may outperform them with a higher number of training samples. This trend persists even with a higher number of training samples. Consequently, one can infer that the works attention Graph, SCSNet, and Transformers partially address the challenges posed by limited training sample availability, particularly when considering disjoint train/test



Fig. 14: University of Houston ground truth maps, disjoint training, validation, and test ground truth maps.

TABLE II: Disjoint Train, Validation, and Test samples selected to train, validate, and test several models.

Indian Pines Dataset				University of Houston Dataset				Pavia University Dataset			
Class	Training	Validation	Test	Class	Training	Validation	Test	Class	Training	Validation	Test
Alfalfa	4	5	37	Healthy grass	125	125	1001	Asphalt	663	663	5305
Corn-notill	142	143	1143	Stressed grass	125	125	1004	Meadows	1864	1865	14920
Corn-mintill	83	83	664	Synthetic grass	69	70	558	Gravel	209	210	1680
Corn	23	24	190	Trees	124	124	996	Trees	306	306	2452
Grass-pasture	48	48	387	Soil	124	124	994	Painted	134	135	1076
Grass-trees	73	73	584	Water	32	33	260	Soil	502	503	4024
Grass-mowed	2	3	23	Residential	126	127	1015	Bitumen	133	133	1064
Hay-windrowed	47	48	383	Commercial	124	124	996	Bricks	368	368	2946
Oats	2	2	16	Road	125	125	1002	Shadows	94	95	758
Soybean-notill	97	97	778	Highway	122	123	982				
Soybean-mintill	245	246	1964	Railway	123	124	988				
Soybean-clean	59	59	475	Parking Lot 1	123	123	987				
Wheat	20	21	164	Parking Lot 2	46	47	376				
Woods	126	127	1012	Tennis Court	42	43	343				
Buildings	38	39	309	Running Track	66	66	528				
Stone-Steel	9	9	75								

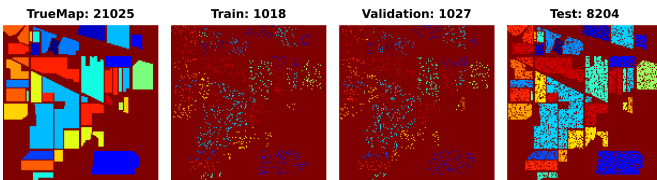


Fig. 15: Indian Pines ground truth maps, disjoint training, validation, and test ground truth maps.

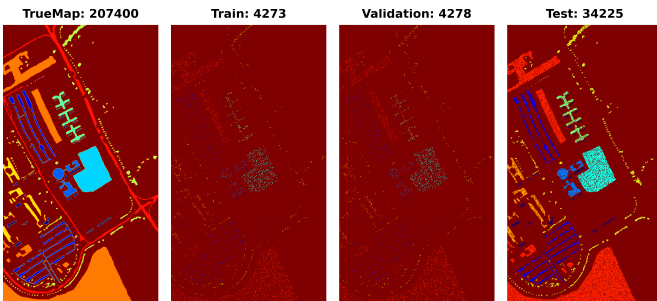


Fig. 16: Pavia University ground truth maps, disjoint training, validation, and test ground truth maps.

samples. Furthermore, it can be deduced that models based on CONVs exhibit subpar performance compared to other models. Despite the advantage of the convolutional process, these models may fail to learn effectively in the absence of constraints. Additionally, the symmetric architecture can lead to an explosion of training parameters, escalating the training difficulty. While the works Attention Graph and SCSNet successfully address these challenges, the approach taken by Exception Net, which neglects the adoption of a greedy layer-wise strategy, results in inferior outcomes. This indicates a potential for enhancing methods in this category.

In summary, Transformer and Graph-based classification

yields significantly better results than CONV-based methods, especially when dealing with limited availability of labeled training samples. While CNNs can capture the internal structure, the resulting feature representation may lack task-specific characteristics, explaining their comparatively lower performance compared to other models. Additionally, Active Learning (AL) and/or Self Learning (SL) benefit from selecting crucial samples for training, allowing the model to focus on challenging instances in HSIC. Few-shot learning (FSL) exploits the relationship between samples to establish a discriminative decision boundary for HSIC. Transfer Learning (TL) leverages similarities among different HSIs to reduce the required training data and the number of trainable parameters, enhancing model robustness. Utilizing raw data without feature extraction/learning, Data Augmentation (DA) generates additional diverse samples.

XV. CONCLUSIONS

This survey has provided a comprehensive exploration of the evolution from conventional methods to the promising era of transformers in the domain of Hyperspectral Image Classification (HSC). By meticulously reviewing a wide array of methodologies, from traditional machine learning techniques to cutting-edge transformer-based models, we aimed to offer a panoramic view of the current landscape and illuminate the prospects of HSC. The journey began with an in-depth analysis of conventional methods, including spectral-spatial and statistical approaches. We delved into the strengths and limitations of these conventional models, acknowledging their contributions to the field while recognizing the inherent challenges they face, particularly in handling the complexity of HS data.

As we transitioned into the era of transformers, we witnessed a paradigm shift in the approach to HSC. The survey meticulously explored the applications of transformer-based models, drawing attention to the remarkable success achieved

TABLE III: Per-class classification results for **Pavia University** using various models with disjoint test set and the complete HSI as the test set with a patch size of 8×8 , 10% allocated for training and validation samples, and the remaining 80% for disjoint test samples.

Class	2D CNN		3D CNN		Hybrid CNN		2D Inception		3D Inception		Hybrid Inception		2D Xception		(2+1D) Xception		SCSNet		Attention Graph		Transformer	
	Test	HSI	Test	HSI	Test	HSI	Test	HSI	Test	HSI	Test	HSI	Test	HSI	Test	HSI	Test	HSI	Test	HSI	Test	HSI
Asphalt	99.24	99.97	99.75	99.99	99.92	99.99	99.18	99.97	99.83	99.99	99.96	99.99	91.40	99.70	99.83	99.99	98.96	99.96	97.66	99.91	97.15	99.90
Meadows	99.67	99.71	99.97	99.96	99.97	99.96	99.71	99.72	100	100	99.97	99.96	98.65	98.78	99.93	99.94	99.75	99.79	99.10	99.13	99.73	99.75
Gravel	90.41	91.61	96.30	96.71	95.29	95.75	88.45	89.75	92.55	93.33	97.67	97.99	73.39	76.08	95.59	95.90	90.23	91.32	94.34	94.90	88.80	90.32
Trees	97.87	98.20	98.93	99.05	99.51	99.57	96.45	96.76	98.00	98.17	99.06	99.18	84.46	85.99	98.57	98.82	97.38	97.45	96.53	96.76	97.14	97.32
Painted	100	100	100	100	100	100	100	100	100	100	100	100	89.96	91.00	100	100	100	100	99.81	99.85	100	100
Soil	98.21	98.46	99.40	99.52	100	100	99.75	99.80	99.90	99.92	100	100	90.53	91.42	99.92	99.94	95.05	95.64	99.72	99.78	98.06	98.30
Bitumen	99.34	99.39	99.15	99.24	99.53	99.62	97.27	97.74	99.90	99.92	99.34	99.39	90.60	91.72	98.96	99.09	94.64	95.11	95.48	95.93	95.95	96.46
Bricks	96.91	97.28	98.40	98.61	99.18	99.26	94.53	95.11	99.76	99.72	99.01	99.15	68.22	71.37	99.01	99.18	92.90	93.48	93.48	93.91	93.04	93.69
Shadows	96.56	97.04	99.60	99.68	99.73	99.78	98.94	99.15	99.47	99.57	99.20	99.26	57.91	61.77	98.15	98.31	90.50	91.12	92.87	93.98	98.28	98.20
Time(S)	2.72	82.92	5.51	97.59	2.96	88.29	5.52	85.66	20.89	140.14	10.64	101.53	10.64	98.41	41.35	272.71	17.63	167.59	4.76	93.31	10.64	138.70
Kappa	98.07	99.15	99.27	99.68	99.50	99.77	97.77	99.00	99.23	99.65	99.57	99.81	87.11	94.16	99.29	99.68	96.68	98.48	97.12	98.65	96.95	98.62
OA	98.54	99.73	99.45	99.90	99.62	99.92	98.32	99.68	99.42	99.89	99.68	99.94	90.27	98.19	99.46	99.90	97.50	99.53	97.83	99.58	97.7	99.57
AA	97.58	97.97	99.06	99.20	99.24	99.33	97.15	97.56	98.83	98.96	99.36	99.44	82.78	85.32	98.89	99.02	95.49	95.99	96.56	97.13	96.47	97.11

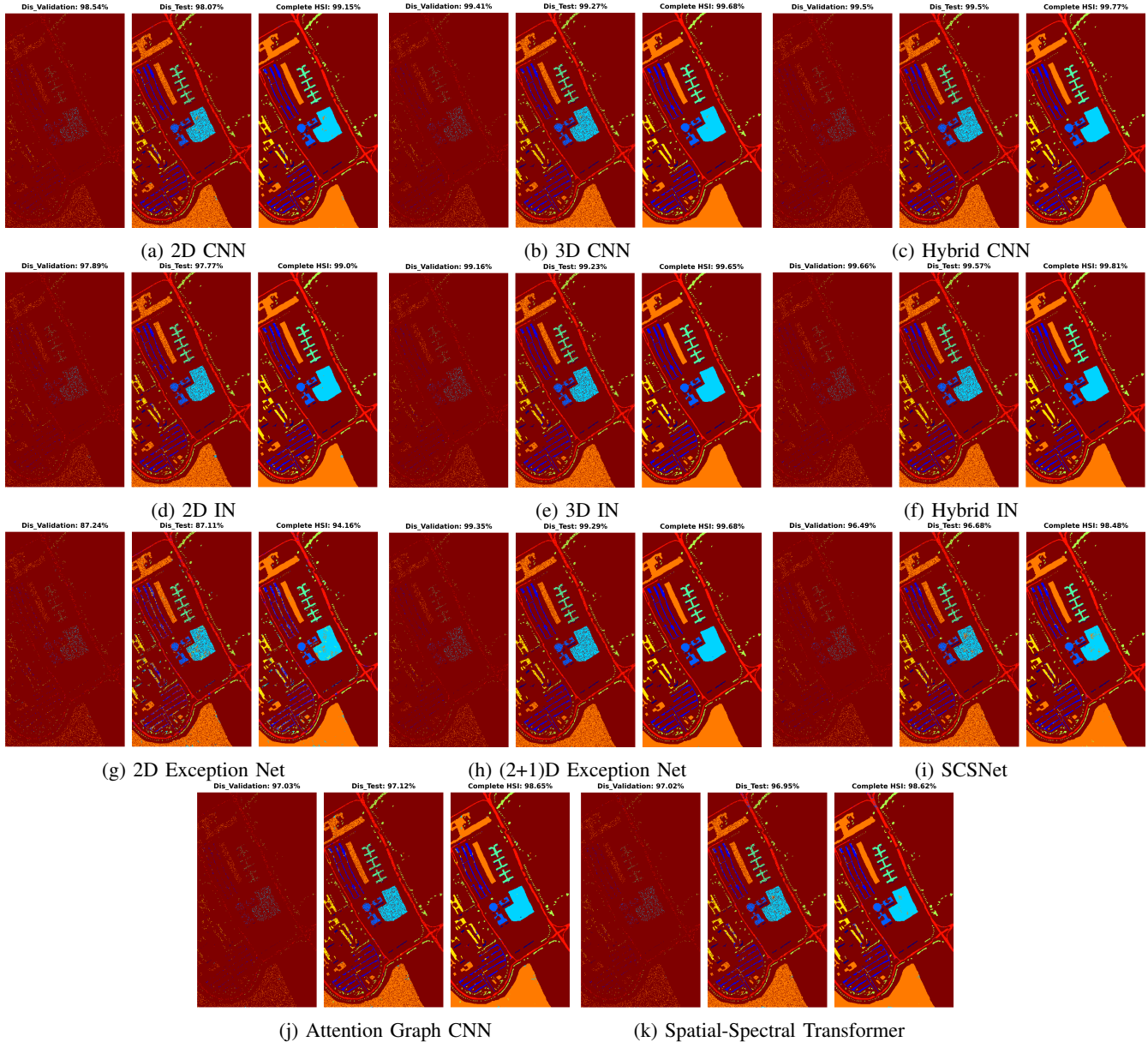


Fig. 17: **Pavia University Dataset**: Predicted land cover maps for disjoint validation, test, and the entire HSI used as a test set are provided. Comprehensive class-wise results can be found in Table III.

by these architectures in various domains. The introduction of self-attention mechanisms, multi-head attention, and positional encoding have empowered transformers to capture intricate

spectral-spatial dependencies, unlocking new possibilities for accurate and context-aware classification.

Our survey also shed light on the challenges that researchers

TABLE IV: Per-class classification results for **Indian Pines** using various models with disjoint test set and the complete HSI as the test set with a patch size of 8×8 , 25% allocated for training and validation samples, and the remaining 50% for disjoint test samples.

Class	2D CNN		3D CNN		Hybrid CNN		2D Inception		3D Inception		Hybrid Inception		2D Xception		(2+1)D Xception		SCSNet		Attention Graph		Transformer	
	Test	HSI	Test	HSI	Test	HSI	Test	HSI	Test	HSI	Test	HSI	Test	HSI	Test	HSI	Test	HSI	Test	HSI	Test	HSI
Alfalfa	47.82	99.81	100	99.99	100	100	100	99.99	100	100	100	100	-	99.57	82.60	99.92	39.13	99.81	86.95	99.95	91.30	99.96
Corn-notill	95.65	96.63	98.03	98.17	99.01	99.22	93.97	95.02	98.73	99.01	98.73	99.01	68.34	7.98	91.31	92.85	90.47	92.15	93.83	95.30	91.73	94.04
Corn-mintill	90.12	93.01	95.42	96.86	97.34	98.55	93.49	95.78	96.86	98.07	96.38	97.71	16.86	0.60	77.34	81.20	80.72	85.18	88.19	92.28	84.33	89.75
Corn	82.35	83.96	96.63	96.62	98.31	97.46	91.59	91.98	100	100	99.15	99.15	31.93	-	84.87	89.02	48.73	54.43	64.70	74.68	74.78	79.74
Grass-pasture	94.21	96.06	98.76	98.96	99.58	99.79	97.93	98.7	98.76	99.37	99.58	99.79	78.09	2.07	92.56	94.40	93.80	94.82	93.80	96.27	95.86	97.10
Grass-trees	98.90	99.45	99.17	99.58	99.72	99.86	98.63	99.31	99.45	98.55	99.72	99.86	79.72	7.67	98.35	99.04	98.35	98.35	98.08	99.04	99.17	99.58
Grass-mowed	50.00	64.28	92.85	96.42	100	100	50	67.85	100	99.72	78.57	85.71	-	-	92.85	96.42	14.28	25	85.71	89.28	92.85	96.42
Hay-windrowed	99.16	99.58	100	100	100	100	100	100	100	100	100	100	73.64	-	99.58	99.79	96.23	97.48	100	100	99.16	99.58
Oats	80	85	90	95	100	100	80	85	80	100	30	45	-	5	70	85	20	30	70	80	60	70
Soybean-notill	90.94	93.41	92.79	95.16	97.53	98.45	88.47	92.28	97.94	90	94.65	95.88	5.96	0.10	79.42	81.79	80.86	86.00	83.74	88.06	83.53	87.75
Soybean-mintill	88.43	91.20	99.02	99.30	98.20	98.77	94.13	95.80	98.94	99.14	98.85	99.22	88.92	-	90.55	93.07	90.55	93.36	95.27	96.65	92.91	94.66
Soybean-clean	93.26	94.26	98.31	98.65	99.32	99.32	93.60	95.61	97.97	98.65	95.28	97.47	39.05	-	97.30	98.31	70.37	77.57	93.93	94.94	83.83	88.02
Wheat	100	100	100	100	100	100	100	100	100	99.51	100	100	20.38	-	97.08	97.56	97.08	97.56	99.02	99.02	100	100
Woods	98.26	98.57	98.57	98.89	99.05	99.28	98.10	98.26	99.52	99.60	98.73	99.20	87.51	-	98.42	99.13	95.89	97.54	97.78	98.41	97.78	98.26
Buildings	94.30	95.59	97.92	98.18	99.48	99.74	92.74	95.07	100	100	100	100	27.46	-	90.15	94.04	78.75	84.45	89.11	93.78	94.30	96.37
Stone-Steel	100	100	95.74	97.84	95.74	97.84	100	100	97.87	98.92	100	100	-	-	95.74	95.69	34.04	43.01	93.61	95.69	97.87	98.92
Time(S)	0.63	8.25	0.66	8.95	0.50	8.81	0.78	9.66	2.19	14.90	1.36	10.60	1.61	11.90	10.32	28.65	5.20	21.46	1.39	9.02	1.78	15.16
Kappa	91.97	96.29	97.51	99.21	98.51	99.38	93.96	97.35	98.62	99.41	97.80	99.08	54.47	29.26	89.71	95.08	85.02	93.07	92.01	96.59	90.72	95.92
OA	92.94	97.37	97.82	99.21	98.69	99.56	94.69	98.12	98.79	99.58	98.07	99.35	60.78	52.14	90.93	96.52	86.91	95.11	93.00	97.59	91.86	97.11
AA	87.72	93.17	97.08	98.11	98.96	99.27	92.04	94.42	97.88	98.79	93.11	94.88	38.62	7.68	89.89	93.58	70.58	78.55	89.61	93.34	89.97	93.14

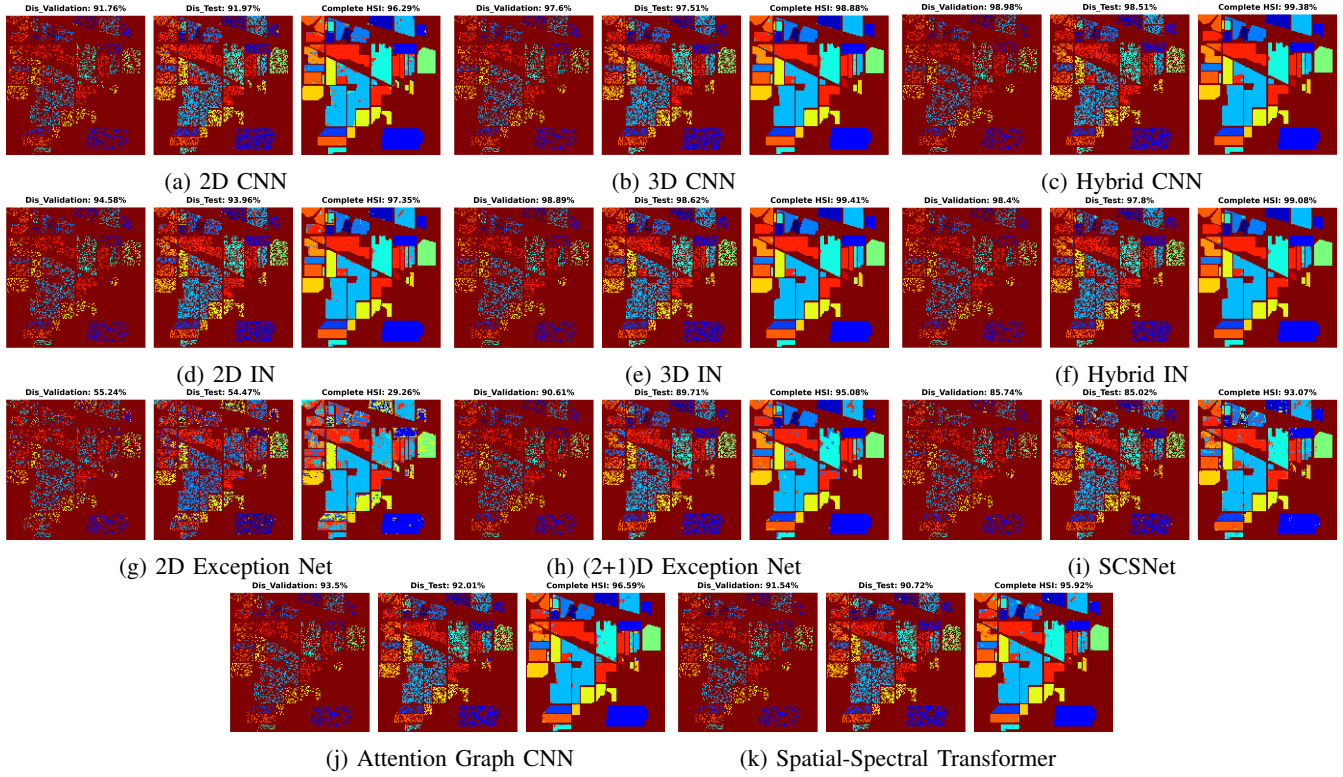


Fig. 18: **Indian Pines Dataset**: Predicted land cover maps for disjoint validation, test, and the entire HSI used as a test set are provided. Comprehensive class-wise results can be found in Table IV.

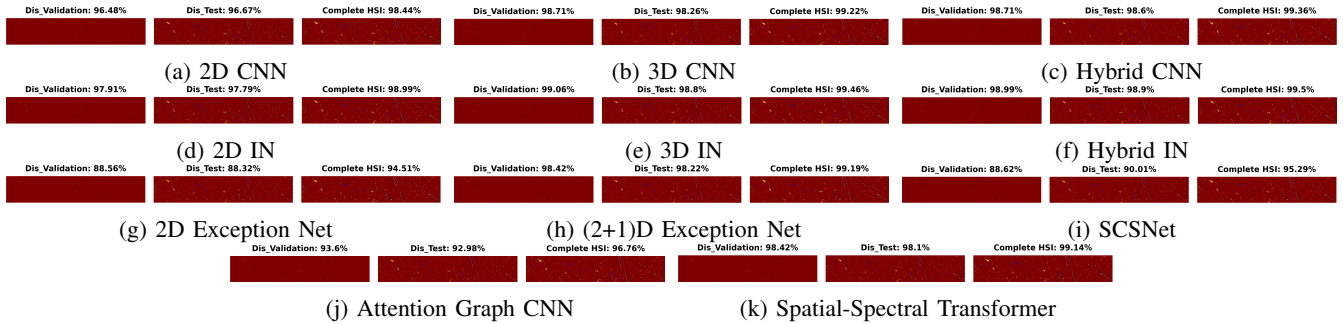


Fig. 19: **University of Houston Dataset**: Predicted land cover maps for disjoint validation, test, and the entire HSI used as a test set are provided. Comprehensive class-wise results can be found in Table V.

TABLE V: Per-class classification results for **University of Houston** using various models with disjoint test set and the complete HSI as the test set with a patch size of 8×8 , 10% allocated for training and validation samples, and the remaining 80% for disjoint test samples.

Class	2D CNN		3D CNN		Hybrid CNN		2D Inception		3D Inception		Hybrid Inception		2D Xception		(2+1)D Xception		SCSNet		Attention Graph		Transformer	
	Test	HSI	Test	HSI	Test	HSI	Test	HSI	Test	HSI	Test	HSI	Test	HSI	Test	HSI	Test	HSI	Test	HSI	Test	HSI
Healthy grass	98.10	99.99	98.60	99.99	98.10	99.99	98.10	99.99	98.80	99.99	98.80	99.99	96.80	99.99	98.60	99.99	95.10	99.99	94.10	99.98	98.10	99.99
Stressed grass	97.70	98.08	97.80	98.16	96.91	97.28	98.00	98.40	98.90	99.12	98.50	98.80	97.80	98.00	98.70	98.96	94.32	94.81	97.41	97.60	97.70	98.08
Synthetic grass	99.64	99.71	97.67	98.13	99.64	99.71	99.64	99.71	99.64	99.71	99.46	99.56	95.87	96.41	98.02	98.42	97.13	97.70	99.64	99.71	99.64	99.71
Trees	99.89	99.91	99.69	99.67	99.69	99.75	98.69	98.87	100	100	100	100	98.99	99.11	99.89	99.91	96.48	96.54	97.08	97.34	99.49	99.59
Soil	100	100	99.89	99.91	100	100	99.89	99.91	100	100	100	100	99.49	99.51	100	100	97.28	97.34	98.79	98.95	100	100
Water	86.92	89.53	96.15	96.92	97.30	97.84	91.53	93.23	96.92	97.53	93.07	94.15	78.46	81.23	94.61	95.38	57.30	60.30	86.15	87.69	99.23	99.38
Residential	95.66	95.74	96.84	97.16	98.42	98.65	97.04	97.08	98.12	98.34	98.91	98.97	90.54	91.71	96.35	96.68	94.87	95.50	88.07	89.11	95.96	96.45
Commercial	94.67	95.01	97.48	97.74	97.89	98.07	97.38	97.66	97.18	97.50	97.89	98.07	86.94	88.58	97.69	97.90	86.44	87.78	94.97	95.25	97.59	97.82
Road	96.00	96.48	98.70	98.88	98.60	98.72	98.90	99.04	99.30	99.44	98.30	98.40	76.64	77.55	98.60	98.72	80.73	82.10	83.83	85.14	98.90	98.96
Highway	96.74	97.06	98.57	98.85	98.77	98.94	98.67	98.69	99.38	99.42	99.28	99.34	81.26	81.98	99.28	99.34	87.16	88.75	93.89	94.45	98.26	98.45
Railway	98.58	98.70	98.88	99.02	98.68	98.94	98.58	98.86	98.58	98.86	99.19	99.35	91.49	92.22	95.74	96.19	96.65	96.84	88.76	89.95	99.69	99.75
Parking Lot 1	92.19	92.37	99.39	99.35	99.08	99.10	98.88	99.02	99.39	99.43	99.69	99.67	84.49	85.23	99.79	99.83	89.26	90.10	99.59	99.67	99.39	99.43
Parking Lot 2	93.88	94.88	93.08	94.24	97.60	97.65	84.04	85.28	94.41	94.88	98.13	98.50	40.95	47.33	94.68	95.52	72.87	73.98	91.22	92.53	84.57	86.56
Tennis Court	100	100	98.83	99.06	100	100	98.83	99.06	100	100	100	100	93.87	93.69	100	100	83.38	84.81	80.46	82.94	100	100
Running Track	98.48	98.48	100	100	100	100	100	100	100	100	100	100	95.07	95.75	100	100	97.72	97.72	98.29	98.63	100	100
Time(S)	1.15	274.67	1.43	285.60	41.12	2932.98	1.41	284.12	4.95	460.70	5.34	351.17	2.56	312.79	20.65	869.61	20.09	122.62	5.26	559.68	7.17	714.78
Kappa	96.67	98.44	98.26	99.22	98.6	99.36	97.79	98.99	98.8	99.46	98.9	99.5	88.32	94.51	98.22	99.19	90.01	95.29	92.98	96.76	98.1	99.14
OA	96.92	99.93	98.39	99.96	98.7	99.97	97.96	99.95	98.89	99.97	98.99	99.97	89.21	99.77	98.35	99.96	90.75	99.80	93.51	99.86	98.25	99.96
AA	96.57	97.07	98.11	98.48	98.72	98.98	97.22	97.66	98.71	98.95	98.75	98.99	87.25	88.56	98.13	98.46	88.44	89.62	92.82	93.94	97.89	98.28

and practitioners encounter in this evolving landscape. From the scarcity of labeled HS data to the interpretability of transformer-based models, each challenge represents an opportunity for further exploration and innovation. We emphasized the significance of interpretable AI, the role of attention mechanisms, and the ongoing quest for efficient models that can operate in real-time or under resource constraints. In short, this survey endeavors to be a guiding beacon for researchers and practitioners venturing into HSC, providing insights into the past, present, and future of this dynamic field. The fusion of conventional wisdom with transformative technologies promises to elevate the accuracy, efficiency, and interpretability of HSC, paving the way for a new era of discoveries and applications.

The future of HSC is poised for transformative developments, with a focus on advancing transformer architectures, improving interpretability, and integrating domain knowledge. Anticipated enhancements in HS data acquisition, labeling techniques, and the emergence of real-time, resource-efficient models underscore the evolution of this field. Cross-domain transfer learning and collaborative interdisciplinary research are expected to play pivotal roles, fostering applications in precision agriculture and environmental monitoring. The collective impact of these advancements promises to revolutionize decision-making processes and promote sustainability across diverse domains. Looking ahead, the future of HSC appears promising, with transformers poised to play a pivotal role. The fusion of domain knowledge, advancements in transformer architectures, and the integration of interpretability measures will shape the next generation of models. As we navigate this transformative journey, collaboration between researchers, domain experts, and technology enthusiasts will be crucial to overcoming challenges and unlocking the full potential of HSI.

REFERENCES

- [1] M. Ahmad, S. Shabbir, S. K. Roy, D. Hong, X. Wu, J. Yao, A. M. Khan, M. Mazzara, S. Distefano, and J. Chanussot, "Hyperspectral image classification—traditional to deep models: A survey for future prospects," *IEEE Journal of Selected Topics in Applied Earth Observations and Remote Sensing*, 2021.
- [2] J. Jiao, Z. Gong, and P. Zhong, "Triplet spectralwise transformer network for hyperspectral target detection," *IEEE Transactions on Geoscience and Remote Sensing*, vol. 61, pp. 1–17, 2023.
- [3] W. Han, X. Zhang, Y. Wang, L. Wang, X. Huang, J. Li, S. Wang, W. Chen, X. Li, R. Feng, R. Fan, X. Zhang, and Y. Wang, "A survey of machine learning and deep learning in remote sensing of geological environment: Challenges, advances, and opportunities," *ISPRS Journal of Photogrammetry and Remote Sensing*, vol. 202, pp. 87–113, 2023.
- [4] X. Cao, Y. Lian, K. Wang, C. Ma, and X. Xu, "Unsupervised hybrid network of transformer and cnn for blind hyperspectral and multi-spectral image fusion," *IEEE Transactions on Geoscience and Remote Sensing*, pp. 1–1, 2024.
- [5] K. Benham, P. Lewis, and J. Richardson, "Effects of loss function choice on one-shot hsi target detection with paired neural networks," *IEEE Journal of Selected Topics in Applied Earth Observations and Remote Sensing*, pp. 1–9, 2024.
- [6] L. Shuai, Z. Li, Z. Chen, D. Luo, and J. Mu, "A research review on deep learning combined with hyperspectral imaging in multiscale agricultural sensing," *Computers and Electronics in Agriculture*, vol. 217, p. 108577, 2024.
- [7] Y. Ma, Y. Zhao, J. Im, Y. Zhao, and Z. Zhen, "A deep-learning-based tree species classification for natural secondary forests using unmanned aerial vehicle hyperspectral images and lidar," *Ecological Indicators*, vol. 159, p. 111608, 2024.
- [8] S. Khorat, D. Das, R. Khatun, S. M. Aziz, P. Anand, A. Khan, M. Santamouris, and D. Niyogi, "Cool roof strategies for urban thermal resilience to extreme heatwaves in tropical cities," *Energy and Buildings*, vol. 302, p. 113751, 2024.
- [9] M. Janeci and L. Dzierzbicka-Glowacka, "Fish module - a prognostic tool for modeling the optimal environmental conditions for fishimage 1," *Applied Soft Computing*, vol. 153, p. 111302, 2024.
- [10] J. Peng, H. Wang, X. Cao, Q. Zhao, J. Yao, H. Zhang, and D. Meng, "Learnable representative coefficient image denoiser for hyperspectral image," *IEEE Transactions on Geoscience and Remote Sensing*, pp. 1–1, 2024.
- [11] M. Ahmad, U. Ghous, M. Usama, and M. Mazzara, "Waveformer: Spectral-spatial wavelet transformer for hyperspectral image classification," *IEEE Geoscience and Remote Sensing Letters*, pp. 1–1, 2024.
- [12] M.-S. Song, J.-J. Lee, H.-S. Yun, and S.-G. Yum, "Projection and identification of vulnerable areas due to heavy snowfall using machine learning and k-means clustering with rcp scenarios," *Climate Services*, vol. 33, p. 100440, 2024.
- [13] M. H. F. Butt, H. Ayaz, M. Ahmad, J. P. Li, and R. Kuleev, "A fast and compact hybrid cnn for hyperspectral imaging-based bloodstain classification," in *2022 IEEE Congress on Evolutionary Computation (CEC)*. IEEE, 2022, pp. 1–8.
- [14] M. Zulfikar, M. Ahmad, A. Sohaib, M. Mazzara, and S. Distefano, "Hyperspectral imaging for bloodstain identification," *Sensors*, vol. 21, no. 9, p. 3045, 2021.
- [15] H. Ayaz, M. Ahmad, A. Sohaib, M. N. Yasir, M. A. Zaidan, M. Ali, M. H. Khan, and Z. Saleem, "Myoglobin-based classification of minced meat using hyperspectral imaging," *Applied Sciences*, vol. 10, no. 19, p. 6862, 2020.
- [16] H. Ayaz, M. Ahmad, M. Mazzara, and A. Sohaib, "Hyperspectral imaging for minced meat classification using nonlinear deep features," *Applied Sciences*, vol. 10, no. 21, p. 7783, 2020.
- [17] M. H. Khan, Z. Saleem, M. Ahmad, A. Sohaib, H. Ayaz, M. Mazzara, and R. A. Raza, "Hyperspectral imaging-based unsupervised adulterated red chili content transformation for classification: Identification

- of red chili adulterants,” *Neural Computing and Applications*, vol. 33, no. 21, pp. 14 507–14 521, 2021.
- [18] M. H. Khan, Z. Saleem, M. Ahmad, A. Sohaib, H. Ayaz, and M. Mazzara, “Hyperspectral imaging for color adulteration detection in red chili,” *Applied Sciences*, vol. 10, no. 17, p. 5955, 2020.
- [19] Z. Saleem, M. H. Khan, M. Ahmad, A. Sohaib, H. Ayaz, and M. Mazzara, “Prediction of microbial spoilage and shelf-life of bakery products through hyperspectral imaging,” *IEEE Access*, vol. 8, pp. 176 986–176 996, 2020.
- [20] M. Ahmad, A. M. Khan, M. Mazzara, S. Distefano, M. Ali, and M. S. Sarfraz, “A fast and compact 3-d cnn for hyperspectral image classification,” *IEEE Geoscience and Remote Sensing Letters*, 2020.
- [21] M. Ahmad and M. Mazzara, “Scs-net: Sharpend cosine similarity based neural network for hyperspectral image classification,” *IEEE Geoscience and Remote Sensing Letters*, pp. 1–1, 2024.
- [22] U. Ghous, M. S. Sarfraz, M. Ahmad, C. Li, and D. Hong, “(2+1)d extreme xception net for hyperspectral image classification,” *IEEE Journal of Selected Topics in Applied Earth Observations and Remote Sensing*, pp. 1–14, 2024.
- [23] X. Xu, W. Kong, L. Wang, T. Wang, P. Luo, and J. Cui, “A novel and dynamic land use/cover change research framework based on an improved plus model and a fuzzy multiobjective programming model,” *Ecological Informatics*, vol. 80, p. 102460, 2024.
- [24] M. Ahmad, “Ground truth labeling and samples selection for hyperspectral image classification,” *Optik*, vol. 230, p. 166267, 2021. [Online]. Available: <https://www.sciencedirect.com/science/article/pii/S0030402621000103>
- [25] M. Ahmad, A. K. Bashir, and A. M. Khan, “Metric similarity regularizer to enhance pixel similarity performance for hyperspectral unmixing,” *Optik*, vol. 140, pp. 86–95, 2017. [Online]. Available: <https://www.sciencedirect.com/science/article/pii/S003040261730311X>
- [26] A. Patel, D. Vyas, N. Chaudhari, R. Patel, K. Patel, and D. Mehta, “Novel approach for the lulc change detection using gis & google earth engine through spatiotemporal analysis to evaluate the urbanization growth of ahmedabad city,” *Results in Engineering*, vol. 21, p. 101788, 2024.
- [27] M. Ahmad, A. M. Khan, M. Mazzara, S. Distefano, S. K. Roy, and X. Wu, “Hybrid dense network with attention mechanism for hyperspectral image classification,” *IEEE Journal of Selected Topics in Applied Earth Observations and Remote Sensing*, vol. 15, pp. 3948–3957, 2022.
- [28] F. Ji, W. Zhao, Q. Wang, W. J. Emery, R. Peng, Y. Man, G. Wang, and K. Jia, “Spectral-spatial evidential learning network for open-set hyperspectral image classification,” *IEEE Transactions on Geoscience and Remote Sensing*, vol. 62, pp. 1–17, 2024.
- [29] M. Ahmad, S. Shabbir, R. A. Raza, M. Mazzara, S. Distefano, and A. M. Khan, “Artifacts of different dimension reduction methods on hybrid cnn feature hierarchy for hyperspectral image classification,” *Optik*, vol. 246, p. 167757, 2021.
- [30] Q. Ran, Y. Zhou, D. Hong, M. Bi, L. Ni, X. Li, and M. Ahmad, “Deep transformer and few-shot learning for hyperspectral image classification,” *CAAI Transactions on Intelligence Technology*, 2023.
- [31] M. Ahmad, U. Ghous, D. Hong, A. M. Khan, J. Yao, S. Wang, and J. Chanussot, “A disjoint samples-based 3d-cnn with active transfer learning for hyperspectral image classification,” *IEEE Transactions on Geoscience and Remote Sensing*, vol. 60, pp. 1–16, 2022.
- [32] Z. Gong, X. Zhou, W. Yao, X. Zheng, and P. Zhong, “Hyperdid: Hyperspectral intrinsic image decomposition with deep feature embedding,” *IEEE Transactions on Geoscience and Remote Sensing*, pp. 1–1, 2024.
- [33] V. C. Gogineni, K. Müller, M. Orlandic, and S. Werner, “Lightweight autonomous autoencoders for timely hyperspectral anomaly detection,” *IEEE Geoscience and Remote Sensing Letters*, vol. 21, pp. 1–5, 2024.
- [34] M. Ahmad, S. Shabbir, D. Oliva, M. Mazzara, and S. Distefano, “Spatial-prior generalized fuzziness extreme learning machine autoencoder-based active learning for hyperspectral image classification,” *Optik*, vol. 206, p. 163712, 2020.
- [35] M. Ahmad, M. A. Alqarni, A. M. Khan, R. Hussain, M. Mazzara, and S. Distefano, “Segmented and non-segmented stacked denoising autoencoder for hyperspectral band reduction,” *Optik*, vol. 180, pp. 370–378, 2019.
- [36] M. Ahmad, A. M. Khan, M. Mazzara, and S. Distefano, “Multi-layer extreme learning machine-based autoencoder for hyperspectral image classification,” in *VISAPP’19*, 2019.
- [37] M. Ahmad, “Sharpnd cosine similarity based neural network for hyperspectral image classification,” *arXiv preprint arXiv:2305.16682*, 2023.
- [38] —, “Deep learning for hyperspectral image classification,” *Diss. Università DEGLI Studi DI Messina*, 2021.
- [39] Y. Zhang, L. Liang, J. Li, A. Plaza, X. Kang, J. Mao, and Y. Wang, “Structural and textural-aware feature extraction for hyperspectral image classification,” *IEEE Geoscience and Remote Sensing Letters*, pp. 1–1, 2024.
- [40] K. Mantripragada and F. Z. Qureshi, “Hyperspectral pixel unmixing with latent dirichlet variational autoencoder,” *IEEE Transactions on Geoscience and Remote Sensing*, pp. 1–1, 2024.
- [41] J. Zhang, W. Li, W. Sun, Y. Zhang, and R. Tao, “Locality robust domain adaptation for cross-scene hyperspectral image classification,” *Expert Systems with Applications*, vol. 238, p. 121822, 2024.
- [42] M. Mahadi, T. Ballal, M. Moineddin, T. Y. Al-Naffouri, and U. M. Al-Saggaf, “Regularized linear discriminant analysis using a nonlinear covariance matrix estimator,” 2024.
- [43] W. Li, S. Prasad, J. E. Fowler, and L. M. Bruce, “Locality-preserving discriminant analysis in kernel-induced feature spaces for hyperspectral image classification,” *IEEE Geoscience and Remote Sensing Letters*, vol. 8, no. 5, pp. 894–898, 2011.
- [44] W. Li, F. Feng, H. Li, and Q. Du, “Discriminant analysis-based dimension reduction for hyperspectral image classification: A survey of the most recent advances and an experimental comparison of different techniques,” *IEEE Geoscience and Remote Sensing Magazine*, vol. 6, no. 1, pp. 15–34, 2018.
- [45] S. Zeng, Z. Wang, C. Gao, Z. Kang, and D. Feng, “Hyperspectral image classification with global-local discriminant analysis and spatial-spectral context,” *IEEE Journal of Selected Topics in Applied Earth Observations and Remote Sensing*, vol. 11, no. 12, pp. 5005–5018, 2018.
- [46] Y. Zhou, J. Peng, and C. L. P. Chen, “Dimension reduction using spatial and spectral regularized local discriminant embedding for hyperspectral image classification,” *IEEE Transactions on Geoscience and Remote Sensing*, vol. 53, no. 2, pp. 1082–1095, 2015.
- [47] M. Ahmad, “Fuzziness-based spatial-spectral class discriminant information preserving active learning for hyperspectral image classification,” *arXiv preprint arXiv:2005.14236*, 2020.
- [48] B.-C. Kuo, C.-H. Li, and J.-M. Yang, “Kernel nonparametric weighted feature extraction for hyperspectral image classification,” *IEEE Transactions on Geoscience and Remote Sensing*, vol. 47, no. 4, pp. 1139–1155, 2009.
- [49] K. Chhapariya, K. M. Buddhiraju, and A. Kumar, “A deep spectral-spatial residual attention network for hyperspectral image classification,” *IEEE Journal of Selected Topics in Applied Earth Observations and Remote Sensing*, pp. 1–13, 2024.
- [50] C. Cheng, L. Zhang, H. Li, L. Dai, and W. Cui, “A deep stochastic adaptive fourier decomposition network for hyperspectral image classification,” *IEEE Transactions on Image Processing*, vol. 33, pp. 1080–1094, 2024.
- [51] W. Tian, Z. Kan, A. Sanchez-Azofeifa, Q. Zhao, and G. He, “Image quality assessment of uav hyperspectral images using radiant, spatial, and spectral features based on fuzzy comprehensive evaluation method,” *IEEE Geoscience and Remote Sensing Letters*, vol. 21, pp. 1–5, 2024.
- [52] Z. Zhang, H. Feng, C. Zhang, Q. Ma, and Y. Li, “S²dcn: Spectral-spatial difference convolution network for hyperspectral image classification,” *IEEE Journal of Selected Topics in Applied Earth Observations and Remote Sensing*, vol. 17, pp. 3053–3068, 2024.
- [53] Y. Gu, T. Liu, X. Jia, J. A. Benediktsson, and J. Chanussot, “Nonlinear multiple kernel learning with multiple-structure-element extended morphological profiles for hyperspectral image classification,” *IEEE Transactions on Geoscience and Remote Sensing*, vol. 54, no. 6, pp. 3235–3247, 2016.
- [54] W. Li, C. Chen, H. Su, and Q. Du, “Local binary patterns and extreme learning machine for hyperspectral imagery classification,” *IEEE Transactions on Geoscience and Remote Sensing*, vol. 53, no. 7, pp. 3681–3693, 2015.
- [55] F. Tsai and J.-S. Lai, “Feature extraction of hyperspectral image cubes using three-dimensional gray-level cooccurrence,” *IEEE Transactions on Geoscience and Remote Sensing*, vol. 51, no. 6, pp. 3504–3513, 2013.
- [56] X. Zhang, Y. Sun, K. Jiang, C. Li, L. Jiao, and H. Zhou, “Spatial sequential recurrent neural network for hyperspectral image classification,” *IEEE Journal of Selected Topics in Applied Earth Observations and Remote Sensing*, vol. 11, no. 11, pp. 4141–4155, 2018.
- [57] Y. Chen, Z. Lin, X. Zhao, G. Wang, and Y. Gu, “Deep learning-based classification of hyperspectral data,” *IEEE Journal of Selected topics*

- in applied earth observations and remote sensing*, vol. 7, no. 6, pp. 2094–2107, 2014.
- [58] Y. Chen, X. Zhao, and X. Jia, “Spectral–spatial classification of hyperspectral data based on deep belief network,” *IEEE Journal of Selected Topics in Applied Earth Observations and Remote Sensing*, vol. 8, no. 6, pp. 2381–2392, 2015.
- [59] M. E. Paoletti, J. M. Haut, J. Plaza, and A. Plaza, “Deep& dense convolutional neural network for hyperspectral image classification,” *Remote Sensing*, vol. 10, no. 9, p. 1454, 2018.
- [60] Z. Chen and B. Wang, “Spectral-spatial classification based on affinity scoring for hyperspectral imagery,” *IEEE Journal of Selected Topics in Applied Earth Observations and Remote Sensing*, vol. 9, no. 6, pp. 2305–2320, 2016.
- [61] P. Ghamisi, M. Dalla Mura, and J. A. Benediktsson, “A survey on spectral–spatial classification techniques based on attribute profiles,” *IEEE Transactions on Geoscience and Remote Sensing*, vol. 53, no. 5, pp. 2335–2353, 2015.
- [62] Y. Sun, B. Liu, X. Yu, A. Yu, K. Gao, and L. Ding, “Perceiving spectral variation: Unsupervised spectrum motion feature learning for hyperspectral image classification,” *IEEE Transactions on Geoscience and Remote Sensing*, vol. 60, pp. 1–17, 2022.
- [63] Z. Wang, S. Zhao, G. Zhao, and X. Song, “Dual-branch domain adaptation few-shot learning for hyperspectral image classification,” *IEEE Transactions on Geoscience and Remote Sensing*, vol. 62, pp. 1–16, 2024.
- [64] I. Dópido, J. Li, P. R. Marpu, A. Plaza, J. M. Bioucas Dias, and J. A. Benediktsson, “Semisupervised self-learning for hyperspectral image classification,” *IEEE Transactions on Geoscience and Remote Sensing*, vol. 51, no. 7, pp. 4032–4044, 2013.
- [65] L. Mou, S. Saha, Y. Hua, F. Bovolo, L. Bruzzone, and X. X. Zhu, “Deep reinforcement learning for band selection in hyperspectral image classification,” *IEEE Transactions on Geoscience and Remote Sensing*, vol. 60, pp. 1–14, 2022.
- [66] C. Zhong, J. Zhang, S. Wu, and Y. Zhang, “Cross-scene deep transfer learning with spectral feature adaptation for hyperspectral image classification,” *IEEE Journal of Selected Topics in Applied Earth Observations and Remote Sensing*, vol. 13, pp. 2861–2873, 2020.
- [67] X. He, Y. Chen, and P. Ghamisi, “Heterogeneous transfer learning for hyperspectral image classification based on convolutional neural network,” *IEEE Transactions on Geoscience and Remote Sensing*, vol. 58, no. 5, pp. 3246–3263, 2020.
- [68] W. Fu, S. Li, L. Fang, and J. A. Benediktsson, “Contextual online dictionary learning for hyperspectral image classification,” *IEEE Transactions on Geoscience and Remote Sensing*, vol. 56, no. 3, pp. 1336–1347, 2018.
- [69] S. Li, W. Song, L. Fang, Y. Chen, P. Ghamisi, and J. A. Benediktsson, “Deep learning for hyperspectral image classification: An overview,” *IEEE Transactions on Geoscience and Remote Sensing*, vol. 57, no. 9, pp. 6690–6709, 2019.
- [70] M. Ahmad, A. M. Khan, M. Mazzara, S. Distefano, M. Ali, and M. S. Sarfraz, “A fast and compact 3-d cnn for hyperspectral image classification,” *IEEE Geoscience and Remote Sensing Letters*, vol. 19, pp. 1–5, 2022.
- [71] M. Ahmad, A. Khan, A. M. Khan, M. Mazzara, S. Distefano, A. Sohaib, and O. Nibouche, “Spatial prior fuzziness pool-based interactive classification of hyperspectral images,” *Remote Sensing*, vol. 11, no. 9, p. 1136, 2019.
- [72] M. Paoletti, J. Haut, J. Plaza, and A. Plaza, “Deep learning classifiers for hyperspectral imaging: A review,” *ISPRS Journal of Photogrammetry and Remote Sensing*, vol. 158, pp. 279–317, 2019.
- [73] F. Ullah, I. Ullah, R. U. Khan, S. Khan, K. Khan, and G. Pau, “Conventional to deep ensemble methods for hyperspectral image classification: A comprehensive survey,” *IEEE Journal of Selected Topics in Applied Earth Observations and Remote Sensing*, vol. 17, pp. 3878–3916, 2024.
- [74] T. Anahara, “A texture-based classification algorithm with histograms of oriented gradients for alos/prism panchromatic imagery,” in *2015 IEEE International Geoscience and Remote Sensing Symposium (IGARSS)*, 2015, pp. 3061–3064.
- [75] H. Ge, L. Wang, M. Liu, X. Zhao, Y. Zhu, H. Pan, and Y. Liu, “Pyramidal multiscale convolutional network with polarized self-attention for pixel-wise hyperspectral image classification,” *IEEE Transactions on Geoscience and Remote Sensing*, vol. 61, pp. 1–18, 2023.
- [76] S. L. Al-khafaji, J. Zhou, A. Zia, and A. W.-C. Liew, “Spectral-spatial scale invariant feature transform for hyperspectral images,” *IEEE Transactions on Image Processing*, vol. 27, no. 2, pp. 837–850, 2018.
- [77] Y. Zhang, G. Cao, X. Li, and B. Wang, “Cascaded random forest for hyperspectral image classification,” *IEEE Journal of Selected Topics in Applied Earth Observations and Remote Sensing*, vol. 11, no. 4, pp. 1082–1094, 2018.
- [78] S. Zhong, C.-I. Chang, and Y. Zhang, “Iterative support vector machine for hyperspectral image classification,” in *2018 25th IEEE International Conference on Image Processing (ICIP)*, 2018, pp. 3309–3312.
- [79] L. Ma, M. M. Crawford, and J. Tian, “Local manifold learning-based k -nearest-neighbor for hyperspectral image classification,” *IEEE Transactions on Geoscience and Remote Sensing*, vol. 48, no. 11, pp. 4099–4109, 2010.
- [80] W. Yang, L. Gao, and D. Chen, “Real-time target detection in hyperspectral images based on spatial-spectral information extraction,” *EURASIP Journal on Advances in Signal Processing*, vol. 2012, 07 2012.
- [81] G. Cheng, P. Zhou, X. Yao, C. Yao, Y. Zhang, and J. Han, “Object detection in vhr optical remote sensing images via learning rotation-invariant hog feature,” in *2016 4th International Workshop on Earth Observation and Remote Sensing Applications (EORSA)*. IEEE, 2016, pp. 433–436.
- [82] R. Wang, P. Song, S. Li, L. Ji, and W. Zheng, “Common latent embedding space for cross-domain facial expression recognition,” *IEEE Transactions on Computational Social Systems*, pp. 1–11, 2023.
- [83] Q. Zhu, Y. Zhong, B. Zhao, G.-S. Xia, and L. Zhang, “Bag-of-visual-words scene classifier with local and global features for high spatial resolution remote sensing imagery,” *IEEE Geoscience and Remote Sensing Letters*, vol. 13, no. 6, pp. 747–751, 2016.
- [84] X. Gong, L. Yuanyuan, and Z. Xie, “An improved bag-of-visual-word based classification method for high-resolution remote sensing scene,” in *2018 26th International Conference on Geoinformatics*, 2018, pp. 1–5.
- [85] L. Huang, C. Chen, W. Li, and Q. Du, “Remote sensing image scene classification using multi-scale completed local binary patterns and fisher vectors,” *Remote Sensing*, vol. 8, no. 6, p. 483, 2016.
- [86] S. Lazebnik, C. Schmid, and J. Ponce, “Beyond bags of features: Spatial pyramid matching for recognizing natural scene categories,” in *2006 IEEE Computer Society Conference on Computer Vision and Pattern Recognition (CVPR’06)*, vol. 2. IEEE, 2006, pp. 2169–2178.
- [87] Y. Zhong, Q. Zhu, and L. Zhang, “Scene classification based on the multifeature fusion probabilistic topic model for high spatial resolution remote sensing imagery,” *IEEE Transactions on Geoscience and Remote Sensing*, vol. 53, no. 11, pp. 6207–6222, 2015.
- [88] D. Hong, L. Gao, N. Yokoya, J. Yao, J. Chanussot, D. Qian, and B. Zhang, “More diverse means better: Multimodal deep learning meets remote-sensing imagery classification,” *IEEE Trans. Geosci. Remote Sens.*, vol. 59, no. 5, pp. 4340–4354, 2021.
- [89] H. T. M. Nhat and V. T. Hoang, “Feature fusion by using lbp, hog, gist descriptors and canonical correlation analysis for face recognition,” in *2019 26th International Conference on Telecommunications (ICT)*. IEEE, 2019, pp. 371–375.
- [90] G. E. Hinton and R. R. Salakhutdinov, “Reducing the dimensionality of data with neural networks,” *science*, vol. 313, no. 5786, pp. 504–507, 2006.
- [91] F. Hu, G.-S. Xia, J. Hu, and L. Zhang, “Transferring deep convolutional neural networks for the scene classification of high-resolution remote sensing imagery,” *Remote Sensing*, vol. 7, no. 11, pp. 14 680–14 707, 2015.
- [92] L. Zhang, L. Zhang, and B. Du, “Deep learning for remote sensing data: A technical tutorial on the state of the art,” *IEEE Geoscience and Remote Sensing Magazine*, vol. 4, no. 2, pp. 22–40, 2016.
- [93] A. Shrestha and A. Mahmood, “Review of deep learning algorithms and architectures,” *IEEE Access*, vol. 7, pp. 53 040–53 065, 2019.
- [94] H. Venkateswara, S. Chakraborty, and S. Panchanathan, “Deep-learning systems for domain adaptation in computer vision: Learning transferable feature representations,” *IEEE Signal Processing Magazine*, vol. 34, no. 6, pp. 117–129, 2017.
- [95] S. Chen and Y. Wang, “Convolutional neural network and convex optimization,” *Dept. of Elect. and Comput. Eng., Univ. of California at San Diego, San Diego, CA, USA, Tech. Rep.*, 2014.
- [96] M. Ahmad, M. Mazzara, and S. Distefano, “Regularized cnn feature hierarchy for hyperspectral image classification,” *Remote Sensing*, vol. 13, no. 12, p. 2275, 2021.
- [97] Z. Niu, W. Liu, J. Zhao, and G. Jiang, “Deeplab-based spatial feature extraction for hyperspectral image classification,” *IEEE Geoscience and Remote Sensing Letters*, vol. 16, no. 2, pp. 251–255, 2019.
- [98] S. Zhong, S. Chen, C.-I. Chang, and Y. Zhang, “Fusion of spectral–spatial classifiers for hyperspectral image classification,” *IEEE*

- Transactions on Geoscience and Remote Sensing*, vol. 59, no. 6, pp. 5008–5027, 2021.
- [99] C. Yu, R. Han, M. Song, C. Liu, and C.-I. Chang, “A simplified 2d-3d cnn architecture for hyperspectral image classification based on spatial-spectral fusion,” *IEEE Journal of Selected Topics in Applied Earth Observations and Remote Sensing*, vol. 13, pp. 2485–2501, 2020.
- [100] B. Pan, X. Xu, Z. Shi, N. Zhang, H. Luo, and X. Lan, “Dssnet: A simple dilated semantic segmentation network for hyperspectral imagery classification,” *IEEE Geoscience and Remote Sensing Letters*, vol. 17, no. 11, pp. 1968–1972, 2020.
- [101] Y. Li, X. Luo, S. Li, and X. Shi, “An end-to-end generative classification model for hyperspectral image,” in *IGARSS 2023 - 2023 IEEE International Geoscience and Remote Sensing Symposium*, 2023, pp. 7621–7624.
- [102] T. Liu, Y. Chen, D. Li, T. Yang, J. Cao, and M. Wu, “Drift compensation for an electronic nose by adaptive subspace learning,” *IEEE Sensors Journal*, vol. 20, no. 1, pp. 337–347, 2020.
- [103] S. J. Pan, I. W. Tsang, J. T. Kwok, and Q. Yang, “Domain adaptation via transfer component analysis,” *IEEE Transactions on Neural Networks*, vol. 22, no. 2, pp. 199–210, 2011.
- [104] F. Ullah, Y. Long, I. Ullah, R. U. Khan, S. Khan, K. Khan, M. Khan, and G. Pau, “Deep hyperspectral shots: Deep snap smooth wavelet convolutional neural network shots ensemble for hyperspectral image classification,” *IEEE Journal of Selected Topics in Applied Earth Observations and Remote Sensing*, vol. 17, pp. 14–34, 2024.
- [105] D. Singh, H. Climente-Gonzalez, M. Petrovich, E. Kawakami, and M. Yamada, “Fsnets: Feature selection network on high-dimensional biological data,” in *2023 International Joint Conference on Neural Networks (IJCNN)*, 2023, pp. 1–9.
- [106] D. H. Hubel and T. N. Wiesel, “Receptive fields, binocular interaction and functional architecture in the cat’s visual cortex,” *The Journal of physiology*, vol. 160, no. 1, pp. 106–154, 1962.
- [107] K. Fukushima, “Neocognitron: A self-organizing neural network model for a mechanism of pattern recognition unaffected by shift in position,” *Biological cybernetics*, vol. 36, no. 4, pp. 193–202, 1980.
- [108] C. Yu, R. Han, M. Song, C. Liu, and C.-I. Chang, “Feedback attention-based dense cnn for hyperspectral image classification,” *IEEE Transactions on Geoscience and Remote Sensing*, vol. 60, pp. 1–16, 2022.
- [109] S. Yu, S. Jia, and C. Xu, “Convolutional neural networks for hyperspectral image classification,” *Neurocomputing*, vol. 219, pp. 88–98, 2017.
- [110] H. Gao, Y. Yang, C. Li, H. Zhou, and X. Qu, “Joint alternate small convolution and feature reuse for hyperspectral image classification,” *ISPRS International Journal of Geo-Information*, vol. 7, no. 9, p. 349, 2018.
- [111] H. Wu and S. Prasad, “Convolutional recurrent neural networks for hyperspectral data classification,” *Remote Sensing*, vol. 9, no. 3, p. 298, 2017.
- [112] X. Jin, L. Jie, S. Wang, H. J. Qi, and S. W. Li, “Classifying wheat hyperspectral pixels of healthy heads and fusarium head blight disease using a deep neural network in the wild field,” *Remote Sensing*, vol. 10, no. 3, p. 395, 2018.
- [113] Z. Qiu, J. Chen, Y. Zhao, S. Zhu, Y. He, and C. Zhang, “Variety identification of single rice seed using hyperspectral imaging combined with convolutional neural network,” *Applied Sciences*, vol. 8, no. 2, p. 212, 2018.
- [114] N. Wu, C. Zhang, X. Bai, X. Du, and Y. He, “Discrimination of chrysanthemum varieties using hyperspectral imaging combined with a deep convolutional neural network,” *Molecules*, vol. 23, no. 11, p. 2831, 2018.
- [115] Q. Huang, W. Li, and X. Xie, “Convolutional neural network for medical hyperspectral image classification with kernel fusion,” in *BIBE 2018; International Conference on Biological Information and Biomedical Engineering*. VDE, 2018, pp. 1–4.
- [116] J. Li, X. Zhao, Y. Li, Q. Du, B. Xi, and J. Hu, “Classification of hyperspectral imagery using a new fully convolutional neural network,” *IEEE Geoscience and Remote Sensing Letters*, vol. 15, no. 2, pp. 292–296, 2018.
- [117] J. M. Haut, M. E. Paoletti, J. Plaza, A. Plaza, and J. Li, “Hyperspectral image classification using random occlusion data augmentation,” *IEEE Geoscience and Remote Sensing Letters*, vol. 16, no. 11, pp. 1751–1755, 2019.
- [118] Y. Xu, B. Du, F. Zhang, and L. Zhang, “Hyperspectral image classification via a random patches network,” *ISPRS journal of photogrammetry and remote sensing*, vol. 142, pp. 344–357, 2018.
- [119] Y. Wang, T. Song, Y. Xie, and S. K. Roy, “A probabilistic neighbourhood pooling-based attention network for hyperspectral image classification,” *Remote Sensing Letters*, vol. 13, no. 1, pp. 65–75, 2021.
- [120] C. Ding, Y. Li, Y. Xia, W. Wei, L. Zhang, and Y. Zhang, “Convolutional neural networks based hyperspectral image classification method with adaptive kernels,” *Remote Sensing*, vol. 9, no. 6, p. 618, 2017.
- [121] Y. Chen, L. Zhu, P. Ghamisi, X. Jia, G. Li, and L. Tang, “Hyperspectral images classification with gabor filtering and convolutional neural network,” *IEEE Geoscience and Remote Sensing Letters*, vol. 14, no. 12, pp. 2355–2359, 2017.
- [122] J. Zhu, L. Fang, and P. Ghamisi, “Deformable convolutional neural networks for hyperspectral image classification,” *IEEE Geoscience and Remote Sensing Letters*, vol. 15, no. 8, pp. 1254–1258, 2018.
- [123] L. Ran, Y. Zhang, W. Wei, and Q. Zhang, “A hyperspectral image classification framework with spatial pixel pair features,” *Sensors*, vol. 17, no. 10, p. 2421, 2017.
- [124] Z. Zhong, J. Li, Z. Luo, and M. Chapman, “Spectral-spatial residual network for hyperspectral image classification: A 3-d deep learning framework,” *IEEE Transactions on Geoscience and Remote Sensing*, vol. 56, no. 2, pp. 847–858, 2018.
- [125] M. Paoletti, J. Haut, J. Plaza, and A. Plaza, “A new deep convolutional neural network for fast hyperspectral image classification,” *ISPRS journal of photogrammetry and remote sensing*, vol. 145, pp. 120–147, 2018.
- [126] S. Li, X. Zhu, Y. Liu, and J. Bao, “Adaptive spatial-spectral feature learning for hyperspectral image classification,” *IEEE Access*, vol. 7, pp. 61 534–61 547, 2019.
- [127] S. K. Roy, S. Manna, T. Song, and L. Bruzzone, “Attention-based adaptive spectral-spatial kernel resnet for hyperspectral image classification,” *IEEE Transactions on Geoscience and Remote Sensing*, vol. 59, no. 9, pp. 7831–7843, 2021.
- [128] S. K. Roy, M. E. Paoletti, J. M. Haut, E. M. T. Hendrix, and A. Plaza, “A new max-min convolutional network for hyperspectral image classification,” in *2021 11th Workshop on Hyperspectral Imaging and Signal Processing: Evolution in Remote Sensing (WHISPERS)*, 2021, pp. 1–5.
- [129] M. E. Paoletti, J. M. Haut, S. K. Roy, and E. M. Hendrix, “Rotation equivariant convolutional neural networks for hyperspectral image classification,” *IEEE Access*, vol. 8, pp. 179 575–179 591, 2020.
- [130] H. Zhang, Y. Li, Y. Jiang, P. Wang, Q. Shen, and C. Shen, “Hyperspectral classification based on lightweight 3-d-cnn with transfer learning,” *IEEE Transactions on Geoscience and Remote Sensing*, vol. 57, no. 8, pp. 5813–5828, 2019.
- [131] S. Jia, Z. Lin, M. Xu, Q. Huang, J. Zhou, X. Jia, and Q. Li, “A lightweight convolutional neural network for hyperspectral image classification,” *IEEE Transactions on Geoscience and Remote Sensing*, vol. 59, no. 5, pp. 4150–4163, 2020.
- [132] S. K. Roy, S. Chatterjee, S. Bhattacharyya, B. B. Chaudhuri, and J. Platoš, “Lightweight spectral-spatial squeeze-and-excitation residual bag-of-features learning for hyperspectral classification,” *IEEE Transactions on Geoscience and Remote Sensing*, vol. 58, no. 8, pp. 5277–5290, 2020.
- [133] S. K. Roy, R. Mondal, M. E. Paoletti, J. M. Haut, and A. Plaza, “Morphological convolutional neural networks for hyperspectral image classification,” *IEEE Journal of Selected Topics in Applied Earth Observations and Remote Sensing*, vol. 14, pp. 8689–8702, 2021.
- [134] Y. Li, H. Zhang, and Q. Shen, “Spectral-spatial classification of hyperspectral imagery with 3d convolutional neural network,” *Remote Sensing*, vol. 9, no. 1, p. 67, 2017.
- [135] S. K. Roy, S. R. Dubey, S. Chatterjee, and B. B. Chaudhuri, “Fusenet: fused squeeze-and-excitation network for spectral-spatial hyperspectral image classification,” *IET Image Processing*, vol. 14, no. 8, pp. 1653–1661, 2020.
- [136] L. Jiao, M. Liang, H. Chen, S. Yang, H. Liu, and X. Cao, “Deep fully convolutional network-based spatial distribution prediction for hyperspectral image classification,” *IEEE Transactions on Geoscience and Remote Sensing*, vol. 55, no. 10, pp. 5585–5599, 2017.
- [137] N. He, M. E. Paoletti, J. M. Haut, L. Fang, S. Li, A. Plaza, and J. Plaza, “Feature extraction with multiscale covariance maps for hyperspectral image classification,” *IEEE Transactions on Geoscience and Remote Sensing*, vol. 57, no. 2, pp. 755–769, 2018.
- [138] H. Zhang, Y. Li, Y. Zhang, and Q. Shen, “Spectral-spatial classification of hyperspectral imagery using a dual-channel convolutional neural network,” *Remote sensing letters*, vol. 8, no. 5, pp. 438–447, 2017.
- [139] M. He, B. Li, and H. Chen, “Multi-scale 3d deep convolutional neural network for hyperspectral image classification,” in *2017 IEEE*

- International Conference on Image Processing (ICIP)*. IEEE, 2017, pp. 3904–3908.
- [140] H. Dong, L. Zhang, and B. Zou, “Band attention convolutional networks for hyperspectral image classification,” *arXiv preprint arXiv:1906.04379*, 2019.
- [141] G. Cheng, Z. Li, J. Han, X. Yao, and L. Guo, “Exploring hierarchical convolutional features for hyperspectral image classification,” *IEEE Transactions on Geoscience and Remote Sensing*, vol. 56, no. 11, pp. 6712–6722, 2018.
- [142] Z. Gong, P. Zhong, Y. Yu, W. Hu, and S. Li, “A cnn with multiscale convolution and diversified metric for hyperspectral image classification,” *IEEE Transactions on Geoscience and Remote Sensing*, vol. 57, no. 6, pp. 3599–3618, 2019.
- [143] P. Zhong, N. Peng, and R. Wang, “Learning to diversify patch-based priors for remote sensing image restoration,” *IEEE Journal of Selected Topics in Applied Earth Observations and Remote Sensing*, vol. 8, no. 11, pp. 5225–5245, 2015.
- [144] L. Liu, Z. Shi, B. Pan, N. Zhang, H. Luo, and X. Lan, “Multiscale deep spatial feature extraction using virtual rgb image for hyperspectral imagery classification,” *Remote Sensing*, vol. 12, no. 2, p. 280, 2020.
- [145] A. Sellami, M. Farah, I. R. Farah, and B. Solaiman, “Hyperspectral imagery classification based on semi-supervised 3-d deep neural network and adaptive band selection,” *Expert Systems with Applications*, vol. 129, pp. 246–259, 2019.
- [146] X. Ma, A. Fu, J. Wang, H. Wang, and B. Yin, “Hyperspectral image classification based on deep deconvolution network with skip architecture,” *IEEE Transactions on Geoscience and Remote Sensing*, vol. 56, no. 8, pp. 4781–4791, 2018.
- [147] S. Mei, J. Ji, Y. Geng, Z. Zhang, X. Li, and Q. Du, “Unsupervised spatial–spectral feature learning by 3d convolutional autoencoder for hyperspectral classification,” *IEEE Transactions on Geoscience and Remote Sensing*, vol. 57, no. 9, pp. 6808–6820, 2019.
- [148] S. K. Roy, S. Das, T. Song, and B. Chanda, “Darecnet-bs: Unsupervised dual-attention reconstruction network for hyperspectral band selection,” *IEEE Geoscience and Remote Sensing Letters*, 2020.
- [149] S. K. Roy, D. Hong, P. Kar, X. Wu, X. Liu, and D. Zhao, “Lightweight heterogeneous kernel convolution for hyperspectral image classification with noisy labels,” *IEEE Geoscience and Remote Sensing Letters*, pp. 1–5, 2021.
- [150] S. K. Roy, G. Krishna, S. R. Dubey, and B. B. Chaudhuri, “HybridSN: Exploring 3-D-2-D CNN feature hierarchy for hyperspectral image classification,” *IEEE Geoscience and Remote Sensing Letters*, vol. 17, no. 2, pp. 277–281, 2020.
- [151] B. Zhang, S. Li, X. Jia, L. Gao, and M. Peng, “Adaptive markov random field approach for classification of hyperspectral imagery,” *IEEE Geoscience and Remote Sensing Letters*, vol. 8, no. 5, pp. 973–977, 2011.
- [152] M. E. Paoletti, J. M. Haut, T. Alipour-Fard, S. K. Roy, E. M. Hendrix, and A. Plaza, “Separable attention network in single-and mixed-precision floating point for land-cover classification of remote sensing images,” *IEEE Geoscience and Remote Sensing Letters*, 2021.
- [153] S. K. Roy, P. Kar, D. Hong, X. Wu, A. Plaza, and J. Chanussot, “Revisiting deep hyperspectral feature extraction networks via gradient centralized convolution,” *IEEE Transactions on Geoscience and Remote Sensing*, pp. 1–20, 2021.
- [154] T. N. Kipf and M. Welling, “Semi-supervised classification with graph convolutional networks,” *arXiv preprint arXiv:1609.02907*, 2016.
- [155] J. Chen, L. Jiao, X. Liu, L. Li, F. Liu, and S. Yang, “Automatic graph learning convolutional networks for hyperspectral image classification,” *IEEE Transactions on Geoscience and Remote Sensing*, vol. 60, pp. 1–16, 2022.
- [156] W. Zhu, C. Zhao, S. Feng, and B. Qin, “Multiscale short and long range graph convolutional network for hyperspectral image classification,” *IEEE Transactions on Geoscience and Remote Sensing*, vol. 60, pp. 1–15, 2022.
- [157] B. Xi, J. Li, Y. Li, and Q. Du, “Semi-supervised graph prototypical networks for hyperspectral image classification,” in *2021 IEEE International Geoscience and Remote Sensing Symposium IGARSS*, 2021, pp. 2851–2854.
- [158] C. Yu, S. Zhou, M. Song, B. Gong, E. Zhao, and C.-I. Chang, “Unsupervised hyperspectral band selection via hybrid graph convolutional network,” *IEEE Transactions on Geoscience and Remote Sensing*, vol. 60, pp. 1–15, 2022.
- [159] B. Xi, J. Li, Y. Li, R. Song, Y. Xiao, Q. Du, and J. Chanussot, “Semisupervised cross-scale graph prototypical network for hyperspectral image classification,” *IEEE Transactions on Neural Networks and Learning Systems*, vol. 34, no. 11, pp. 9337–9351, 2023.
- [160] J. Bai, W. Shi, Z. Xiao, A. C. Regan, T. A. A. Ali, Y. Zhu, R. Zhang, and L. Jiao, “Hyperspectral image classification based on superpixel feature subdivision and adaptive graph structure,” *IEEE Transactions on Geoscience and Remote Sensing*, vol. 60, pp. 1–15, 2022.
- [161] C. Yu, J. Huang, M. Song, Y. Wang, and C.-I. Chang, “Edge-inferring graph neural network with dynamic task-guided self-diagnosis for few-shot hyperspectral image classification,” *IEEE Transactions on Geoscience and Remote Sensing*, vol. 60, pp. 1–13, 2022.
- [162] C. Ding, M. Zheng, S. Zheng, Y. Xu, L. Zhang, W. Wei, and Y. Zhang, “Integrating prototype learning with graph convolution network for effective active hyperspectral image classification,” *IEEE Transactions on Geoscience and Remote Sensing*, vol. 62, pp. 1–16, 2024.
- [163] J. Zhao, J. Wang, C. Ruan, Y. Dong, and L. Huang, “Dual-branch spectral–spatial attention network for hyperspectral image classification,” *IEEE Transactions on Geoscience and Remote Sensing*, vol. 62, pp. 1–18, 2024.
- [164] A. Jamali, S. K. Roy, D. Hong, P. M. Atkinson, and P. Ghamisi, “Attention graph convolutional network for disjoint hyperspectral image classification,” *IEEE Geoscience and Remote Sensing Letters*, pp. 1–1, 2024.
- [165] D. Hong, L. Gao, J. Yao, B. Zhang, A. Plaza, and J. Chanussot, “Graph convolutional networks for hyperspectral image classification,” *IEEE Trans. Geosci. Remote Sens.*, vol. 59, no. 7, pp. 5966–5978, 2021.
- [166] A. Qin, Z. Shang, J. Tian, Y. Wang, T. Zhang, and Y. Y. Tang, “Spectral–spatial graph convolutional networks for semisupervised hyperspectral image classification,” *IEEE Geosci. Remote Sens. Lett.*, vol. 16, no. 2, pp. 241–245, 2018.
- [167] S. Wan, C. Gong, P. Zhong, S. Pan, G. Li, and J. Yang, “Hyperspectral image classification with context-aware dynamic graph convolutional network,” *arXiv preprint arXiv:1909.11953*, 2019.
- [168] G. E. Hinton, S. Osindero, and Y.-W. Teh, “A fast learning algorithm for deep belief nets,” *Neural computation*, vol. 18, no. 7, pp. 1527–1554, 2006.
- [169] N. Zhang, S. Ding, J. Zhang, and Y. Xue, “An overview on restricted boltzmann machines,” *Neurocomputing*, vol. 275, pp. 1186–1199, 2018.
- [170] B. Ayhan and C. Kwan, “Application of deep belief network to land cover classification using hyperspectral images,” in *Advances in Neural Networks - ISNN 2017*, F. Cong, A. Leung, and Q. Wei, Eds. Cham: Springer International Publishing, 2017, pp. 269–276.
- [171] U. Shaham, X. Cheng, O. Dror, A. Jaffe, B. Nadler, J. Chang, and Y. Kluger, “A deep learning approach to unsupervised ensemble learning,” in *International conference on machine learning*, 2016, pp. 30–39.
- [172] H. Xiong, A. J. Rodríguez-Sánchez, S. Szedmak, and J. Piater, “Diversity priors for learning early visual features,” *Frontiers in computational neuroscience*, vol. 9, p. 104, 2015.
- [173] P. Zhong, Z. Gong, S. Li, and C.-B. Schönlieb, “Learning to diversify deep belief networks for hyperspectral image classification,” *IEEE Transactions on Geoscience and Remote Sensing*, vol. 55, no. 6, pp. 3516–3530, 2017.
- [174] J. Li, B. Xi, Y. Li, Q. Du, and K. Wang, “Hyperspectral classification based on texture feature enhancement and deep belief networks,” *Remote Sensing*, vol. 10, no. 3, p. 396, 2018.
- [175] K. Tan, F. Wu, Q. Du, P. Du, and Y. Chen, “A parallel gaussian-bernoulli restricted boltzmann machine for mining area classification with hyperspectral imagery,” *IEEE Journal of Selected Topics in Applied Earth Observations and Remote Sensing*, vol. 12, no. 2, pp. 627–636, 2019.
- [176] S. Li, W. Song, L. Fang, Y. Chen, P. Ghamisi, and J. A. Benediktsson, “Deep learning for hyperspectral image classification: An overview,” *IEEE Transactions on Geoscience and Remote Sensing*, vol. 57, no. 9, pp. 6690–6709, 2019.
- [177] A. Sellami and I. Farah, “Spectra-spatial graph-based deep restricted boltzmann networks for hyperspectral image classification,” in *2019 Photonics & Electromagnetics Research Symposium-Spring (PIERS-Spring)*. IEEE, 2019, pp. 1055–1062.
- [178] R. J. Williams and D. Zipser, “A learning algorithm for continually running fully recurrent neural networks,” *Neural computation*, vol. 1, no. 2, pp. 270–280, 1989.
- [179] M. E. Paoletti, J. M. Haut, J. Plaza, and A. Plaza, “Scalable recurrent neural network for hyperspectral image classification,” *The Journal of Supercomputing*, pp. 1–17, 2020.
- [180] R. Hang, Q. Liu, D. Hong, and P. Ghamisi, “Cascaded recurrent neural networks for hyperspectral image classification,” *IEEE Transactions on Geoscience and Remote Sensing*, vol. 57, no. 8, pp. 5384–5394, 2019.

- [181] F. Zhou, R. Hang, Q. Liu, and X. Yuan, "Hyperspectral image classification using spectral-spatial lstms," *Neurocomputing*, vol. 328, pp. 39–47, 2019.
- [182] A. Sharma, X. Liu, and X. Yang, "Land cover classification from multi-temporal, multi-spectral remotely sensed imagery using patch-based recurrent neural networks," *Neural Networks*, vol. 105, pp. 346 – 355, 2018. [Online]. Available: <http://www.sciencedirect.com/science/article/pii/S0893608018301813>
- [183] H. Wu and S. Prasad, "Semi-supervised deep learning using pseudo labels for hyperspectral image classification," *IEEE Transactions on Image Processing*, vol. 27, no. 3, pp. 1259–1270, 2017.
- [184] F. Zhou, R. Hang, Q. Liu, and X. Yuan, "Integrating convolutional neural network and gated recurrent unit for hyperspectral image spectral-spatial classification," in *Chinese Conference on Pattern Recognition and Computer Vision (PRCV)*. Springer, 2018, pp. 409–420.
- [185] H. Luo, "Shorten spatial-spectral rnn with parallel-gru for hyperspectral image classification," *arXiv preprint arXiv:1810.12563*, 2018.
- [186] Q. Liu, F. Zhou, R. Hang, and X. Yuan, "Bidirectional-convolutional lstm based spectral-spatial feature learning for hyperspectral image classification," *Remote Sensing*, vol. 9, no. 12, p. 1330, 2017.
- [187] C. Shi and C.-M. Pun, "Multi-scale hierarchical recurrent neural networks for hyperspectral image classification," *Neurocomputing*, vol. 294, pp. 82–93, 2018.
- [188] X. Yang, Y. Ye, X. Li, R. Y. Lau, X. Zhang, and X. Huang, "Hyperspectral image classification with deep learning models," *IEEE Transactions on Geoscience and Remote Sensing*, vol. 56, no. 9, pp. 5408–5423, 2018.
- [189] M. Seydgar, A. Alizadeh Naeni, M. Zhang, W. Li, and M. Satari, "3-d convolution-recurrent networks for spectral-spatial classification of hyperspectral images," *Remote Sensing*, vol. 11, no. 7, p. 883, 2019.
- [190] J. Zhu, L. Wu, H. Hao, X. Song, and Y. Lu, "Auto-encoder based for high spectral dimensional data classification and visualization," in *2017 IEEE Second International Conference on Data Science in Cyberspace (DSC)*. IEEE, 2017, pp. 350–354.
- [191] A. Hassanzadeh, A. Kaarna, and T. Kauranne, "Unsupervised multi-manifold classification of hyperspectral remote sensing images with contractive autoencoder," in *Scandinavian Conference on Image Analysis*. Springer, 2017, pp. 169–180.
- [192] X. Zhang, Y. Liang, C. Li, N. Huyan, L. Jiao, and H. Zhou, "Recursive autoencoders-based unsupervised feature learning for hyperspectral image classification," *IEEE Geoscience and Remote Sensing Letters*, vol. 14, no. 11, pp. 1928–1932, 2017.
- [193] S. Hao, W. Wang, Y. Ye, T. Nie, and L. Bruzzone, "Two-stream deep architecture for hyperspectral image classification," *IEEE Transactions on Geoscience and Remote Sensing*, vol. 56, no. 4, pp. 2349–2361, 2017.
- [194] X. Sun, F. Zhou, J. Dong, F. Gao, Q. Mu, and X. Wang, "Encoding spectral and spatial context information for hyperspectral image classification," *IEEE Geoscience and Remote Sensing Letters*, vol. 14, no. 12, pp. 2250–2254, 2017.
- [195] C. Zhao, X. Wan, G. Zhao, B. Cui, W. Liu, and B. Qi, "Spectral-spatial classification of hyperspectral imagery based on stacked sparse autoencoder and random forest," *European journal of remote sensing*, vol. 50, no. 1, pp. 47–63, 2017.
- [196] X. Wan, C. Zhao, Y. Wang, and W. Liu, "Stacked sparse autoencoder in hyperspectral data classification using spectral-spatial, higher order statistics and multifractal spectrum features," *Infrared Physics & Technology*, vol. 86, pp. 77–89, 2017.
- [197] F. Lv, M. Han, and T. Qiu, "Remote sensing image classification based on ensemble extreme learning machine with stacked autoencoder," *IEEE Access*, vol. 5, pp. 9021–9031, 2017.
- [198] P. Zhou, J. Han, G. Cheng, and B. Zhang, "Learning compact and discriminative stacked autoencoder for hyperspectral image classification," *IEEE Transactions on Geoscience and Remote Sensing*, vol. 57, no. 7, pp. 4823–4833, 2019.
- [199] R. Lan, Z. Li, Z. Liu, T. Gu, and X. Luo, "Hyperspectral image classification using k-sparse denoising autoencoder and spectral-restricted spatial characteristics," *Applied Soft Computing*, vol. 74, pp. 693–708, 2019.
- [200] S. Paul and D. N. Kumar, "Spectral-spatial classification of hyperspectral data with mutual information based segmented stacked autoencoder approach," *ISPRS journal of photogrammetry and remote sensing*, vol. 138, pp. 265–280, 2018.
- [201] B. Liu, Q. Zhang, L. Ying, W. Chang, and M. Zhou, "Spatial-spectral jointed stacked auto-encoder-based deep learning for oil slick extraction from hyperspectral images," *Journal of the Indian Society of Remote Sensing*, vol. 47, no. 12, pp. 1989–1997, 2019.
- [202] Q. Nguyen and M. Hein, "Optimization landscape and expressivity of deep cnns," *arXiv preprint arXiv:1710.10928*, 2017.
- [203] L. Bottou, "Stochastic gradient learning in neural networks," *Proceedings of Neuro-Nimes*, vol. 91, no. 8, p. 12, 1991.
- [204] N. Qian, "On the momentum term in gradient descent learning algorithms," *Neural networks*, vol. 12, no. 1, pp. 145–151, 1999.
- [205] G. Hinton, N. Srivastava, and K. Swersky, "Neural networks for machine learning lecture 6a overview of mini-batch gradient descent," *Cited on*, vol. 14, no. 8, 2012.
- [206] D. P. Kingma and J. Ba, "Adam: A method for stochastic optimization," *arXiv preprint arXiv:1412.6980*, 2014.
- [207] I. Loshchilov and F. Hutter, "Decoupled weight decay regularization," *arXiv preprint arXiv:1711.05101*, 2017.
- [208] S. R. Dubey, S. Chakraborty, S. K. Roy, S. Mukherjee, S. K. Singh, and B. B. Chaudhuri, "diffgrad: An optimization method for convolutional neural networks," *IEEE transactions on neural networks and learning systems*, vol. 31, no. 11, pp. 4500–4511, 2019.
- [209] L. Liu, H. Jiang, P. He, W. Chen, X. Liu, J. Gao, and J. Han, "On the variance of the adaptive learning rate and beyond," *arXiv preprint arXiv:1908.03265*, 2019.
- [210] H. Yong, J. Huang, X. Hua, and L. Zhang, "Gradient centralization: A new optimization technique for deep neural networks," in *European Conference on Computer Vision*. Springer, 2020, pp. 635–652.
- [211] S. Roy, M. Paoletti, J. Haut, S. Dubey, P. Kar, A. Plaza, and B. Chaudhuri, "Angulargrad: A new optimization technique for angular convergence of convolutional neural networks," *arXiv preprint arXiv:2105.10190*, 2021.
- [212] D. Erhan, Y. Bengio, A. Courville, P.-A. Manzagol, P. Vincent, and S. Bengio, "Why does unsupervised pre-training help deep learning?" *Journal of Machine Learning Research*, vol. 11, no. Feb, pp. 625–660, 2010.
- [213] M. Z. Alom, T. M. Taha, C. Yakopcic, S. Westberg, P. Sidike, M. S. Nasrin, M. Hasan, B. C. Van Essen, A. A. Awwal, and V. K. Asari, "A state-of-the-art survey on deep learning theory and architectures," *Electronics*, vol. 8, no. 3, p. 292, 2019.
- [214] A. Plaza, J. Plaza, A. Paz, and S. Sanchez, "Parallel hyperspectral image and signal processing [applications corner]," *IEEE Signal Processing Magazine*, vol. 28, no. 3, pp. 119–126, 2011.
- [215] A. Plaza, D. Valencia, and J. Plaza, "An experimental comparison of parallel algorithms for hyperspectral analysis using heterogeneous and homogeneous networks of workstations," *Parallel Computing*, vol. 34, no. 2, pp. 92–114, 2008.
- [216] J. M. Bioucas-Dias, A. Plaza, G. Camps-Valls, P. Scheunders, N. Nasrabadi, and J. Chanussot, "Hyperspectral remote sensing data analysis and future challenges," *IEEE Geoscience and remote sensing magazine*, vol. 1, no. 2, pp. 6–36, 2013.
- [217] K. He, X. Zhang, S. Ren, and J. Sun, "Deep residual learning for image recognition," in *Proceedings of the IEEE conference on computer vision and pattern recognition*, 2016, pp. 770–778.
- [218] Y. Bengio, P. Simard, and P. Frasconi, "Learning long-term dependencies with gradient descent is difficult," *IEEE transactions on neural networks*, vol. 5, no. 2, pp. 157–166, 1994.
- [219] A. Vaswani, N. Shazeer, N. Parmar, J. Uszkoreit, L. Jones, A. N. Gomez, L. u. Kaiser, and I. Polosukhin, "Attention is all you need," in *Advances in Neural Information Processing Systems*, I. Guyon, U. V. Luxburg, S. Bengio, H. Wallach, R. Fergus, S. Vishwanathan, and R. Garnett, Eds., vol. 30. Curran Associates, Inc., 2017.
- [220] N. Chen, L. Fang, Y. Xia, S. Xia, H. Liu, and J. Yue, "Spectral query spatial: Revisiting the role of center pixel in transformer for hyperspectral image classification," *IEEE Transactions on Geoscience and Remote Sensing*, pp. 1–1, 2024.
- [221] J. Fang, J. Yang, A. Khader, and L. Xiao, "Mimo-sst: Multi-input multi-output spatial-spectral transformer for hyperspectral and multispectral image fusion," *IEEE Transactions on Geoscience and Remote Sensing*, pp. 1–1, 2024.
- [222] M. Böhle, N. Singh, M. Fritz, and B. Schiele, "B-cos alignment for inherently interpretable cnns and vision transformers," *IEEE Transactions on Pattern Analysis and Machine Intelligence*, pp. 1–15, 2024.
- [223] P. Ghosh, S. K. Roy, B. Koirala, B. Rasti, and P. Scheunders, "Hyperspectral unmixing using transformer network," *IEEE Transactions on Geoscience and Remote Sensing*, vol. 60, pp. 1–16, 2022.
- [224] W. Rao, L. Gao, Y. Qu, X. Sun, B. Zhang, and J. Chanussot, "Siamese transformer network for hyperspectral image target detection," *IEEE Transactions on Geoscience and Remote Sensing*, vol. 60, pp. 1–19, 2022.

- [225] Z. Zhong, Y. Li, L. Ma, J. Li, and W.-S. Zheng, "Spectral-spatial transformer network for hyperspectral image classification: A factorized architecture search framework," *IEEE Transactions on Geoscience and Remote Sensing*, vol. 60, pp. 1–15, 2022.
- [226] H. Yu, Z. Xu, K. Zheng, D. Hong, H. Yang, and M. Song, "Mstnet: A multilevel spectral-spatial transformer network for hyperspectral image classification," *IEEE Transactions on Geoscience and Remote Sensing*, vol. 60, pp. 1–13, 2022.
- [227] X. He and Y. Chen, "Optimized input for cnn-based hyperspectral image classification using spatial transformer network," *IEEE Geoscience and Remote Sensing Letters*, vol. 16, no. 12, pp. 1884–1888, 2019.
- [228] J. Bai, Z. Wen, Z. Xiao, F. Ye, Y. Zhu, M. Alazab, and L. Jiao, "Hyperspectral image classification based on multibranch attention transformer networks," *IEEE Transactions on Geoscience and Remote Sensing*, vol. 60, pp. 1–17, 2022.
- [229] X. Yang, W. Cao, Y. Lu, and Y. Zhou, "Hyperspectral image transformer classification networks," *IEEE Transactions on Geoscience and Remote Sensing*, vol. 60, pp. 1–15, 2022.
- [230] X. Qiao and W. Huang, "A dual frequency transformer network for hyperspectral image classification," *IEEE Journal of Selected Topics in Applied Earth Observations and Remote Sensing*, vol. 16, pp. 10344–10358, 2023.
- [231] X. Zhao, J. Niu, C. Liu, Y. Ding, and D. Hong, "Hyperspectral image classification based on graph transformer network and graph attention mechanism," *IEEE Geoscience and Remote Sensing Letters*, vol. 19, pp. 1–5, 2022.
- [232] Y. Zhang, S. Xu, D. Hong, H. Gao, C. Zhang, M. Bi, and C. Li, "Multimodal transformer network for hyperspectral and lidar classification," *IEEE Transactions on Geoscience and Remote Sensing*, vol. 61, pp. 1–17, 2023.
- [233] W. Zhang, L. Su, Y. Zhang, and X. Lu, "A spectrum-aware transformer network for change detection in hyperspectral imagery," *IEEE Transactions on Geoscience and Remote Sensing*, vol. 61, pp. 1–12, 2023.
- [234] D. Hong, Z. Han, J. Yao, L. Gao, B. Zhang, A. Plaza, and J. Chanussot, "Spectralformer: Rethinking hyperspectral image classification with transformers," *IEEE Transactions on Geoscience and Remote Sensing*, vol. 60, pp. 1–15, 2022.
- [235] B. Zhang, Y. Chen, Y. Rong, S. Xiong, and X. Lu, "Matnet: A combining multi-attention and transformer network for hyperspectral image classification," *IEEE Transactions on Geoscience and Remote Sensing*, vol. 61, pp. 1–15, 2023.
- [236] J.-F. Hu, T.-Z. Huang, L.-J. Deng, H.-X. Dou, D. Hong, and G. Vivone, "Fusformer: A transformer-based fusion network for hyperspectral image super-resolution," *IEEE Geoscience and Remote Sensing Letters*, vol. 19, pp. 1–5, 2022.
- [237] Y. Liu, J. Hu, X. Kang, J. Luo, and S. Fan, "Interactformer: Interactive transformer and cnn for hyperspectral image super-resolution," *IEEE Transactions on Geoscience and Remote Sensing*, vol. 60, pp. 1–15, 2022.
- [238] Z. Yang, M. Xu, S. Liu, H. Sheng, and J. Wan, "Ust-net: A u-shaped transformer network using shifted windows for hyperspectral unmixing," *IEEE Transactions on Geoscience and Remote Sensing*, vol. 61, pp. 1–15, 2023.
- [239] Z. He, K. Xia, P. Ghamisi, Y. Hu, S. Fan, and B. Zu, "Hypervitgan: Semisupervised generative adversarial network with transformer for hyperspectral image classification," *IEEE Journal of Selected Topics in Applied Earth Observations and Remote Sensing*, vol. 15, pp. 6053–6068, 2022.
- [240] Y. Liu, X. Li, Z. Xu, and Z. Hua, "Bsformer: Transformer-based reconstruction network for hyperspectral band selection," *IEEE Geoscience and Remote Sensing Letters*, vol. 20, pp. 1–5, 2023.
- [241] S. Zhang, J. Zhang, X. Wang, J. Wang, and Z. Wu, "Els2t: Efficient lightweight spectral-spatial transformer for hyperspectral image classification," *IEEE Transactions on Geoscience and Remote Sensing*, vol. 61, pp. 1–16, 2023.
- [242] D. Wang, J. Zhang, B. Du, L. Zhang, and D. Tao, "Dcn-t: Dual context network with transformer for hyperspectral image classification," *IEEE Transactions on Image Processing*, vol. 32, pp. 2536–2551, 2023.
- [243] J. Zou, W. He, and H. Zhang, "Lessformer: Local-enhanced spectral-spatial transformer for hyperspectral image classification," *IEEE Transactions on Geoscience and Remote Sensing*, vol. 60, pp. 1–16, 2022.
- [244] C. Zhao, H. Liu, N. Su, and Y. Yan, "Tftn: A transformer-based fusion tracking framework of hyperspectral and rgb," *IEEE Transactions on Geoscience and Remote Sensing*, vol. 60, pp. 1–15, 2022.
- [245] W. Qi, C. Huang, Y. Wang, X. Zhang, W. Sun, and L. Zhang, "Global-local 3-d convolutional transformer network for hyperspectral image classification," *IEEE Transactions on Geoscience and Remote Sensing*, vol. 61, pp. 1–20, 2023.
- [246] X. Huang, M. Dong, J. Li, and X. Guo, "A 3-d-swin transformer-based hierarchical contrastive learning method for hyperspectral image classification," *IEEE Transactions on Geoscience and Remote Sensing*, vol. 60, pp. 1–15, 2022.
- [247] B. Zu, T. Cao, Y. Li, J. Li, F. Ju, and H. Wang, "Swint-srnet: Swin transformer with image super-resolution reconstruction network for pollen images classification," *Engineering Applications of Artificial Intelligence*, vol. 133, p. 108041, 2024.
- [248] B. Liu, Y. Liu, W. Zhang, Y. Tian, and W. Kong, "Spectral swin transformer network for hyperspectral image classification," *Remote Sensing*, vol. 15, no. 15, 2023.
- [249] G. Farooque, Q. Liu, A. B. Sargano, and L. Xiao, "Swin transformer with multiscale 3d atrous convolution for hyperspectral image classification," *Engineering Applications of Artificial Intelligence*, vol. 126, p. 107070, 2023.
- [250] J. Xie, J. Hua, S. Chen, P. Wu, P. Gao, D. Sun, Z. Lyu, S. Lyu, X. Xue, and J. Lu, "Hypersformer: A transformer-based end-to-end hyperspectral image classification method for crop classification," *Remote Sensing*, vol. 15, no. 14, 2023.
- [251] S. Ayas and E. Tunc-Gormus, "Spectralswin: a spectral-swin transformer network for hyperspectral image classification," *International Journal of Remote Sensing*, vol. 43, no. 11, pp. 4025–4044, 2022.
- [252] Y. Peng, J. Ren, J. Wang, and M. Shi, "Spectral-swin transformer with spatial feature extraction enhancement for hyperspectral image classification," *Remote Sensing*, vol. 15, no. 10, 2023.
- [253] Y. Long, X. Wang, M. Xu, S. Zhang, S. Jiang, and S. Jia, "Dual self-attention swin transformer for hyperspectral image super-resolution," *IEEE Transactions on Geoscience and Remote Sensing*, vol. 61, pp. 1–12, 2023.
- [254] L. Wang, Z. Zheng, N. Kumar, C. Wang, F. Guo, and P. Zhang, "Multilevel class token transformer with cross tokenmixer for hyperspectral images classification," *IEEE Transactions on Geoscience and Remote Sensing*, vol. 62, pp. 1–13, 2024.
- [255] X. He, Y. Chen, and Z. Lin, "Spatial-spectral transformer for hyperspectral image classification," *Remote Sensing*, vol. 13, no. 3, 2021.
- [256] G. Wang, Y. Wang, Z. Pan, X. Wang, J. Zhang, and J. Pan, "Vitfsl-baseline: A simple baseline of vision transformer network for few-shot image classification," *IEEE Access*, vol. 12, pp. 11836–11849, 2024.
- [257] Y. Ma, Y. Lan, Y. Xie, L. Yu, C. Chen, Y. Wu, and X. Dai, "A spatial-spectral transformer for hyperspectral image classification based on global dependencies of multi-scale features," *Remote Sensing*, vol. 16, no. 2, 2024.
- [258] J. Lian, L. Wang, H. Sun, and H. Huang, "Gt-had: Gated transformer for hyperspectral anomaly detection," *IEEE Transactions on Neural Networks and Learning Systems*, pp. 1–15, 2024.
- [259] S. Mei, Z. Han, M. Ma, F. Xu, and X. Li, "A novel center-boundary metric loss to learn discriminative features for hyperspectral image classification," *IEEE Transactions on Geoscience and Remote Sensing*, vol. 62, pp. 1–16, 2024.
- [260] A. Jamali, S. K. Roy, D. Hong, P. M. Atkinson, and P. Ghamisi, "Spatial-gated multilayer perceptron for land use and land cover mapping," *IEEE Geoscience and Remote Sensing Letters*, vol. 21, pp. 1–5, 2024.
- [261] Y. Xiao, Q. Yuan, K. Jiang, J. He, C.-W. Lin, and L. Zhang, "Ttst: A top-k token selective transformer for remote sensing image super-resolution," *IEEE Transactions on Image Processing*, vol. 33, pp. 738–752, 2024.
- [262] S. Mei, C. Song, M. Ma, and F. Xu, "Hyperspectral image classification using group-aware hierarchical transformer," *IEEE Transactions on Geoscience and Remote Sensing*, vol. 60, pp. 1–14, 2022.
- [263] J. Chen, C. Yang, L. Zhang, L. Yang, L. Bian, Z. Luo, and J. Wang, "Tccu-net: Transformer and cnn collaborative unmixing network for hyperspectral image," *IEEE Journal of Selected Topics in Applied Earth Observations and Remote Sensing*, pp. 1–20, 2024.
- [264] M. Ye, J. Chen, F. Xiong, and Y. Qian, "Adaptive graph modeling with self-training for heterogeneous cross-scene hyperspectral image classification," *IEEE Transactions on Geoscience and Remote Sensing*, vol. 62, pp. 1–15, 2024.
- [265] W. Huang, Y. Deng, S. Hui, Y. Wu, S. Zhou, and J. Wang, "Sparse self-attention transformer for image inpainting," *Pattern Recognition*, vol. 145, p. 109897, 2024.
- [266] Y. Sun, X. Zhi, S. Jiang, G. Fan, X. Yan, and W. Zhang, "Image fusion for the novelty rotating synthetic aperture system based on vision transformer," *Information Fusion*, vol. 104, p. 102163, 2024.

- [267] T. Kim, J. Kim, H. Oh, and J. Kang, "Deep transformer based video inpainting using fast fourier tokenization," *IEEE Access*, vol. 12, pp. 21 723–21 736, 2024.
- [268] Y. Shi, J. Xia, M. Zhou, and Z. Cao, "A dual-feature-based adaptive shared transformer network for image captioning," *IEEE Transactions on Instrumentation and Measurement*, vol. 73, pp. 1–13, 2024.
- [269] J. Li, Z. Zhang, R. Song, Y. Li, and Q. Du, "Sformer: Spectral coordinate transformer for cross-domain few-shot hyperspectral image classification," *IEEE Transactions on Image Processing*, vol. 33, pp. 840–855, 2024.
- [270] Z. Shu, Y. Wang, and Z. Yu, "Dual attention transformer network for hyperspectral image classification," *Engineering Applications of Artificial Intelligence*, vol. 127, p. 107351, 2024.
- [271] Q. Ma, J. Jiang, X. Liu, and J. Ma, "Reciprocal transformer for hyperspectral and multispectral image fusion," *Information Fusion*, vol. 104, p. 102148, 2024.
- [272] Y. Zhang, C. Lan, H. Zhang, G. Ma, and H. Li, "Multimodal remote sensing image matching via learning features and attention mechanism," *IEEE Transactions on Geoscience and Remote Sensing*, vol. 62, pp. 1–20, 2024.
- [273] B. Li, L. Fang, N. Chen, J. Kang, and J. Yue, "Enhancing hyperspectral image classification: Leveraging unsupervised information with guided group contrastive learning," *IEEE Transactions on Geoscience and Remote Sensing*, vol. 62, pp. 1–17, 2024.
- [274] S. Miao, Q. Xu, W. Li, C. Yang, B. Sheng, F. Liu, T. T. Bezabih, and X. Yu, "Mmtfn: Multi-modal multi-scale transformer fusion network for alzheimer's disease diagnosis," *International Journal of Imaging Systems and Technology*, vol. 34, no. 1, p. e22970, 2024.
- [275] L. Qu, S. Liu, M. Wang, S. Li, S. Yin, and Z. Song, "Trans2fuse: Empowering image fusion through self-supervised learning and multi-modal transformations via transformer networks," *Expert Systems with Applications*, vol. 236, p. 121363, 2024.
- [276] J. Yang, Y.-Q. Zhao, and J. C.-W. Chan, "Learning and transferring deep joint spectral-spatial features for hyperspectral classification," *IEEE Transactions on Geoscience and Remote Sensing*, vol. 55, no. 8, pp. 4729–4742, 2017.
- [277] L. Windrim, A. Melkumyan, R. J. Murphy, A. Chlingaryan, and R. Ramakrishnan, "Pretraining for hyperspectral convolutional neural network classification," *IEEE Transactions on Geoscience and Remote Sensing*, vol. 56, no. 5, pp. 2798–2810, 2018.
- [278] X. Liu, Q. Sun, Y. Meng, M. Fu, and S. Bourennane, "Hyperspectral image classification based on parameter-optimized 3d-cnns combined with transfer learning and virtual samples," *Remote Sensing*, vol. 10, no. 9, p. 1425, 2018.
- [279] O. Day and T. M. Khoshgoftaar, "A survey on heterogeneous transfer learning," *Journal of Big Data*, vol. 4, no. 1, p. 29, 2017.
- [280] X. Li, L. Zhang, B. Du, L. Zhang, and Q. Shi, "Iterative reweighting heterogeneous transfer learning framework for supervised remote sensing image classification," *IEEE Journal of Selected Topics in Applied Earth Observations and Remote Sensing*, vol. 10, no. 5, pp. 2022–2035, 2017.
- [281] Y. Liu and C. Xiao, "Transfer learning for hyperspectral image classification using convolutional neural network," in *MIPPR 2019: Remote Sensing Image Processing, Geographic Information Systems, and Other Applications*, vol. 11432. International Society for Optics and Photonics, 2020, p. 114320E.
- [282] J. Lin, C. He, Z. J. Wang, and S. Li, "Structure preserving transfer learning for unsupervised hyperspectral image classification," *IEEE Geoscience and Remote Sensing Letters*, vol. 14, no. 10, pp. 1656–1660, 2017.
- [283] R. Pires de Lima and K. Marfurt, "Convolutional neural network for remote-sensing scene classification: Transfer learning analysis," *Remote Sensing*, vol. 12, no. 1, p. 86, 2020.
- [284] C. Shorten and T. M. Khoshgoftaar, "A survey on image data augmentation for deep learning," *Journal of Big Data*, vol. 6, no. 1, p. 60, 2019.
- [285] X. Yu, X. Wu, C. Luo, and P. Ren, "Deep learning in remote sensing scene classification: a data augmentation enhanced convolutional neural network framework," *GIScience & Remote Sensing*, vol. 54, no. 5, pp. 741–758, 2017.
- [286] W. Li, C. Chen, M. Zhang, H. Li, and Q. Du, "Data augmentation for hyperspectral image classification with deep cnn," *IEEE Geoscience and Remote Sensing Letters*, vol. 16, no. 4, pp. 593–597, 2018.
- [287] X. Cao, J. Yao, Z. Xu, and D. Meng, "Hyperspectral image classification with convolutional neural network and active learning," *IEEE Transactions on Geoscience and Remote Sensing*, 2020.
- [288] J. F. R. Rochac, N. Zhang, L. Thompson, and T. Oladunni, "A data augmentation-assisted deep learning model for high dimensional and highly imbalanced hyperspectral imaging data," in *2019 9th International Conference on Information Science and Technology (ICIST)*. IEEE, 2019, pp. 362–367.
- [289] J. Nalepa, M. Myller, and M. Kawulok, "Training-and test-time data augmentation for hyperspectral image segmentation," *IEEE Geoscience and Remote Sensing Letters*, 2019.
- [290] —, "Hyperspectral data augmentation," *arXiv preprint arXiv:1903.05580*, 2019.
- [291] I. Goodfellow, J. Pouget-Abadie, M. Mirza, B. Xu, D. Warde-Farley, S. Ozair, A. Courville, and Y. Bengio, "Generative adversarial nets," in *Advances in neural information processing systems*, 2014, pp. 2672–2680.
- [292] Y. Zhan, D. Hu, Y. Wang, and X. Yu, "Semisupervised hyperspectral image classification based on generative adversarial networks," *IEEE Geoscience and Remote Sensing Letters*, vol. 15, no. 2, pp. 212–216, 2017.
- [293] Z. He, H. Liu, Y. Wang, and J. Hu, "Generative adversarial networks-based semi-supervised learning for hyperspectral image classification," *Remote Sensing*, vol. 9, no. 10, p. 1042, 2017.
- [294] L. Zhu, Y. Chen, P. Ghamisi, and J. A. Benediktsson, "Generative adversarial networks for hyperspectral image classification," *IEEE Transactions on Geoscience and Remote Sensing*, vol. 56, no. 9, pp. 5046–5063, 2018.
- [295] Y. Zhan, K. Wu, W. Liu, J. Qin, Z. Yang, Y. Medjadba, G. Wang, and X. Yu, "Semi-supervised classification of hyperspectral data based on generative adversarial networks and neighborhood majority voting," in *IGARSS 2018-2018 IEEE International Geoscience and Remote Sensing Symposium*. IEEE, 2018, pp. 5756–5759.
- [296] J. Feng, H. Yu, L. Wang, X. Cao, X. Zhang, and L. Jiao, "Classification of hyperspectral images based on multiclass spatial-spectral generative adversarial networks," *IEEE Transactions on Geoscience and Remote Sensing*, vol. 57, no. 8, pp. 5329–5343, 2019.
- [297] Z. Zhong, J. Li, D. A. Clausi, and A. Wong, "Generative adversarial networks and conditional random fields for hyperspectral image classification," *IEEE transactions on cybernetics*, 2019.
- [298] X. Wang, K. Tan, Q. Du, Y. Chen, and P. Du, "Caps-triplegan: Gan-assisted capsnet for hyperspectral image classification," *IEEE Transactions on Geoscience and Remote Sensing*, vol. 57, no. 9, pp. 7232–7245, 2019.
- [299] Z. Xue, "Semi-supervised convolutional generative adversarial network for hyperspectral image classification," *IET Image Processing*, vol. 14, no. 4, pp. 709–719, 2019.
- [300] W.-Y. Wang, H.-C. Li, Y.-J. Deng, L.-Y. Shao, X.-Q. Lu, and Q. Du, "Generative adversarial capsule network with convlstm for hyperspectral image classification," *IEEE Geoscience and Remote Sensing Letters*, 2020.
- [301] T. Alipour-Fard and H. Arefi, "Structure aware generative adversarial networks for hyperspectral image classification," *IEEE Journal of Selected Topics in Applied Earth Observations and Remote Sensing*, vol. 13, pp. 5424–5438, 2020.
- [302] S. K. Roy, J. M. Haut, M. E. Paoletti, S. R. Dubey, and A. Plaza, "Generative adversarial minority oversampling for spectral-spatial hyperspectral image classification," *IEEE Transactions on Geoscience and Remote Sensing*, 2021.
- [303] R. Ganti and A. Gray, "Upal: Unbiased pool based active learning," in *Artificial Intelligence and Statistics*, 2012, pp. 422–431.
- [304] C. C. Aggarwal, X. Kong, Q. Gu, J. Han, and S. Y. Philip, "Active learning: A survey," in *Data Classification: Algorithms and Applications*. CRC Press, 2014, pp. 571–605.
- [305] B. Settles, "Active learning literature survey," University of Wisconsin-Madison Department of Computer Sciences, Tech. Rep., 2009.
- [306] C. Liu, L. He, Z. Li, and J. Li, "Feature-driven active learning for hyperspectral image classification," *IEEE Transactions on Geoscience and Remote Sensing*, vol. 56, no. 1, pp. 341–354, 2017.
- [307] Y. Zhang, G. Cao, X. Li, B. Wang, and P. Fu, "Active semi-supervised random forest for hyperspectral image classification," *Remote Sensing*, vol. 11, no. 24, p. 2974, 2019.
- [308] J. Guo, X. Zhou, J. Li, A. Plaza, and S. Prasad, "Superpixel-based active learning and online feature importance learning for hyperspectral image analysis," *IEEE Journal of Selected Topics in Applied Earth Observations and Remote Sensing*, vol. 10, no. 1, pp. 347–359, 2016.
- [309] Z. Xue, S. Zhou, and P. Zhao, "Active learning improved by neighborhoods and superpixels for hyperspectral image classification," *IEEE Geoscience and Remote Sensing Letters*, vol. 15, no. 3, pp. 469–473, 2018.

- [310] K. Bhardwaj, A. Das, and S. Patra, "Spectral-spatial active learning with attribute profile for hyperspectral image classification," in *International Conference on Intelligent Computing and Smart Communication 2019*. Springer, 2020, pp. 1219–1229.
- [311] S. Patra, K. Bhardwaj, and L. Bruzzone, "A spectral-spatial multicriteria active learning technique for hyperspectral image classification," *IEEE Journal of Selected Topics in Applied Earth Observations and Remote Sensing*, vol. 10, no. 12, pp. 5213–5227, 2017.
- [312] Z. Zhang and M. M. Crawford, "A batch-mode regularized multimetric active learning framework for classification of hyperspectral images," *IEEE Transactions on Geoscience and Remote Sensing*, vol. 55, no. 11, pp. 6594–6609, 2017.
- [313] X. Xu, J. Li, and S. Li, "Multiview intensity-based active learning for hyperspectral image classification," *IEEE Transactions on Geoscience and Remote Sensing*, vol. 56, no. 2, pp. 669–680, 2017.
- [314] M. K. Pradhan, S. Minz, and V. K. Shrivastava, "Fisher discriminant ratio based multiview active learning for the classification of remote sensing images," in *2018 4th International Conference on Recent Advances in Information Technology (RAIT)*. IEEE, 2018, pp. 1–6.
- [315] Z. Zhang, E. Pasolli, and M. M. Crawford, "An adaptive multiview active learning approach for spectral-spatial classification of hyperspectral images," *IEEE Transactions on Geoscience and Remote Sensing*, vol. 58, no. 4, pp. 2557–2570, 2019.
- [316] Y. Li, T. Lu, and S. Li, "Subpixel-pixel-superpixel-based multiview active learning for hyperspectral images classification," *IEEE Transactions on Geoscience and Remote Sensing*, 2020.
- [317] Y. Sun, J. Li, W. Wang, A. Plaza, and Z. Chen, "Active learning based autoencoder for hyperspectral imagery classification," in *2016 IEEE International Geoscience and Remote Sensing Symposium (IGARSS)*. IEEE, 2016, pp. 469–472.
- [318] P. Liu, H. Zhang, and K. B. Eom, "Active deep learning for classification of hyperspectral images," *IEEE Journal of Selected Topics in Applied Earth Observations and Remote Sensing*, vol. 10, no. 2, pp. 712–724, 2016.
- [319] J. M. Haut, M. E. Paoletti, J. Plaza, J. Li, and A. Plaza, "Active learning with convolutional neural networks for hyperspectral image classification using a new bayesian approach," *IEEE Transactions on Geoscience and Remote Sensing*, vol. 56, no. 11, pp. 6440–6461, 2018.
- [320] J. Lin, L. Zhao, S. Li, R. Ward, and Z. J. Wang, "Active-learning-incorporated deep transfer learning for hyperspectral image classification," *IEEE Journal of Selected Topics in Applied Earth Observations and Remote Sensing*, vol. 11, no. 11, pp. 4048–4062, 2018.
- [321] C. Deng, Y. Xue, X. Liu, C. Li, and D. Tao, "Active transfer learning network: A unified deep joint spectral-spatial feature learning model for hyperspectral image classification," *IEEE Transactions on Geoscience and Remote Sensing*, vol. 57, no. 3, pp. 1741–1754, 2018.
- [322] C. Deng, X. Liu, C. Li, and D. Tao, "Active multi-kernel domain adaptation for hyperspectral image classification," *Pattern Recognition*, vol. 77, pp. 306–315, 2018.
- [323] M. Ahmad, S. Protasov, A. M. Khan, R. Hussain, A. M. Khattak, and W. A. Khan, "Fuzziness-based active learning framework to enhance hyperspectral image classification performance for discriminative and generative classifiers," *PLoS ONE*, vol. 13, no. 1, p. e0188996, January 2018.
- [324] M. Ahmad, R. A. Raza, and M. Mazzara, "Multiclass non-randomized spectral-spatial active learning for hyperspectral image classification," *Applied Sciences*, vol. 10, p. 4739, 07 2020.
- [325] X. Xu, J. Li, and A. Plaza, "Fusion of hyperspectral and lidar data using morphological component analysis," in *2016 IEEE International Geoscience and Remote Sensing Symposium (IGARSS)*. IEEE, 2016, pp. 3575–3578.
- [326] R. O. Green, M. L. Eastwood, C. M. Sarture, T. G. Chrien, M. Aronsson, B. J. Chippendale, J. A. Faust, B. E. Pavri, C. J. Chovit, M. Solis *et al.*, "Imaging spectroscopy and the airborne visible/infrared imaging spectrometer (aviris)," *Remote sensing of environment*, vol. 65, no. 3, pp. 227–248, 1998.
- [327] X. Huang and L. Zhang, "A comparative study of spatial approaches for urban mapping using hyperspectral rosis images over pavia city, northern italy," *International Journal of Remote Sensing*, vol. 30, no. 12, pp. 3205–3221, 2009.